# FINAL REPORT

## RL-34 RING LASER GYRO
## LABORATORY EVALUATION

### FOR THE

## DEEP SPACE NETWORK
## ANTENNA APPLICATION

## JPL CONTRACT NO. 959072

## 28 NOVEMBER 1991

**Allied-Signal Aerospace Company**

*Bendix Guidance Systems Division*

**Allied Signal**

# Table of Contents

# List of Figures

## List of Tables

# I. Introduction

The Bendix designed RL-34 high accuracy ring laser gyro is the basis of the testing done under this gyro evaluation contract (see Figure 1). Three of these gyros were incorporated into an Inertial Sensor Assembly(ISA) with three Sundstrand QA 2000 accelerometers. This ISA was installed into one of our Advanced Land Navigation Systems which was then tested for pointing accuracy (see Figure 2). The overall system pointing results agree very well with the measured individual gyro performance, such that pointing accuracy of a few millidegrees is feasible.

## Pointing Performance vs. Objectives

### Initialization

The initialization goal was to demonstrate the angular rate error of an individual RLG to be less than 0.0002 deg/hr, rms, in the determination of the Earth's spin vector. This translates to an initialization pointing error of 0.001 degrees (3.7 arc-seconds) at the BGSD latitude of 40.86 degrees. The final initialization pointing results were 0.00086 degrees (3.1 arc-seconds), one sigma, thus meeting the goal. These results encompassed 9 positions in the level plane (azimuth), spanning the entire 360 degree range.

### Blind Target Acquisition

The objective for the target acquisition mode was 0.0001 degrees (0.36 arc-seconds) individual RLG pointing error, after a 20 degree rotation at 0.1 degrees per second. Final tracking results were limited by the digital quantization of the gyro output to 0.77 arc-seconds. An existing BGSD system electronics modification will bring this value down to 0.18 arc-seconds, as explained in the recommendations section later.

### Target Tracking

The angular position error objective for target tracking was 0.001 degrees, rms, with a zero input rate for a period of 10 hours. The best recorded test was 0.00136 degrees (4.9 arc-seconds) rms, for 10 hours. This was one of two tests that we believe were representative of performance capabilities with proper calibration. Together, they had a mean of 0.0022 degrees, rms.

The overall average tracking performance was 0.0038 degrees (13.8 arc-seconds, all 12 tests). It should be noted that most of this error occurs in azimuth, with average elevation error being less than 0.001 degrees. This difference is due to the strapdown system
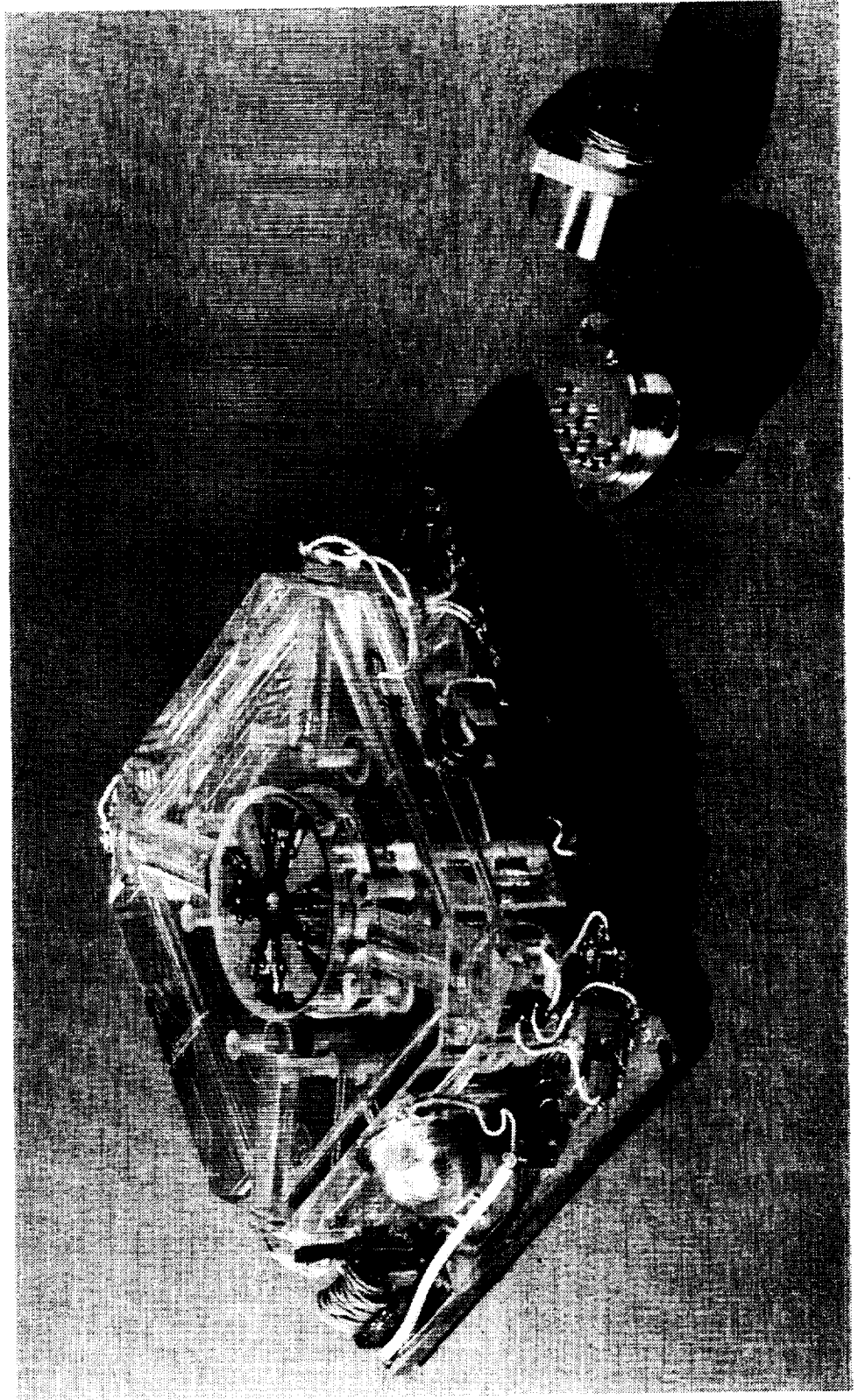
Figure 1    RL-34 High Accuracy RLG

2
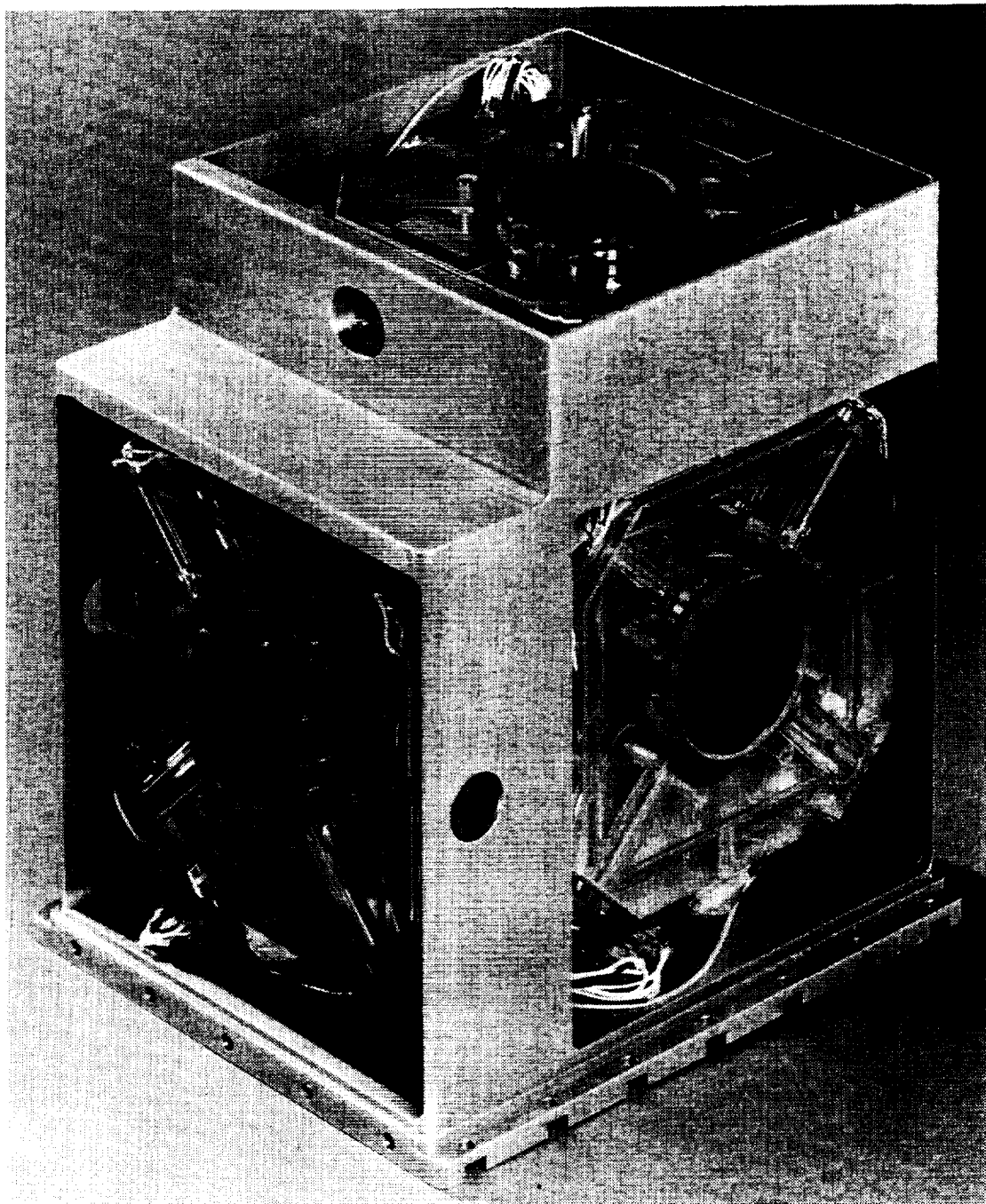
Figure 2        RL-34  ISA  Assembly

implementation, which is further explained in the body of the report, and in Appendix B.

## Definition of System Roll, Pitch, and Heading

The standard nomenclature of a navigation system is defined in terms of roll, pitch and heading. Figure 3 shows roll, pitch and heading with respect to a North, East, and Up coordinate system. Pitch is defined as the angle between the X system axis and the local level plane. Heading is defined as the angle between North and the projection of the X system axis onto the local level plane. Roll is the angle of rotation around the X system axis. For the JPL/DSN application, the two degrees of freedom for the antenna are azimuth and elevation. They are related to the navigation system's heading and pitch outputs, respectively. Throughout this report, heading and azimuth will both be used, with azimuth being preferred. The same is true for pitch and elevation, with elevation preferred. The navigation system outputs all the angles in "mils" with 6400 mils in 360 degs. Figure 4 shows this convention applied to azimuth. North corresponds to 0/6400 mils and East is 1600 mils. Most of the analyzed data presented in this report has been converted to arc-sec where 0.001 deg equal 3.6 arc-sec.
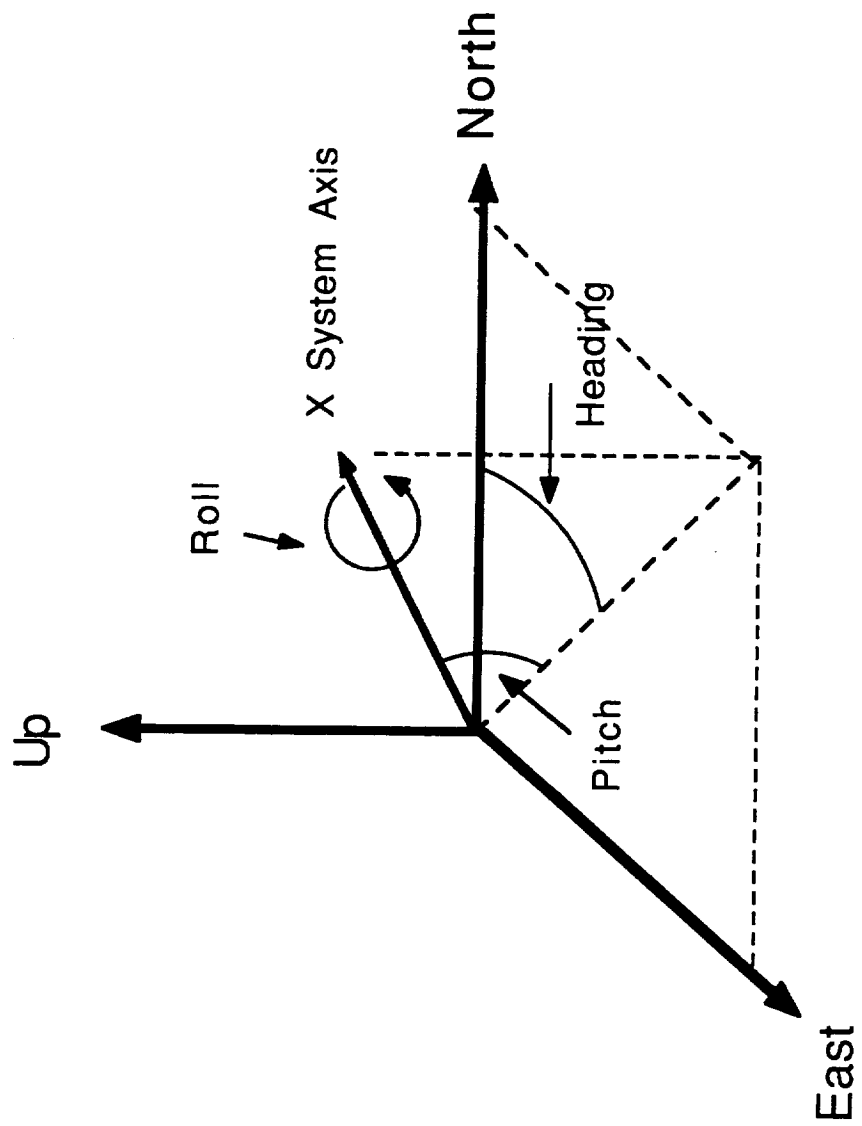
Figure 3    Definition of System's Roll, Pitch, and Heading

North
0 mils

5600 mils

800 mils

West
4800 mils

East
1600 mils

4000 mils

2400 mils

South
3200 mils
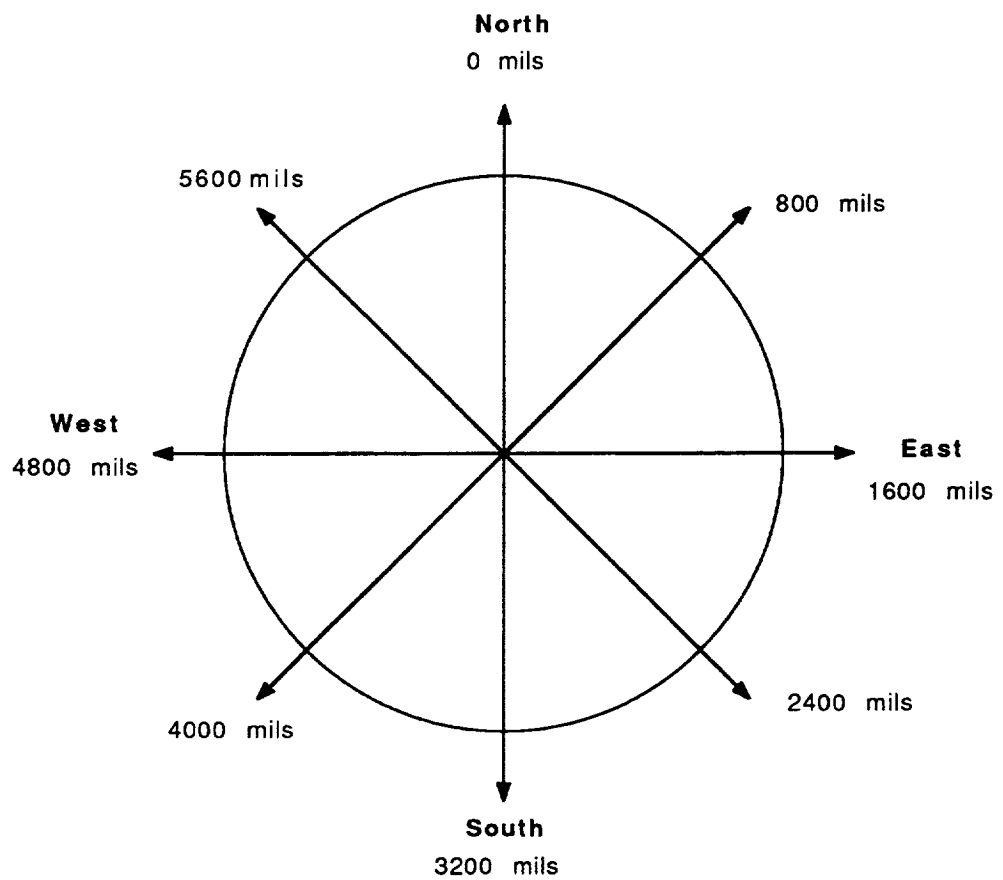
The relationship between the system azimuth readout in Mils and Degrees.

Figure 4    System Readout in Mils and Degs

## II. Test Plans

According to the statement of work, the test plan was separated into three different areas: initialization, acquisition, and tracking. We also realized the need for a more accurate gyro bias calibration procedure and developed one accordingly. Please note that the pointing accuracy objectives are such that gyro biases be known to 0.0001 deg/hr. Our existing automated production calibration techniques were designed to calibrate to 0.001 deg/hr, which is required for high accuracy RLG based navigators.

### Calibration Tests

To fine calibrate the gyro biases, a four position gyrocompass test was performed (North, South, East, West). Each position required 6-8 hours of testing to average the random noise errors down to the gyro bias stability limit (see appendix A on gyro data). The new gyro biases were then changed and stored in the system for use in future tests.

### Initialization Tests

Once calibrated, the system gyrocompassed to determine its attitude (see appendix B for system implementation). Since the longest gyrocompass time allowed (production software limitation) was 15 minutes, multiple gyro compasses were performed for 4-8 hr test times. The qualification of the gyrocompass accuracy was accomplished by testing 8 azimuth positions at 45 deg intervals.

### Acquisition Tests

Once the system was initialized, the acquisition capability was tested by rotating the system azimuth and elevation to acquire a target. The rate table was used to rotate at various rates. The elevation was changed with the Ultradex. The length of each test was limited by the 100 second data update rate for the high rotation rate tests or by the longer time of the low rotation rate test. Each test was performed multiple times to generate performance and test statistics.

### Tracking Tests

All the tracking tests involved a 10 hour static navigation test. Eight were performed at 0 deg elevation and 4 were performed at 60 deg elevation.

## III. Test Facility and Metrology Description

### Bendix Facility

The geodetic latitude of Bendix's Teterboro complex is 40.86056 degrees. Within the facility, there are four outdoor geodetic survey monuments to identify our geophysical location so we can cross check each monument for accuracy. The monuments are calibrated every 10 years by using a telescope-theodolite referring to the "North Star" -- Polaris. The most recent calibration was done in October, 1991. The overall accuracy to true north is within 2 arc-sec. Using this as a primary north reference, "North" is transferred and aligned to an indoor monument for all of our test measurements The indoor "North" reference is located in our temperature controlled system test area. The room temperature is controlled around 70 +/-5 deg F all year long.

For the purposes of this evaluation, two test sites were utilized. The primary site was a Contraves rate table model 51C, with an air-bearing table. On top of this table was mounted an Ultradex table. Due to the time limitations of this contract, early results were obtained on a three axis dividing head which was quickly set up while the primary site was being prepared and calibrated. These two sites are shown in Figure 5 and 6.

### Detailed descriptions of Test Equipment

#### Theodolites

There are two different models (model T-1600 and model T-2000) of theodolites used in our system alignment. Both theodolites were manufactured by Wild Heerbrugg of Switzerland. The resolution of these instruments are one arc-sec and one-tenth arc-sec for models T-1600 and T-2000, respectively. The high precision model T-2000 theodolite was used in the air-bearing table calibration only, all the other theodolite measurements were done by with model T-1600. A precision polished cube was mounted on the ISA as the reference for all external reference measurements. The cube is calibrated to one arc-sec for each polished surface.

Due to the limited amount of light reflected from the cube, a small modification was made to improve the theodolite reading and we believe this modification had no effect on theodolite accuracy. We added a fiber optic light source to increase the intensity of the light sent out from the theodolite to the cube, thus increasing the reflected signal.

The theodolite measurement was made in both stationary and dynamic testing of the navigation system. In the stationary mode
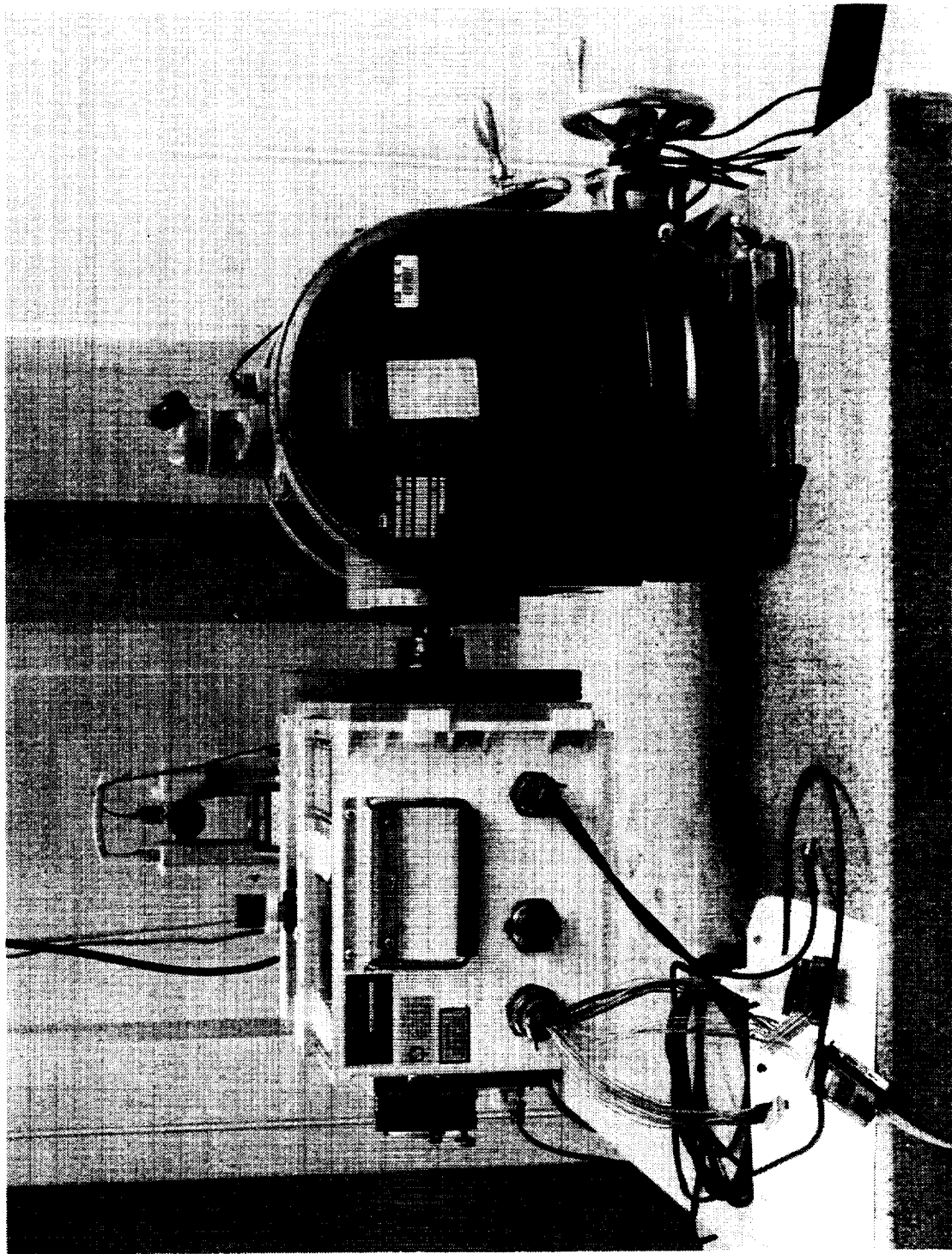
A picture of the three axis dividing head table, the external reference cube and the theodolite for external reference measurements.

Figure 5      Three Axis Dividing Head Test Site

9

A front view of the air-bearing table and its control console.
The table is installed on an isolation pad to isolate any
building vibrations.

Figure 6          Air Bearing Test Site

with the system at rest, there were sharp line images in the theodolite in both the vertical and horizontal. In the dynamic mode when the system was in operation, the horizontal line was foggy and oscillated around the stationary line. The blurred line was due to "dither" reaction motion of the ISA. The theodolite horizontal icon corresponded to the system local level and vertical icon corresponded to the system heading- azimuth angle.

Table alignment

The test table "North" was based on our indoor north monument by using two theodolites to transfer north in three steps to the table. Two T-1600 model theodolites were used to complete the transfer alignment operation. The first theodolite was aligned to indoor north, then transferred the alignment to the second theodolite and finally transferred to the ISA external reference-cube in a third step by moving the first theodolite (see Figure 7 for conceptual drawing). This is a time consuming and difficult operation, and we eliminated error and saved time by using a combination of the precision Ultradex table and a porro prism to establish "North" on the test table top ( see Figure 8 for conceptual drawing).

Three Axis Dividing Head Table

The initial system testing was conducted on a three axis dividing head table ( see Figure 5). This setup allowed us to adjust the system azimuth, elevation and roll. The table resolutions in azimuth and elevation are 5 arc-seconds and adjustment in roll is limited to the "worm" gear resolution. At each test position, the exact position was confirmed by using theodolites in all angles. Using this technique, we were able to complete our first system calibration run before moving to the newly installed high precision air-bearing rate table.

Air-bearing Table

A high precision air-bearing rate table model 51C manufactured by Contraves was installed in our laboratory for these tests (see Figure 6). The table was designed for testing high accuracy mechanical and laser inertial systems. The aerostatic table axis bearing exhibits very low axis friction and minimizes axis wobble for effective evaluation of gyro performance. The servo driven table axis (azimuth) provides precise control of table position which is displayed at the control console with a resolution of .0001 deg (0.36 arc-sec). The table payload is rated at 800 lbs in the vertical axis. The table was installed on an isolation pad to isolate the test stand from the rest of the building. A 12 inch Ultradex table was mounted on top of the table for system elevation adjustment. The Ultradex

EXTERNAL REFERENCE-1

NORTH → theodolite-1 → theodolite-2 → theodolite-3 → Cube-ISA → AZIMUTH LEVEL X-Y
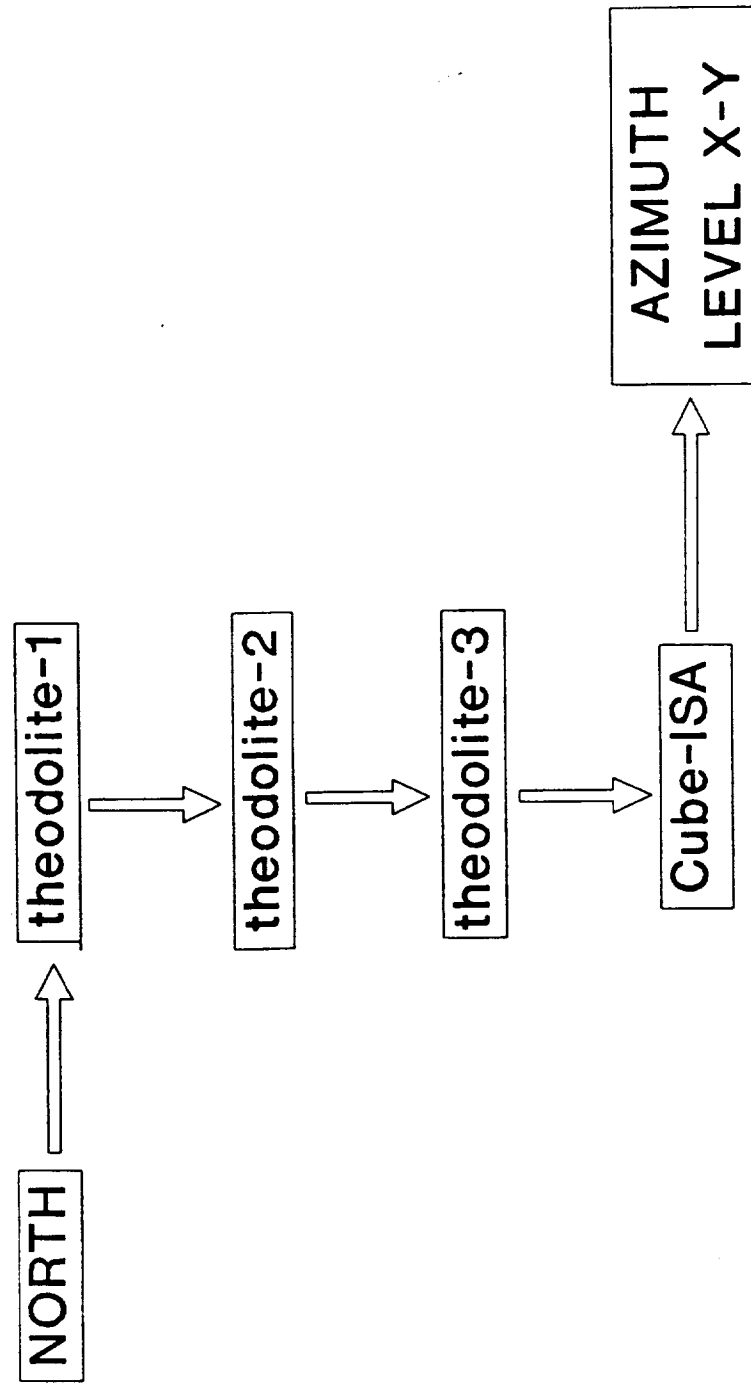
A conceptual drawing of the initial theodolite setup for the external reference measurement.

Figure 7    Theodolite   Setup

12

# EXTERNAL REFERENCE-2
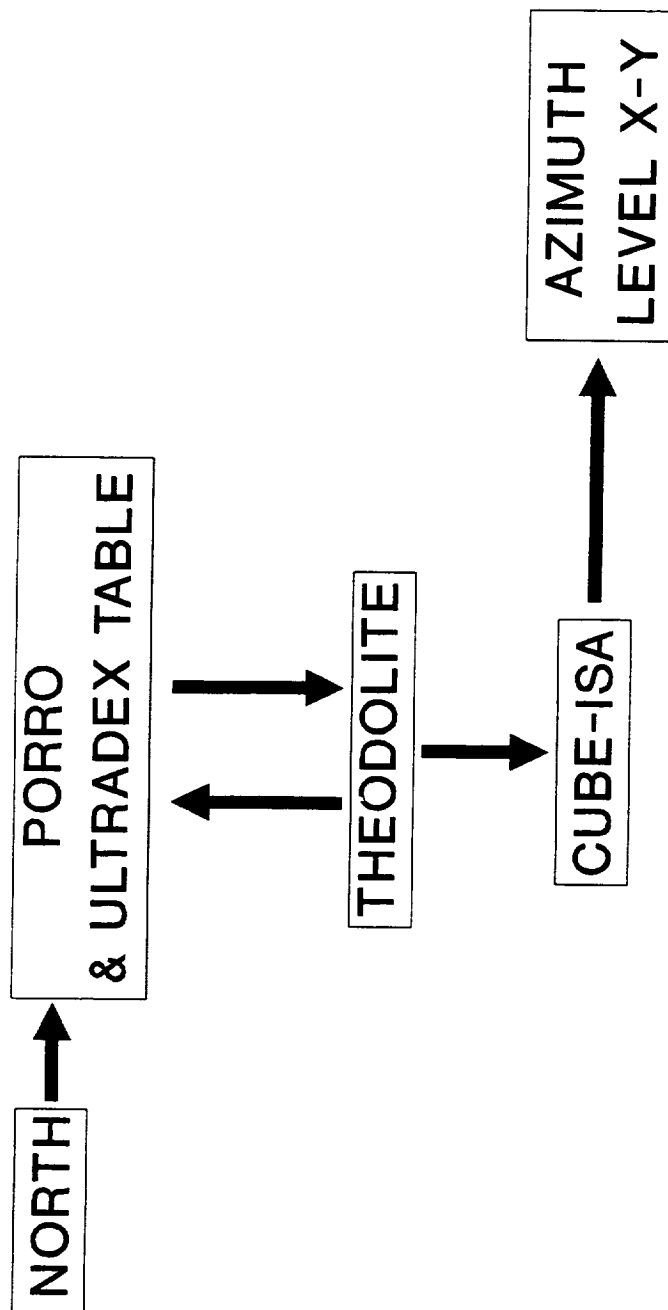


A simplified theodolite setup using the combination of porro prism and a small Ultradex as a "North" on the test table for external reference measurement.

Figure 8    Theodolite Setup with porro prism

13

table model R-13722-3 was manufactured by Absolute Accuracy Gage Inc. with horizontal recommended load limit of 300 lbs. The Ultradex table accuracy is better than 0.25 arc-sec with 0.25 degree incremental resolution.

Table Calibration

A high precision theodolite model T-2000 and an autocollimator were used to calibrate the air-bearing azimuth table and Ultradex elevation table. The spindle axis of the air-bearing azimuth table was adjusted within 2 arc-sec for 8 different table positions(0, 45, 90, 135, 180, 225, 270, 315). These 8 positions were used for system calibration operation. The air-bearing table azimuth resolution of 0.0001 deg (0.36 arc-sec) was confirmed by using the combination of the high precision theodolite and the autocollimator.

The Ultradex table used for elevation movement was aligned to the local level and the 1/4 arc-sec table resolution was confirmed by using the high precision theodolite.

Test environment

All tests were conducted in an air-conditioned, temperature controlled standard laboratory environment. No special attentions were made to control room temperature better than +/- 2 deg F nor were there any attempts to control room humidity.

# IV. RLG Array Description, and Test Configurations

## Inertial Sensor Assembly Description

The Inertial Sensor Assembly(ISA) includes three RLG's and three Sundstrand QA 2000 accelerometers (see Figure 2). For this testing, the three gyros that were installed into the ISA were

|          |            |
|----------|------------|
| X gyro   | SN: B2003  |
| Y gyro   | SN: B4500  |
| Z gyro   | SN: Z2002  |

It also includes the High Voltage Power Supply and the current regulator assemblies needed to start and run the plasma discharges for the three RLG's. Additional low-voltage support electronics exist in the system cards that are interfaced to the ISA through two 50-pin connectors. The RLG's are mounted orthogonally and the three accelerometers are similarly mounted so their respective axes are collinear with the gyros. The accelerometer triad is mounted close to the center of gravity of the ISA to minimize lever-arm effects.

The ISA also has magnetic shielding(50:1) to reduce any magnetic effects from sensor outputs to values below instrument stability levels. Typical gyro sensitivity when mounted in the ISA is 0.0002 dph/gauss. The areas where testing is done show field fluctuations less than 1 gauss for the tests that were conducted for this gyro evaluation.

The ISA assembly is suspended by eight vibration isolators that are matched in transfer characteristics to keep the center of suspension co-incident with the center of gravity and thus minimize dynamic motion. The isolators are arranged in a symmetric fashion to aid in balancing the entire assembly. The eight mounting points of the ISA are arranged such that four are through the top of the system chassis, and four are through the bottom of the system chassis.

## Ring Laser Gyro Noise Sources

There are three basic noise sources for the RL-34 gyro in this application: quantization noise, random walk noise and gyro bias instability noise. Each error appears differently as a function of testing time and system output (rate or angle). At short test times for angle measurements the error is dominated by the gyro quantization, while the gyro random walk error increases as a square root function of time and the bias instability contribution grows linearly as a function of time. The overall Noise Equivalent Angle (NEA) and Noise Equivalent Rate (NER) equations are given as :

$$NEA = \sqrt{\left(\frac{Q}{\sqrt{6}}\right)^2 + \left(RWC\sqrt{3600\ T}\right)^2 + \left(BI*T\right)^2}$$

and

$$NER = \sqrt{\left(\frac{Q}{\sqrt{6}\ T}\right)^2 + \left(RWC\sqrt{\frac{3600}{T}}\right)^2 + \left(BI\right)^2}$$

where Q is the gyro quantization error in arc-sec, RWC is the gyro random walk in deg/root-hr, BI is gyro in-run bias instability in deg/hr, and T is the data sampling time in seconds.

## Sigma Plot Generation

One useful method to estimate the quantization, RWC and bias instability errors for an RLG is to plot the standard deviation of the gyro output vs integration time. Table 1 shows the first 60 points of data for B4500 from data file 06-30-91.g (see appendix A for details on datafile). The first column shows run time in seconds for the 100 seconds/sample data. The second column shows the gyro pulses per 100 second sample. The scale factor (SF) for the RL-34 with X4 logic is 0.3838 arc-sec/pulse. This SF was used to scale the gyro pulses/100 sec to deg/hr (column 3). This data represents the gyro output integrated for 100 seconds. At the bottom of column 3 is shown the integration time of 100 seconds with a standard deviation for the 60 points of .0072 deg/hr. Column 4 shows the data integrated for 200 seconds with a standard deviation for the 30 points of 0.0042. Similarly, the data was integrated into 300 and 400 second samples. The maximum integration time was limited at 400 because longer integration times gave less than 15 samples (an arbitrary limit for a statistically valid sample size).

A plot on a log-log scale of standard deviation vs integration time allows graphical analysis of the various noise terms described above. It can be seen that from the NER equation that on a log-log plot the quantization noise has a slope of -1, the RWC noise has a slope of -1/2, and Bias instability has a slope of 0. Figure 9 shows a graphical estimation of the three errors by drawing the appropriate slope lines through the data. In order to reduce time and increase accuracy, a computer program was developed which fits the NER equation to the data. It still plots out the data and draws the appropriately sloped lines for visual confirmation of the fit to the data. Figure 10 show the computer generated lines and the

16

# Table I
### Example of Calculations for a Sigma Plot

| Data file: 06-30-91.g | | Gyro SN: B4500 | | Scale Factor: 0.3838 arc-sec/pulse | |
|---|---|---|---|---|---|
| Run Time (sec) | Gyro Output SN: B4500 (Pulses/100 sec) | Scaled to Deg/hr (deg/hr) | Summed to 200 sec/sample (deg/hr) | Summed to 300 sec/sample (deg/hr) | Summed to 400 sec/sample (deg/hr) |
| 100 | 2572 | 9.8713 | | | |
| 200 | 2571 | 9.8675 | 9.8694 | | |
| 300 | 2570 | 9.8637 | | 9.8675 | |
| 400 | 2568 | 9.8560 | 9.8598 | | 9.8646 |
| 500 | 2569 | 9.8598 | | | |
| 600 | 2564 | 9.8406 | 9.8502 | 9.8521 | |
| 700 | 2574 | 9.8790 | | | |
| 800 | 2564 | 9.8406 | 9.8598 | | 9.8550 |
| 900 | 2569 | 9.8598 | | 9.8598 | |
| 1000 | 2569 | 9.8598 | 9.8598 | | |
| 1100 | 2568 | 9.8560 | | | |
| 1200 | 2568 | 9.8560 | 9.8560 | 9.8573 | 9.8579 |
| 1300 | 2569 | 9.8598 | | | |
| 1400 | 2567 | 9.8521 | 9.8560 | | |
| 1500 | 2571 | 9.8675 | | 9.8598 | |
| 1600 | 2568 | 9.8560 | 9.8617 | | 9.8589 |
| 1700 | 2568 | 9.8560 | | | |
| 1800 | 2566 | 9.8483 | 9.8521 | 9.8534 | |
| 1900 | 2569 | 9.8598 | | | |
| 2000 | 2572 | 9.8713 | 9.8656 | | 9.8589 |
| 2100 | 2567 | 9.8521 | | 9.8611 | |
| 2200 | 2567 | 9.8521 | 9.8521 | | |
| 2300 | 2568 | 9.8560 | | | |
| 2400 | 2570 | 9.8637 | 9.8598 | 9.8573 | 9.8560 |
| 2500 | 2569 | 9.8598 | | | |
| 2600 | 2566 | 9.8483 | 9.8541 | | |
| 2700 | 2570 | 9.8637 | | 9.8573 | |
| 2800 | 2568 | 9.8560 | 9.8598 | | 9.8569 |
| 2900 | 2568 | 9.8560 | | | |
| 3000 | 2571 | 9.8675 | 9.8617 | 9.8598 | |
| 3100 | 2569 | 9.8598 | | | |
| 3200 | 2565 | 9.8445 | 9.8521 | | 9.8569 |
| 3300 | 2569 | 9.8598 | | 9.8547 | |
| 3400 | 2568 | 9.8560 | 9.8579 | | |
| 3500 | 2570 | 9.8637 | | | |
| 3600 | 2570 | 9.8637 | 9.8637 | 9.8611 | 9.8608 |
| 3700 | 2568 | 9.8560 | | | |
| 3800 | 2567 | 9.8521 | 9.8541 | | |
| 3900 | 2569 | 9.8598 | | 9.8560 | |
| 4000 | 2568 | 9.8560 | 9.8579 | | 9.8560 |
| 4100 | 2570 | 9.8637 | | | |
| 4200 | 2567 | 9.8521 | 9.8579 | 9.8573 | |
| 4300 | 2567 | 9.8521 | | | |
| 4400 | 2571 | 9.8675 | 9.8598 | | 9.8589 |
| 4500 | 2568 | 9.8560 | | 9.8585 | |
| 4600 | 2570 | 9.8637 | 9.8598 | | |
| 4700 | 2569 | 9.8598 | | | |
| 4800 | 2568 | 9.8560 | 9.8579 | 9.8598 | 9.8589 |
| 4900 | 2569 | 9.8598 | | | |
| 5000 | 2566 | 9.8483 | 9.8541 | | |
| 5100 | 2571 | 9.8675 | | 9.8585 | |
| 5200 | 2568 | 9.8560 | 9.8617 | | 9.8579 |
| 5300 | 2570 | 9.8637 | | | |
| 5400 | 2567 | 9.8521 | 9.8579 | 9.8573 | |
| 5500 | 2567 | 9.8521 | | | |
| 5600 | 2570 | 9.8637 | 9.8579 | | 9.8579 |
| 5700 | 2568 | 9.8560 | | 9.8573 | |
| 5800 | 2569 | 9.8598 | 9.8579 | | |
| 5900 | 2567 | 9.8521 | | | |
| 6000 | 2570 | 9.8637 | 9.8579 | 9.8585 | 9.8579 |
| Number of Samples | | 60 | 30 | 20 | 15 |
| Integration Time (sec) | | 100 | 200 | 300 | 400 |
| Standard Deviation (deg/hr) | | 0.0072 | 0.0042 | 0.0032 | 0.0023 |
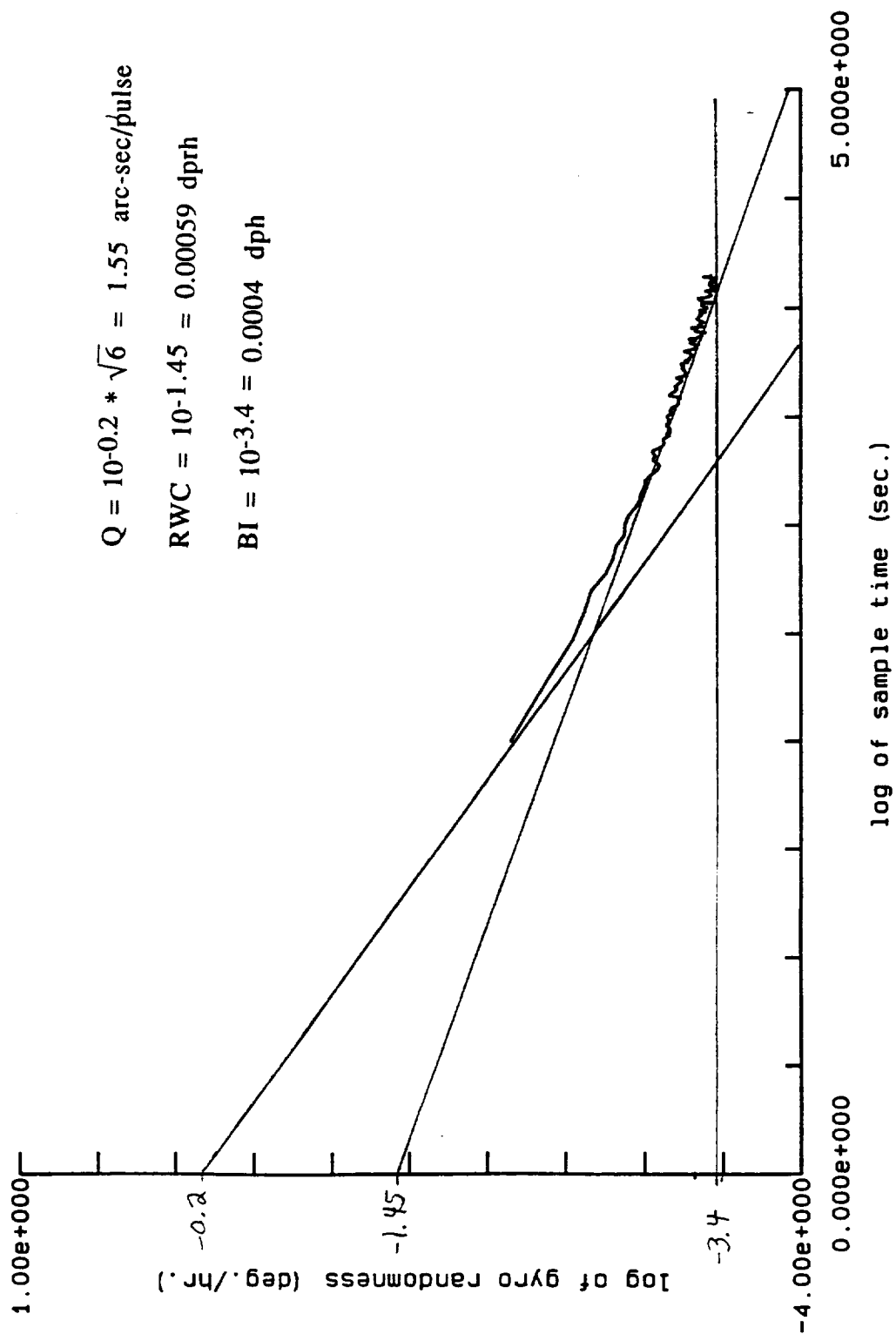
$Q = 10^{-0.2} * \sqrt{6} = 1.55$ arc-sec/pulse

$RWC = 10^{-1.45} = 0.00059$ dprh

$BI = 10^{-3.4} = 0.0004$ dph

log of sample time (sec.)

log of gyro randomness (deg./hr.)

GYRO: B2003     DATA FILE: 06-30-91.g01     07-24-91

Figure 9    Sigma Plot with Graphical Curve Fit

18

Figure 10  Sigma Plot with Computer Curve Fit

Q = 1.48 arc-sec/pulse

RWC = 0.00060 dprh

BI = 0.0002 dph

log of gyro randomness (deg./hr.)

log of sample time (sec.)

1.00e+000

-4.00e+000

0.000e+000

5.000e+000

GYRO: B2003     DATA FILE: 06-30-91.g01     07-24-91

19
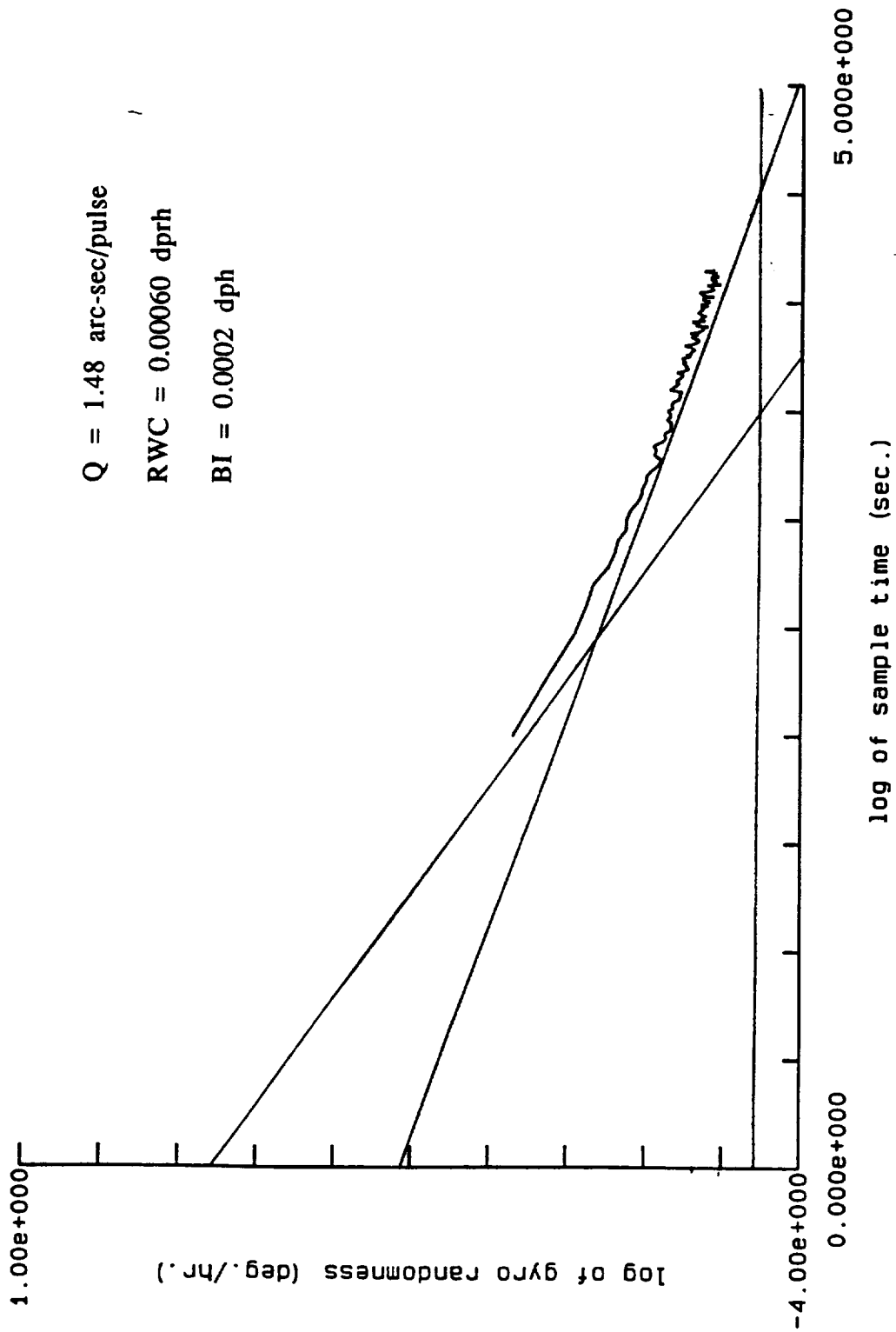
calculated values. Notice that they agree except for the bias instability value. The computer value is more accurate than the graphical analysis because the test was not long enough to graphically determine the bias instability yet the computer can still estimate the information.

## Individual Gyro Information

An RL-34 gyro is generally biased at less than 0.04 degrees per hour. This is a fixed bias magnitude which does not imply bias stability, one of the features of RLG technology. Typical RL-34 gyros have bias stabilities of less than 0.0005 dph, which is more than sufficient for the their navigational system requirements, but needs to be better for the DSN pointing application. In-run stabilities of RL-34 gyros at constant temperature have been as good as 0.00015 dph.

During the gyro evaluation, there was a unique opportunity for GSD to evaluate the RL-34 gyroscope for the DSN application. We utilized three RL-34 gyros set aside for our high-accuracy navigation systems demonstrator. These three units are representative of GSD's high accuracy RLG development. While all have been tested and accepted for our navigations system requirements, GSD felt they came close to the requirements for the DSN application.

Gyro S/N B4500 was built under last year's IR& D program and has demonstrated 0.00046 dprh random walk, with bias repeatability of less than 0.0004 dph, one sigma. The bias repeatability is the residual error left after thermal modeling over the temperature range of -55 to + 70 degrees Celsius. A significant portion of this error resides below -10 Celsius, and as such significant performance improvement is possible for a DSN application. Also note that turn-on to turn-on bias repeatability at room temperature has been shown to be within the RL-34's in-run bias stability and is less than thermal residual bias repeatability.

S/N B4500 is part of constant improvement of RLG technology, and it has capability for in-run bias stability of less than 0.0002 dph. This unit is part of our newest series of RL-34 gyros designed under IR&D funding, which have been better performers than previous RL-34 gyros built at GSD. They have lower environmental sensitivities, improved bias performance, and are more producible than previous RL-34 gyros.

Gyro S/N B2003 was built in 1989, and was evaluated at the Army MICOM laboratories, as part of our entry into RLG based land navigation systems and north finding modules. At that time, this unit demonstrated 0.0005 deg/hr bias repeatability over temperature, and 0.001 deg/rt-hr random walk coefficient. At GSD

this unit has tested to bias repeatabilities better than 0.0007 dph, and RWC of better than 0.00055 dprh. In addition, this unit has shown in-run bias stability of 0.0002 dph.

Gyro S/N Z2002 was built in 1988 under our IR& D program, and has tested at better than 0.001 dph bias repeatability over temnperature, while having a random walk of 0.00059 dprh.

These three gyros are representative of our high accuracy RLG program at GSD, and all are tested, proven performers which GSD utilized during the gyro evaluation program for DSN applications. They were installed into the ISA as listed below:

| | | |
|---|---|---|
| X gyro | SN: | B2003 |
| Y gyro | SN: | B4500 |
| Z gyro | SN: | Z2002 |

Appendix A includes plots of individual gyro data for each of the three gyros. Each of the sigma plots has been marked graphically to estimate the random walk coefficient and the in-run bias stability for each gyro. This data was previously provided to JPL under separate cover on July 10, 1991, including the actual data records on a floppy disk.

# V. Data acquisition and processing description

The standard input/output port of the navigation system used for these tests is an RS-232 serial port. The data acquisition computer used this RS-232 serial port to interrogate various system variables every 100 seconds during the course of a test. These system variables include compensated and uncompensated gyro and accelerometer outputs as well as attitude and navigation variables like roll, pitch, heading, latitude and longitude. The data acquisition computer stored all 60 system variables while providing the capability to plot up to 6 variables real time. The stored datafile names contain the date of the test and the number of tests started that day. For example 092091b.dat is the second test started on 9/20/91.

All of the detailed data analysis and plots were generated on an additional computer using a custom software package. Most of the summary data was tabulated and analyzed using either Lotus 123 or Microsoft Excel. A detailed description of the analysis will be included in the next section as the processed test data summaries are presented.

# VI. Processed test data summary records

## Initialization

The gyro bias requirements for the JPL application require the gyro biases be calibrated to <0.0001 dph. This specification was based on the need to track a target for 10 hours to within 0.001 degrees¯rather than the requirement for intialization of <0.0002 dph. The long term bias stability (months - years) will maintain this accuracy only with periodic re-calibration. A calibration procedure was designed that will allow the gyro biases to be periodically calibrated in a manner consistent with the DSN application. This procedure entails mounting the system on an indexing table or equivalent and testing at 4 different positions. From these four positions, the gyro and accelerometer biases can be determined. To evaluate if this procedure was plausible, we used it to calibrate the gyro biases. It is estimated that this 24 hr calibration procedure (6 hrs at 4 positions) will have to be performed monthly to maintain the bias requirements for the JPL application.

To calibrate the gyro biases, the table was set to 4 positions: 0, 180, 90 and 270 deg. When the rate table is set to 0 deg, the X axis of the system is North. At position 90 deg, the X axis is East. At each position, multiple 15 minute alignments were performed for over 4 hrs. The heading value at the end of each alignment was recorded. The table below summarizes the four calibration positions.

## Table II
### Calibration Data at Four Positions

| Data File | Table Azimuth Degrees | Table Azimuth Mils | System Output Mean Mils | Standard Deviation Mils | Number of Aligns |
|---|---|---|---|---|---|
| 090691b.dat | 180 | 3200 | 3200.74215 | 0.05792 | 176 |
| 090991a.dat | 360 | 6400 | 6398.79999 | 0.06929 | 26 |
| 090991b.dat | 90 | 1600 | 1600.74174 | 0.14317 | 46 |
| 091091a.dat | 270 | 4800 | 4898.81603 | 0.11603 | 18 |

To clarify this data, the calibration test performed at the 360 degree position will be examined in detail. This test was performed for over 6.5 hrs with 26 fifteen minute aligns being performed. The table below shows the heading for all 26 aligns. These aligns have a mean of 6398.800 mils with a standard deviation of 0.0693 mils, or

23

## TABLE III
### List of Azimuth at Completion of Alignment

Datafile 090991a.dat

| | | | |
|---|---|---|---|
| 1 | 6398.715 | 14 | 6398.863 |
| 2 | 6398.838 | 15 | 6398.831 |
| 3 | 6398.793 | 16 | 6398.863 |
| 4 | 6398.876 | 17 | 6398.879 |
| 5 | 6398.729 | 18 | 6398.773 |
| 6 | 6398.927 | 19 | 6398.705 |
| 7 | 6398.855 | 20 | 6398.841 |
| 8 | 6398.732 | 21 | 6398.705 |
| 9 | 6398.843 | 22 | 6398.902 |
| 10 | 6398.775 | 23 | 6398.671 |
| 11 | 6398.790 | 24 | 6398.821 |
| 12 | 6398.723 | 25 | 6398.833 |
| 13 | 6398.747 | 26 | 6398.764 |

| | | |
|---|---|---|
| Standard Dev. | 0.0693 | mils |
| MEAN | 6398.800 | mils |

0.0039 degrees. Recall that 6400 mils = 1 revolution. This datafile (090991a.dat) will be included with the raw data records.

The old bias values for the X, Y, Z gyro were -0.00388, -0.002112, and 0.00449 deg/hr, respectively. From these four calibrations runs, the bias corrections for the X and Y gyros were calculated to be +0.01075 and -0.010845, respectively. The new bias values of +0.00687 and -0.01296 (x and y, respectively) were entered and stored into the system to be used in all future tests. The Z gyro bias was not adjusted for these initialization tests since Z gyro bias errors do not affect gyro compass accuracy in these positions.

The additional advantage of this calibration procedure is its ability to determine the boresite error. The boresite error for this mounting configuration is -0.225 mils. This means that as the table is set to different azimuth positions, there will be a consistent -0.225 mils difference in the system azimuth output.

With the boresite known and the gyros biased, a test was performed to evaluate the overall gyro compass accuracy at 8 different table azimuth positions. Table IV show a summary of these tests. The last column is the azimuth system error representing the difference between the actual value and the expected value. The mean and standard deviation for the 8 azimuth errors are calculated.

## Table IV
### Summary of Gyro Compass Accuracy at 8 Positions

| Data File | Table Azimuth (degs) | Table Azimuth (mils) | System Azimuth Mean (mils) | System Azimuth 1 sigma (mils) | No of Aligns | Azimuth Error (arc-sec)* |
|---|---|---|---|---|---|---|
| 091091d.dat | 360 | 6400.0000 | 6399.75506 | 0.04638 | 11 | 4.0 |
| | 180 | 3200.0000 | 3199.79102 | 0.04608 | 11 | -3.2 |
| | 90 | 1600.0000 | 1599.74164 | 0.15098 | 25 | 6.7 |
| 091191f.dat | 270 | 4800.0000 | 4799.79106 | 0.15118 | 23 | -3.3 |
| | 315 | 5600.0000 | 5599.8117 | 0.08254 | 17 | -7.4 |
| | 135 | 2400.0000 | 2399.76465 | 0.16084 | 16 | 2.1 |
| 091291c.dat | 45 | 800.0000 | 799.75719 | 0.15622 | 24 | 3.6 |
| | 225 | 4000.0000 | 3999.83993 | 0.11582 | 23 | -13.1 |
| | | | | STD | | 6.7 |
| | | | | MEAN | | -1.3 |

* Azimuth Error = (Table Azimuth - System Azimuth Mean + Boresite) *360/6400*3600

Boresite (mils)          -0.22504

Some additional initialization tests were performed at other table azimuth positions and are summarized on table V. The overall performance was obtained by analyzing these 14 table positions and the 8 table positions shown on table 3. These 22 table positions had a mean of -0.82 arc-sec with a standard deviation of 6.1 arc-sec.

## Table V
### Summary of Additional Gyro Compass Positions

| Data File | Table Azimuth (degs) | Table Azimuth (mils) | System Azimuth Mean (mils) | System Azimuth 1 sigma (mils) | No of Aligns | Azimuth Error (arc-sec)* |
|---|---|---|---|---|---|---|
| 091391f.dat | 360 | 6400.0000 | 6399.75715 | 0.04001 | 22 | 3.6 |
| | 180 | 3200.0000 | 3199.79099 | 0.03832 | 23 | -3.2 |
| | 200.0500 | 3556.4444 | 3556.23502 | 0.0726 | 22 | -3.2 |
| | 200.1000 | 3557.3333 | 3557.13241 | 0.08962 | 22 | -4.9 |
| | 200.1500 | 3558.2222 | 3558.02457 | 0.08043 | 22 | -5.5 |
| | 200.2000 | 3559.1111 | 3558.90043 | 0.0772 | 22 | -2.9 |
| | 200.2500 | 3560.0000 | 3559.82402 | 0.07599 | 22 | -9.9 |
| | 200.3000 | 3560.8889 | 3560.71208 | 0.06746 | 22 | -9.7 |
| 092391b.dat | 360 | 6400.0000 | 6399.75317 | 0.0472 | 8 | 4.4 |
| | 0.1308 | 2.3253 | 2.08827 | 0.05194 | 11 | 2.4 |
| | 0.1336 | 2.3751 | 2.11725 | 0.05027 | 11 | 6.6 |
| | 0.1364 | 2.4249 | 2.17122 | 0.04679 | 11 | 5.8 |
| | 0.1392 | 2.4747 | 2.20722 | 0.05784 | 12 | 8.6 |
| | 0.1420 | 2.5244 | 2.29645 | 0.05182 | 12 | 0.6 |
| | | | | STD | | 6.0 |
| | | | | MEAN | | -0.5 |
| | | | For All 22 table azimuth positions | | | |
| | | | | STD | | 6.1 |
| | | | | MEAN | | -0.8 |

* Azimuth Error = (Table Azimuth - System Azimuth Mean + Boresite) *360/6400*3600

Boresite (mils)          -0.22504

The ability to calibrate the gyros in the system to < 0.0002 dph bias with the above calibration procedure did not prove completely effective the first time. The data in table IV shows the gyrocompass accuracy at 8 positions after initially calibrating the gyro biases. Note that the first four positions are a repeat of those used during the calibration. If these tests were considered to be a second calibration, the X and Y gyro biases should still be adjusted by -0.00028 and 0.0002 dph, respectively. These small bias errors remained due to the approximate equations used to calculate the gyro biases from the calibration data. Because of earlier experiments with the system software, the biases values required considerable changes (.01 dph) after the first calibration. Once the system is calibrated, the monthly changes will be much smaller in magnitude and the approximate equations will be acceptable to bias the gyros to 0.0001 dph.

Due to the limited test time available on this program, the biases were not changed and testing continued. This data was later post processed to correct for the bias errors. Table VI shows the azimuth error (from table IV & V), the correction based on the bias errors, and the corrected azimuth error. This reduced the initialization error by a factor of 2 (to 3.1 arc-sec, one sigma) showing that the system performance slightly exceeded the expected limit (see error analysis section).

Even though bias errors were included, they remained constant during the initialization portion of the tests. Table VII shows a summary of tests repeated at table position 360 and 180 degs (based on the corrected azimuth error from table VI). At the 360 deg position, the azimuth error had a standard deviation of 0.4 arc-sec over a 13 day period. Even though this standard deviation is slightly lower than expected (see error analysis section), it indicates an extremely stable gyro bias.

## Table VI
### Azimuth Error Corrected for Bias Errors

X Bias Error     -0.00028
Y Bias Error     0.0002

| Datafile | Table Azimuth (degs) | Azimuth Error* (arc-sec) | Azimuth Correction for bias Error** (arc-sec) | Corrected Azimuth Error*** (arc-sec) |
|---|---|---|---|---|
| 091091d.dat | 360.00 | 4.00 | 3.63 | 0.37 |
|  | 180.00 | -3.20 | -3.63 | 0.43 |
|  | 90.00 | 6.70 | 5.08 | 1.62 |
| 091191f.dat | 270.00 | -3.30 | -5.08 | 1.78 |
|  | 315.00 | -7.40 | -1.03 | -6.37 |
|  | 135.00 | 2.10 | 1.03 | 1.07 |
| 091291c.dat | 45.00 | 3.60 | 6.16 | -2.56 |
|  | 225.00 | -13.10 | -6.16 | -6.94 |
| 091391f.dat | 360.00 | 3.60 | 3.63 | -0.03 |
|  | 180.00 | -3.20 | -3.63 | 0.43 |
|  | 200.05 | -3.20 | -5.15 | 1.95 |
|  | 200.10 | -4.96 | -5.15 | 0.19 |
|  | 200.15 | -5.50 | -5.16 | -0.34 |
|  | 200.20 | -2.90 | -5.16 | 2.26 |
|  | 200.25 | -9.90 | -5.16 | -4.74 |
|  | 200.30 | -9.70 | -5.17 | -4.53 |
| 092391b.dat | 360.00 | 4.40 | 3.63 | 0.77 |
|  | 0.1308 | 2.40 | 3.64 | -1.24 |
|  | 0.1336 | 6.60 | 3.64 | 2.96 |
|  | 0.1364 | 5.80 | 3.64 | 2.16 |
|  | 0.1392 | 8.60 | 3.64 | 4.96 |
|  | 0.1420 | 0.60 | 3.64 | -3.04 |
|  | STD | 6.08 |  | 3.09 |
|  | MEAN | -0.82 |  | -0.40 |

\* From table IV & V
\*\*Azimuth Correction =Table_pos -
         ATAN((11.37*SIN(Table_Pos)+ybias)/(11.37*COS(Table_Pos)+Xbias))
\*\*\* Corrected Azimuth Error = Azimuth error - Azimuth Correction

## Table VII
## Summary of Repeated Alignment Tests

| Datafile | Corrected azimuth error * Table Azimuth Position (arc-sec) | |
|---|---|---|
| | 360 | 180 |
| 091091d.dat | 0.37 | 0.43 |
| 091391f.dat | -0.03 | 0.43 |
| 092391b.dat | 0.77 | |
| Standard Dev. | 0.40 | ---- |

* From table VI

### Error Analysis of Initialization tests

The initialization is a gyrocompass operation where the two level gyros (Gyro X and Gyro Y) are used to measure the horizontal component of Earth's rate. The Azimuth angle is equal to the arctan(GyroY/GyroX). Depending on length of time spent gyro compassing, the accuracy will improve and can be predicted from the NER for each gyro. A propagation of error analysis can predict the uncertainty in azimuth based on the NER of the X and Y Gyro. This was done in Table VIII.

Since there was a substantial difference between the RWC of the X and Y gyros, the uncertainty in azimuth should vary depending on which gyro is primarily used to gyrocompass. Table VIII shows the predicted uncertainty in azimuth as of function of azimuth. There is fair agreement with actual system azimuth uncertainties. Note that table azimuth positions 360 and 180 show a lower noise than the 90 and 270 azimuth positions. This is because at the 360/180 positions, the gyrocompass is dominated by the Y gyro. At the 90/270 positions, the gyro compass is dominated by the X gyro. Since the Y gyro has lower noise in 15 minute samples then the X gyro, the gyrocompass noise is lower at the 360/180 positions compared to the 90/270 positions. Future tests were initialized near 360 table azimuth to take advantage of the reduced noise in this orientation.

## Table VIII
### Initialization Error Based on Gyro Noise Model

|  | Gyro X | Gyro Y |
|---|---|---|
| Quantization Noise (arc-sec)*** | 1.2 | 1.2 |
| RWC (dprh)*** | 0.0008 | 0.0003 |
| Bias Instability (dph)*** | 0.0002 | 0.0002 |
|  |  |  |
| NER for 15 minute alignment time | 0.00170 | 0.00083 |

| Table Azimuth | Uncertainty in Azimuth Predicted* (Mils) | Actual** (Mils) |
|---|---|---|
|  | Mils |  |
| 360 | 0.074 | 0.046 |
| 180 | 0.074 | 0.046 |
| 90 | 0.152 | 0.151 |
| 270 | 0.152 | 0.151 |
| 315 | 0.120 | 0.083 |
| 135 | 0.120 | 0.161 |
| 45 | 0.120 | 0.156 |
| 225 | 0.120 | 0.116 |

Horizontal Earth's Rate (dph) at BGSD Latitude = 11.37 deg/hr
*Predicted = ((SigmaX*SIN(table))^2+(SigmaY*COS(table))^2)^0.5
*180/PI()*3600/ERH/3600/360*6400
** From Table IV
*** Based on sigma plot analysis with system in current configuration

The above analysis also predicts what the ultimate gyrocompass accuracy will be for longer gyrocompass times. The gyro noise for time periods longer than 4-6 hrs is dominated by the bias stability of the gyro. If a 0.0002 dph bias stability and 0.0003 dprh RWC gyro is used to gyrocompass for 6 hrs, the expected gyro and azimuth noise are 0.00023 dph and 4.2 arc-sec, respectively. Taking another look at the data on table VI shows there is fair agreement to the actual data. The "Azimuth Error" shows a 6.1 arc-sec noise (sigma) and the "Corrected Azimuth Error" shows a 3.1 arc-sec noise. Both of these numbers are close to the expected azimuth noise with the "Corrected Azimuth Error" even slightly better than expected.

## System turn on and off repeatability test

The system was locked at table position 3200 mils (south) and tested for on-off repeatability. The system was turned off for 24 hrs in between each turn on as required in the statement of work. During the turn on periods, gyro compass data was recorded for 8 hrs and the mean value calculated. The results were :

> 1st turn on and system heading : 3200.830 mils
> system off for 24 hrs
> 2nd turn on and system heading : 3200.852 mils
> system off for 24 hrs
> 3rd turn on and system heading : 3200.845 mils

This data shows that the system has excellent repeatability with a 2.3 arc-sec 1 sigma.

## Initialization Testing Conclusion

The statement of work's objective for initialization translates to an accuracy of 3.7 arc-sec (0.0002 deg/hr bias error at BGSD latitude). When the data is post processed to remove the remaining small bias errors, the initialization results yield 3.1 arc-sec, 1 sigma. This indicates that the two gyros whose input axes lie in the level plane clearly have bias stabilities < 0.0002 deg/hr. It further indicates the potential of the BGSD RL-34 RLG-based pointing system to initialize to within the 0.001 degree angular objective.

31

## Blind Acquisition Testing

The first series of acquisition tests were 20 degree azimuth rotations at 0 degree elevation. In this test series, the experiments were conducted by rotating the air-bearing azimuth table from either east-to-west or west-to-east for exact 20 degree angles at various rotation rates of 0.5 deg/sec, 0.2 deg/sec, 0.07 deg/sec, and 0.05 deg/sec rates as required by the statement of work.

The test data was recorded in the form of system heading, pitch and roll information. The objective was to compare the system heading raw data before and after 20 degrees air-table rotation. The azimuth error was defined as any heading deviation from 20 degrees rotation as shown below:

$$Azimuth\ error = Abs.Value\{heading1 - heading2\} - 20\ degrees$$

where heading 1 is the system heading reading before the 20 degrees rotation and heading 2 is the system heading reading after 20 degrees rotation.

The system information is updated every 100 seconds with our current data acquisition design and no attempt was made to change the system readout software for instant update after rotation.

A summary of these test results is given in Table IX, showing one sigma azimuth error as a function of azimuth rotation rate. The one sigma of these measurements clearly demonstrated that the system error is a function of rotation rate. This is consistent with the theoretical noise equivalent angle (NEA) model as predicted in the NEA equation (see the ring laser gyro noise section).

In addition to the theoretical NEA error, there was an air-bearing oscillation problem at the end of table rotation when the table was rotated at low rotation rates. By hand locking the table at the end of rotation, the table oscillation problem was eliminated and the one sigma of the measurement was improved from 3.02 arc-sec to 2.29 arc-sec which represented an improvement of 25%.

Table  IX

| rotation rate :<br>0.5 deg/sec | | rotation rate :<br>0.2 deg/sec | | rotation rate :<br>0.07 deg/sec | | hand locked the table<br>at end of rotation<br>rotation rate:<br>0.05 deg/sec | |
|---|---|---|---|---|---|---|---|
| system pointing<br>error (arc-sec) | | system pointing<br>error (arc-sec) | | system pointing<br>error (arc-sec) | | system pointing<br>error (arc-sec) | |
| E-W | -0.75 | E-W | 1.99 | E-W | 1.19 | E-W | 1.79 |
|  | 0.41 |  | 0.99 |  | 3.35 |  | 4.51 |
|  | 0.21 |  | 0.79 |  | 3.93 |  | 3.09 |
|  | -0.75 |  | 0.99 |  | -2.71 |  | 0.01 |
|  | 0.79 |  | 0.79 |  | -4.27 |  | -1.93 |
|  | 0.23 |  | 1.39 | W-E | 1.8 |  | 0.03 |
|  | 0.81 |  | 0.01 |  | 2.57 |  | 0.03 |
|  | 0.61 | W-E | 1.19 |  | -1.91 |  | 0.99 |
|  | 0.81 |  | -0.75 |  | -3.29 |  | 2.17 |
|  | -0.37 |  | -0.17 |  | 0.41 |  | 1.39 |
|  | -0.17 |  | -1.55 |  | 3.35 | W-E | -3.89 |
| W-E | -1.93 |  | -2.33 |  | 5.31 |  | -2.91 |
|  | -1.73 |  | -1.55 |  |  |  | -4.53 |
|  | -1.15 |  | -2.15 |  |  |  | -0.77 |
|  | -1.35 |  | -2.13 |  |  |  | 1.57 |
|  | -0.37 |  | 0.01 |  |  |  | -1.33 |
|  | -0.55 |  | -0.75 |  |  |  | -1.15 |
|  | -0.57 |  |  |  |  |  | 2.53 |
|  | -0.35 |  |  |  |  |  | -1.73 |
|  | -0.57 |  |  |  |  |  | -0.95 |
|  | -0.37 |  |  |  |  |  |  |
| MEAN | -0.34 |  | -0.19 |  | 0.81 |  | -0.05 |
| SIGMA | 0.78 |  | 1.34 |  | 3.02 |  | 2.29 |

**Table  IX :** Summary of target acquisition test results for 20 deg azimuth rotation at 0 deg elevation. The data is given as system pointing errors resulting from 20 deg azimuth rotation. In both rotation directions, east-to-west(E-W)and west-to-east(W-E), there is no significant difference in the pointing errors. The near "zero" mean value of these measurements shows that the system input vertical axis is well aligned with the rotation axis of air-bearing table.

In all these tests, the near "zero" mean value suggests that the system vertical axis is well aligned with rotation axis of air-bearing table and the test data also indicates that there is no significant difference between east-to-west and west-to-east rotation directions. Further analysis of the test results by removing the known table error showed the true system error is only 0.55 arc-sec. for the rotation rate of 0.5 deg/sec. This compares favorably with the statement of work objective of 0.36 arc-sec.

$$\sigma^2_{measured} = \sqrt{2}\,\sigma^2_{system} + \sqrt{2}\,\sigma^2_{az\text{-}table}$$

$$\sigma_{az\text{-}table} = 0.36 \text{ arc-sec.}$$
$$\sigma_{measured} = 0.78 \text{ arc-sec}$$
$$\sigma_{system} = 0.55 \text{ arc-sec}$$

## Compound Angle Acquisition Tests

To demonstrate the system repeatability in the blind target acquisition mode, we decided to conduct the tests at the worst case scenario by rotating the system 20 degrees in air-bearing table to simulate the azimuth rotation and +/- 60 degrees in Ultradex table to simulate the elevation rotation for northern and southern hemispheres. One of great strengths of a ring laser gyro is the inherent precision scale factor with no apparent upper rotation rate limitations. And the gyro often shows the scale factor is better than 1 ppm from near zero rotation rate to 2 revolutions/sec.

The blind target acquisition requirement for this Deep Space Network (DSN) gyro evaluation is 0.36 arc-sec accuracy over 20 degrees rotation which corresponds to a gyro scale factor linearity of 5 ppm. This is a "relative easy target" to meet in a ring laser gyro based navigation system except where there is a short time duration. The gyro angular resolution(Least Significant Bit or LSB) limits the angular accuracy that can be achieved in short time intervals(see previous discussion of noise equivalent angle). The RL-34 gyro based system used in our tests has an LSB resolution of 0.38 arc-sec/pulse, meaning a one pulse error is the entire budget for this test series.

Fortunately the LSB of the gyro is only limited by how we sample the gyro analog output. For the purposes of present production navigators, the existing 0.38 arc-sec sampling works acceptably. However, we recognized that space and ground based pointing applications require Bendix to improve our current RL-34 resolution. We developed circuitry in early 1991 that modifies the RL-34 resolution from 0.38 arc-sec/pulse to 0.05 arc-sec/pulse which will be able to meet the DSN pointing requirements (see Recommended Alternatives to Improve Performance Section)

All the test results were recorded as a system outputs of heading, pitch and roll. The system data is updated every 100 sec and data is compared between the system reading before moving and after moving for both heading and pitch. The repeatability of the test is presented as an azimuth error and pitch error. The definition of these errors are given as the following:

34

*Azimuth error= AbsValue{heading1-heading2} - 20 deg - mean value*

*Elevation error= AbsValue{pitch1-pitch2}- 60 deg - mean value*

where heading1 is the system heading reading before the rotation operation and the heading2 is the system heading reading after the rotation operation, and the same is true for the system pitch reading.

Table X showed a typical compound angle acquisition test results. The data recorded as system's heading, roll and pitch in the unit of mils. The compound angle was made by rotating air-bearing table 20 degs and Ultradex table +60 degs. In Table X, the delta heading is the absolute value of heading difference before and after rotations minus 20 deg azimuth rotation, and the azimuth error is by removing the mean value generated in the delta heading. Similar mathematical operation is also applied to the pitch data to generate the elevation error, then, the overall system pointing error is plotted in both azimuth and elevation errors as shown in Figure 13 and Figure 14.

The mean value represents a constant misalignment/boresite artifact that was removed in the post processing. When the rate table and Ultradex were installed, they were leveled and aligned to true North as previously described. When the navigation system was mounted onto the rate table/Ultradex, no fine adjustments were provided to mechanically align the system input axis to the rotation axis of table/Ultradex, thereby creating a fixed mean value in angle which would need to be removed later.

During the initialization and initial acquisition tests (with only azimuth rotations), the data was corrected for the azimuth boresite. This was straightforward since the azimuth boresite error was a constant value with no cross coupling terms. This was expected since the rate table was leveled to within several arc-sec. As the table was rotated, the rotation was truly about system azimuth (remember the system azimuth is defined as the angle from North in a level plane).

TABLE X

| TEST POINTS | HEADING MILS | DELTA HEADING ARC-SEC | AZIMUTH ERROR ARC-SEC | ROLL MILS | PITCH MILS | DELTA PITCH ARC-SEC | ELEVATION ERROR ARC-SEC |
|---|---|---|---|---|---|---|---|
| 1 | 5866.43 | | | -0.88 | -0.08 | | |
| 2 | 6222.59 | 123.22 | -1.01 | -0.43 | 1066.62 | 7.51 | -0.30 |
| 3 | 5866.43 | 122.43 | -1.80 | -0.87 | -0.08 | 7.30 | -0.51 |
| 4 | 6222.61 | 125.40 | 1.17 | -0.42 | 1066.63 | 8.88 | 1.07 |
| 5 | 5866.44 | 124.01 | -0.22 | -0.87 | -0.08 | 7.89 | 0.08 |
| 6 | 6222.62 | 125.20 | 0.97 | -0.42 | 1066.63 | 7.40 | -0.41 |
| 7 | 5866.44 | 124.61 | 0.38 | -0.87 | -0.08 | 7.16 | -0.65 |
| 8 | 6222.62 | 124.80 | 0.57 | -0.42 | 1066.63 | 6.92 | -0.89 |
| 10 | 5866.45 | 123.62 | -0.61 | -0.87 | -0.08 | 7.40 | -0.40 |
| 11 | 6222.62 | 124.41 | 0.18 | -0.42 | 1066.63 | 8.99 | 1.18 |
| 12 | 5866.45 | 124.61 | 0.38 | -0.87 | -0.08 | 8.64 | 0.84 |
| | MEAN SIGMA | 124.23 0.87 | | | | 7.81 0.72 | |

**TABLE X:** Typical compound angle acquisition test results. The data was recorded as system's heading, roll and pitch in the unit of mils as a result of repeating compound rotation of 20 deg azimuth and +60 deg elevation. For the first test point, the system box is located at air-bearing table 350 deg and Ultradex table 0 deg. The second test point is for system box located at air-bearing table 330 deg and Ultradex table +60 deg. The third test point was repeated at the same location as the first test point, and so on for the rest of test points.

During the initialization and initial acquisition tests (with only azimuth rotations), the data was corrected for the azimuth boresite. This was straightforward since the azimuth boresite error was a constant value with no cross coupling terms. This was expected since the rate table was leveled to within several arc-sec. As the table was rotated, the rotation was truly about system azimuth (remember the system azimuth is defined as the angle from North in a level plane).

The more complicated problem to be post-processed was the effect that boresite errors have on azimuth, elevation, and roll with an Ultradex elevation(i.e. target acquisition). Since the rotation axis of the Ultradex is not coincident with the pitch axis of the system, as the Ultradex was rotated, a component of that rotation was coupled into the system azimuth and roll. Figures 11 & 12 show the system azimuth and elevation errors versus Ultradex elevation. These errors were caused by the inability to mechanically align the system to the

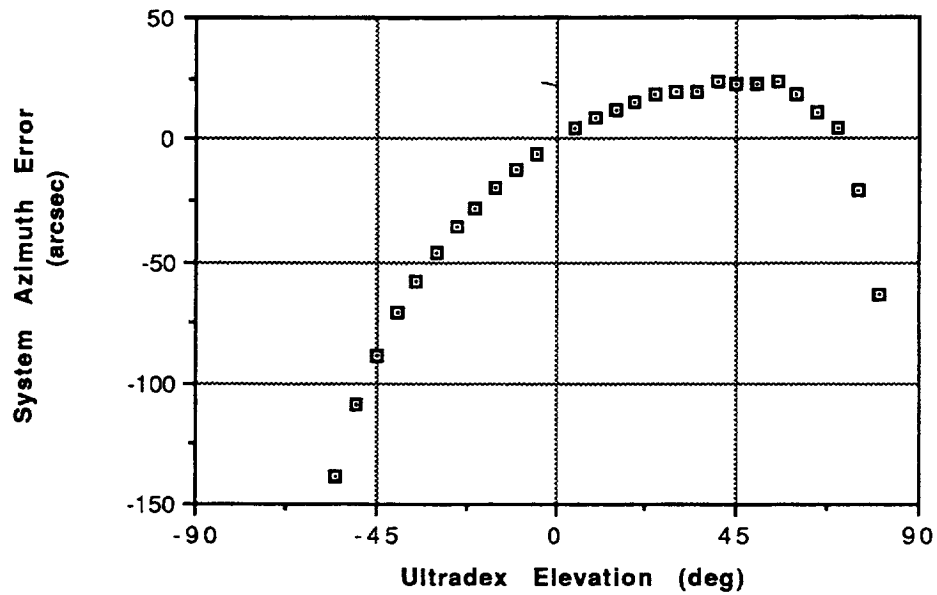**Error Between System Azimuth and Table Azimuth during Ultradex Elevation Changes**



Figure 11        Azimuth Error Due to Boresite Errors

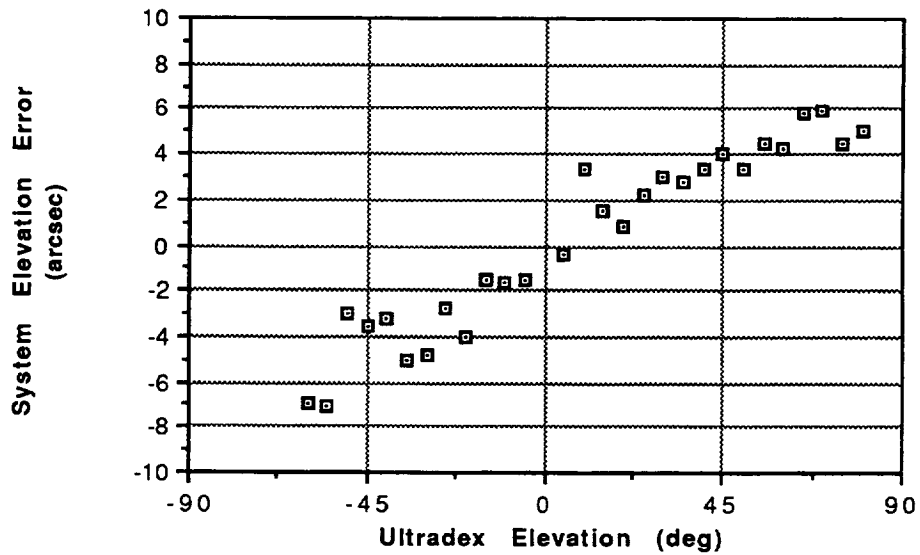**Error Between System Elevation and Ultradex Elevation**



Figure 12        Elevation Error Due to Boresite Errors

37

air-bearing table/Ultradex. When the system was rotated to a rate table azimuth and Ultradex elevation, the system reads out a certain attitude. When the system was re-initialized at this position, the system still read out the same attitude. The system's ability to locate attitude was very repeatable throughout the testing.

To use this system for the final DSN pointing application, the above results indicate that an alignment between the antenna and the system must be performed. There are two options which will solve this problem. Mechanical adjustments can be provided to allow alignment of the system to the antenna or a transformation matrix can be developed that will transform the system coordinate system to the antenna coordinate system. Both options require additional investigation to determine which is best suited for the DSN pointing application. Since the target acquisition data showed that the system has excellent repeatability, then with proper adjustments either in mechanical alignment or transformation matrix operation the final result will have no impact to the DSN application.

Blind Acquisition Test Conclusions:

The results of these tests are shown in Figure 13 and Figure 14 for air-bearing table rotation rates of 0.5 deg/sec and 0.2 deg/sec respectively. A circle of 6-sigma of DSN specification(0.36 arc-sec* 6) represents a target of interest. Within 27 tests, 11 times the system reached the target which indicated the possibility is better than 40% with a rotation rate of 0.5 deg/sec and the possibility reduced as the rotation rate decreased as shown in Figure 14 (10/35 reach the target). Faster rotation rates and lower angular quantization(e.g. 0.05 arc-sec) will improve these results to within the desired values.

The data also suggested that the system had more error in heading(azimuth) than in pitch(elevation) and this can be explained by the fact that the system pitch is bounded by the Schuler loop but not the system heading(see appendix B). The test results are also tabulated in Table XI, where the RSS is defined as a root-sum-square of azimuth error and elevation error. By separating the errors between the table and the true system error, we found the true system RSS error is in order of 0.77 arc-sec for the best case and 1.14 arc-sec for a typical result.
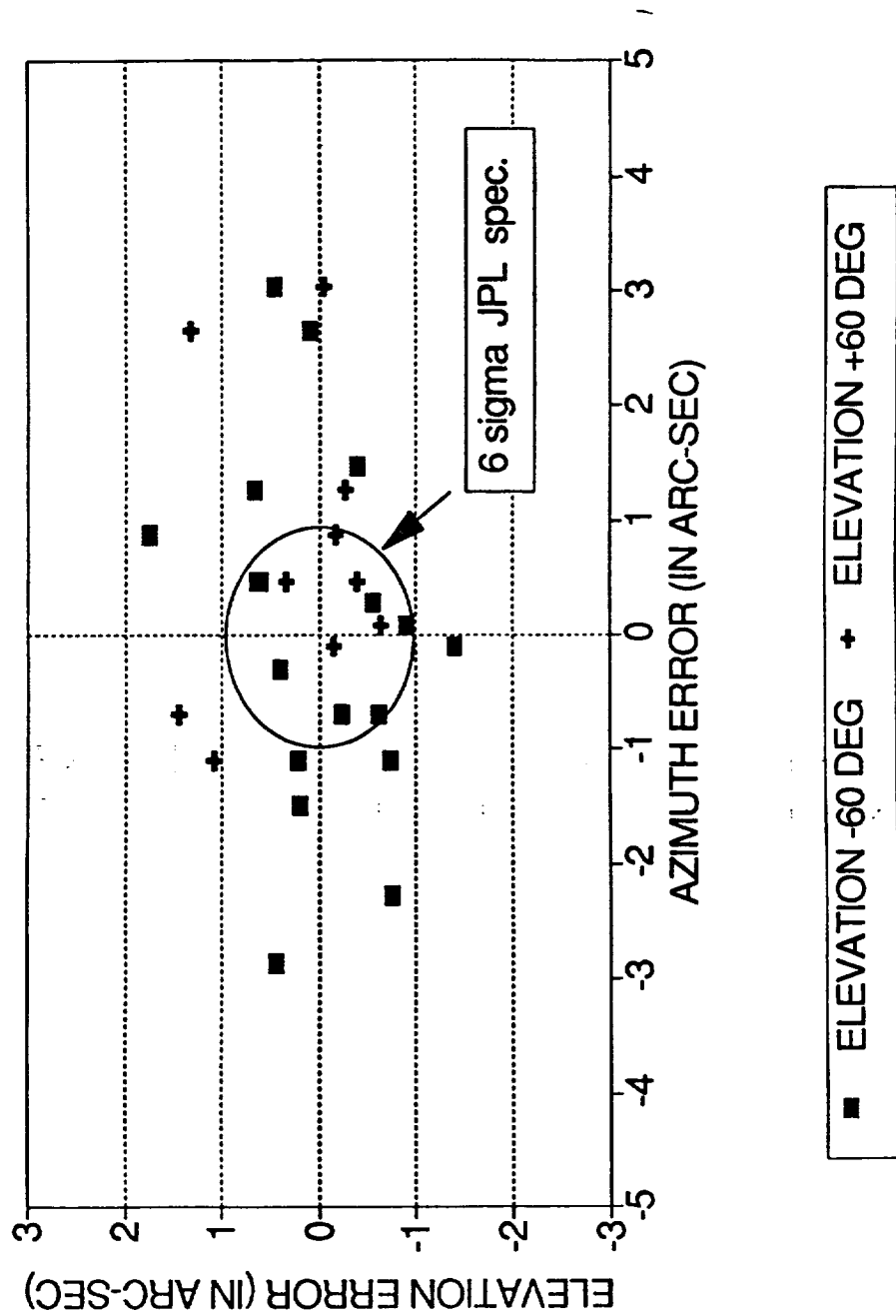
The test results of blind target acquisition after 20 deg air-bearing table rotation and +/- 60 deg of elevation. The results showed the repeatability of the system measurement as a functions of position errors in both azimuth and pitch directions. In this test, the air-bearing rotation rate is 0.5 dps.

Figure 13    Blind Target Acquisition Test Results at 0.5 dps
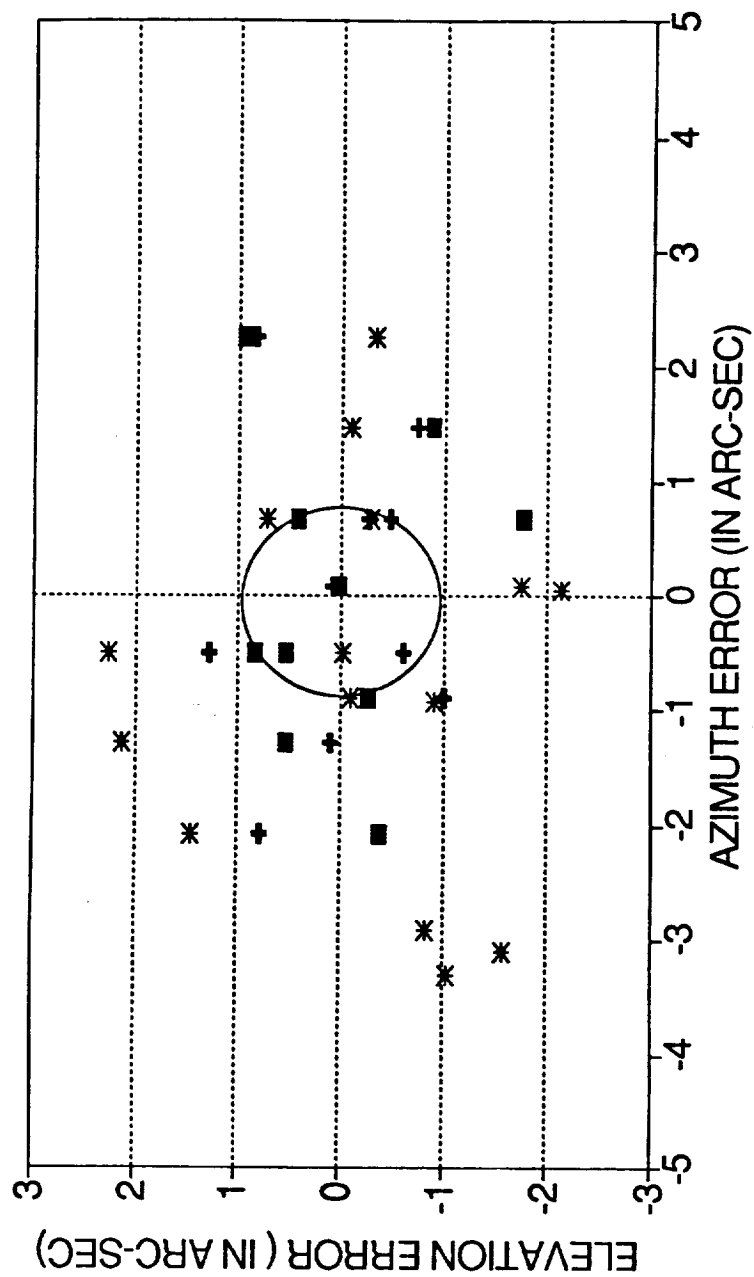
Figure 14    Blind Target Acquisition Test Results at 0.2 dps

The same test as Figure 13 but at lower air-bearing rotation rate of 0.2 dps.

40

TABLE XI

| FILES | TABLE (DEG) | ELEVATION (DEG) | HEADING MEAN VALUE (ARC-SEC) | SIGMA (ARC-SEC) | PITCH MEAN VALUE (ARC-SEC) | SIGMA (ARC-SEC) | RSS (ARC-SEC) | ROTATION RATE (DEG/SEC) |
|---|---|---|---|---|---|---|---|---|
| 101191A | 0--340 | -60 | -74.6 | 1.5 | 11.03 | 0.73 | 1.67 | 0.5 |
| 101191D | 350--330 | -60 | -71.3 | 1.2 | 10.44 | 0.81 | 1.49 | 0.2 |
| 101191C | 350--330 | 60 | 124.2 | 0.9 | 0.72 | 0.72 | 1.13 | 0.5 |
| 101191E | 350--330 | 60 | 123.6 | 2.3 | 2.3 | 2.3 | 2.41 | 0.2 |
| 101191F | 350--330 | 60 | 127.5 | 2.5 | 1.3 | 1.3 | 2.83 | 0.2 |

**TABLE XI** : Summary of compound angle target acquisition test results for a combination of 20 deg azimuth rotation and +/- 60 deg elevation rotation. The data is given as one sigma of measurement error in both heading (azimuth) and pitch (elevation) directions.

Acquisition Test Error sources

The measurement errors presented in the Figure 13 and Figure 14 are a total error which is a combination of apparent table error and true system error. The table error was measured during the table calibration and the RSS table error between the air-bearing table and the Ultradex table is given as:

$$\sigma_{table} = \sqrt{\sigma^2_{az-table} + \sigma^2_{ultradex}} = .55 \text{ arc-sec.}$$

The relationship between the true system error and the measured error (RSS) for the best case shown in Table X file 101191C is given as :

$$\sigma^2_{measured} = \sqrt{2}\, \sigma^2_{system} + \sqrt{2}\, \sigma^2_{table}$$

$$\sigma_{measured} = 1.13 \text{ arc-sec.}$$

$$\sigma_{system} = 0.77 \text{ arc-sec.}$$

It is quite clear that we have demonstrated a true system

41

error of 0.77 arc-sec RSS for combination of azimuth and elevation errors. However, for a typical blind target acquisition measurement the true system error is on the order of 1.14 arc-sec RSS. Again, it is important to note that faster rotation rates and decreased gyro quantization will reduce this error to within the objective of 0.36 arc-seconds.

From our previous sigma analysis, the values of quantization error, random walk and in-run bias stability were 1.2 arc-sec, 0.0003 deg/rt-hr, 0.0002 deg/hr, respectively, and the calculated NEA for our gyro is on the order of 0.52 arc-sec which is in fair agreement with our best case result of 0.77 arc-sec.

By breaking down the error components in the NEA equation, it is quite easy to realize that the gyro quantization error is the dominant error source in our blind target acquisition operation. By improving the gyro quantization error to 0.05 arc-sec, we can make a great impact in this measurement. A quick calculation shows that the improved NEA shall be on the order of 0.18 arc-sec which is better than the stated objective.

The NEA equation also explains why the one sigma of the measurement is larger at low rotation rates. At low rotation, it requires more time to complete the 20 degree rotation so that the gyro random walk error term starts to contribute as a square root of time and eventually dominates the error term. It is therefore helpful to move the antenna as fast as possible, so that the system resolution is limited by quantization error and this error is fairly independent of rotation rate.

### Inertial Sensor Assembly Orientation Stability

Since the system is mounted on 8 elastomeric isolators, there is some concern about the mechanical alignment of isolators in the high elevation orientation. To initially test the mechanical stability of the isolators, we elevated the system to 40 degrees and used a theodolite to measure any possible angular changes. The test results showed no significant change in angle in this setup which implied that the system mechanical stability is better than one arc-sec. However, in cold start up conditions, when the system is gradually warming up, we observed system changes in pitch and small offsets in heading. The measured results are given in Table XII, and the system temperature warm up profile is shown in Figure 15. The sagging stops when the system reaches thermal equilibrium and since most of our tests are conducted in thermal equilibrium and level, this finding had no effect on our measured results. This mechanical instability is only present during a cold start up, therefore it will have no impact on the DSN application.

TABLE XII

| | SYSTEM START UP | | OVERNIGHT SYSTEM WARM UP | |
|---|---|---|---|---|
| | theodolite readout azimuth (in arc-sec) | pitch | theodolite readout azimuth (in arc-sec) | pitch |
| | 0 | -1 | -2 | -5 |
| | -1 | 0 | -3 | -6 |
| | 0 | -1 | -3 | -6 |
| | 1 | 0 | -2 | -7 |
| | -2 | 1 | -3 | -4 |
| | 0 | 0 | -3 | -5 |
| | 0 | -1 | -6 | -6 |
| | 0 | 2 | -4 | -6 |
| | 1 | 0 | -4 | -8 |
| | -1 | 0 | -3 | -7 |
| MEAN | -0.2 | 0 | -3.3 | -6 |
| SIGMA | 0.92 | 0.94 | 1.16 | 1.15 |

**TABLE XII** : Inertial Sensor Assembly Stability Measurements. The system box was elevated at an angle of -30 degrees and azimuth and pitch were recorded. The instability between the cold start up and overnight warm up were 6 arc-sec and 3.1 arc-sec, in pitch and azimuth directions, respectively. The temperature warm-up profile is shown in Figure 15.

43
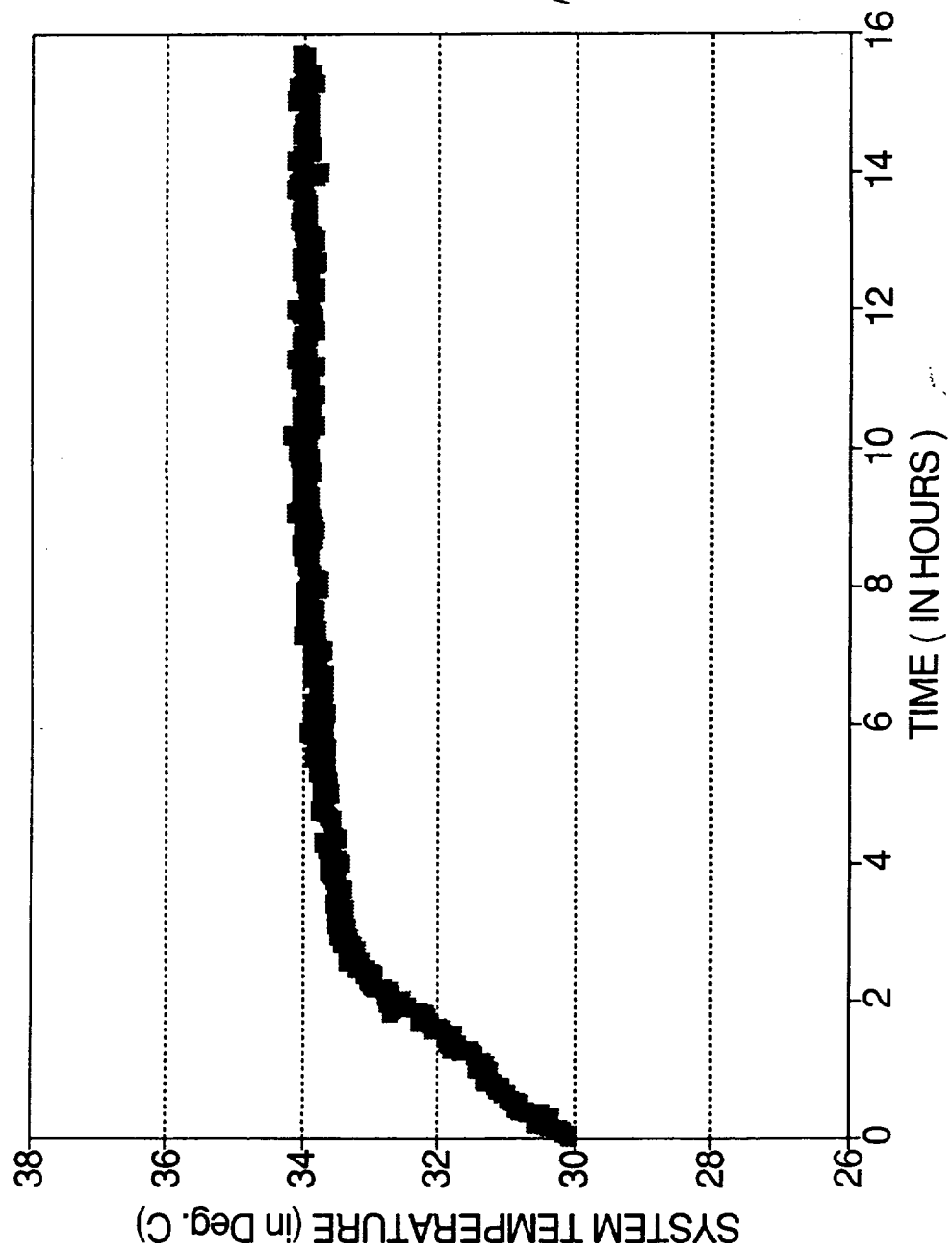
The system warm up temperature profile as a function of time.

Figure 15    System Temperature Warm Up

## Target Tracking Tests

Once the target is acquired, the goal is to track within 0.001 degrees (3.6 arc-sec), rms, for 10 hours. To evaluate the system's ability to track a target, the system was held stationary on the rate table. Any change in system attitude output was an error since the actual attitude of the system was not changing (other than small changes due to the isolator temperature sensitivities described earlier). The system maintained this constant attitude by transforming the inertial inputs from the gyros and accelerometers to a fixed Earth coordinate system. This essentially removes Earth's rate from the gyro inputs and gravity from the accelerometers.

## Calibration

Previously during the initialization testing, the X and Y gyro biases were determined with the calibration procedure. At the time, the Z gyro bias was not changed because it did not affect the initialization testing. The Z gyro bias errors only affect the azimuth output during the 10 hr tracking tests. Upon starting the tracking tests, an acquisition software error was found that limited the length of the tracking test that could successfully be performed. While debugging this problem, these short tracking tests were analyzed and a Z gyro bias error was observed. The bias was changed 4 times over this 2 day period and the table below shows these changes.

Table XIII
Z gyro bias changes made during
acquisition software corrections
(deg/hr)

| Old Bias | Correction | New Bias |
|----------|------------|----------|
| 0.00449 | 0.00450 | 0.00899 |
| 0.00899 | 0.00200 | 0.01099 |
| 0.01099 | 0.00200 | 0.01299 |
| 0.01299 | -0.00150 | 0.01149 |

At this point, a weekend test was set up to execute multiple 10 hr tracking tests. These tests comprise the first 6 tracking tests (datafile: 092091a.dat and 092591b.dat). These tests all showed a Z gyro bias error of about 0.0009 deg/hr. It was realized that a complete re-calibration should be performed before any additional tracking tests were run. At this point various other experiments were performed, including the acquisition tests.

On 10/4/91, a Friday, a calibration test was performed over the weekend in preparation for some additional tracking tests. The actual test was about 24 hours long, 6 hrs at the four positions (0, 90, 180, 270). The data is shown in below.

## Table XIV

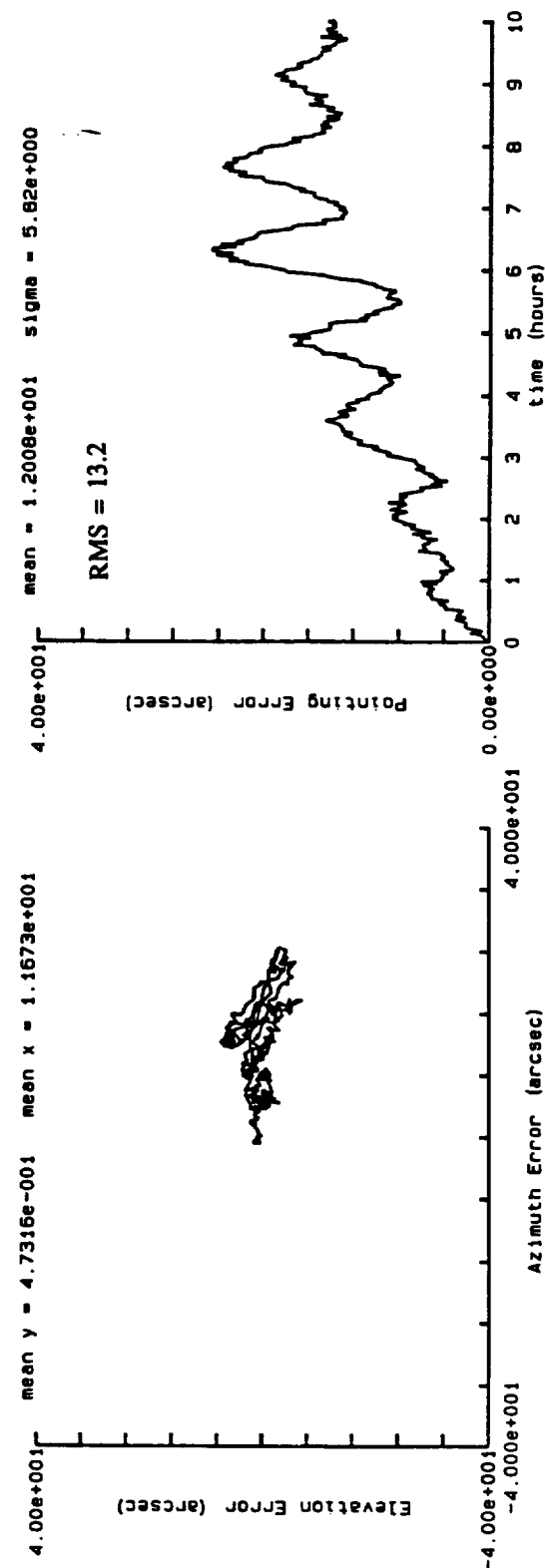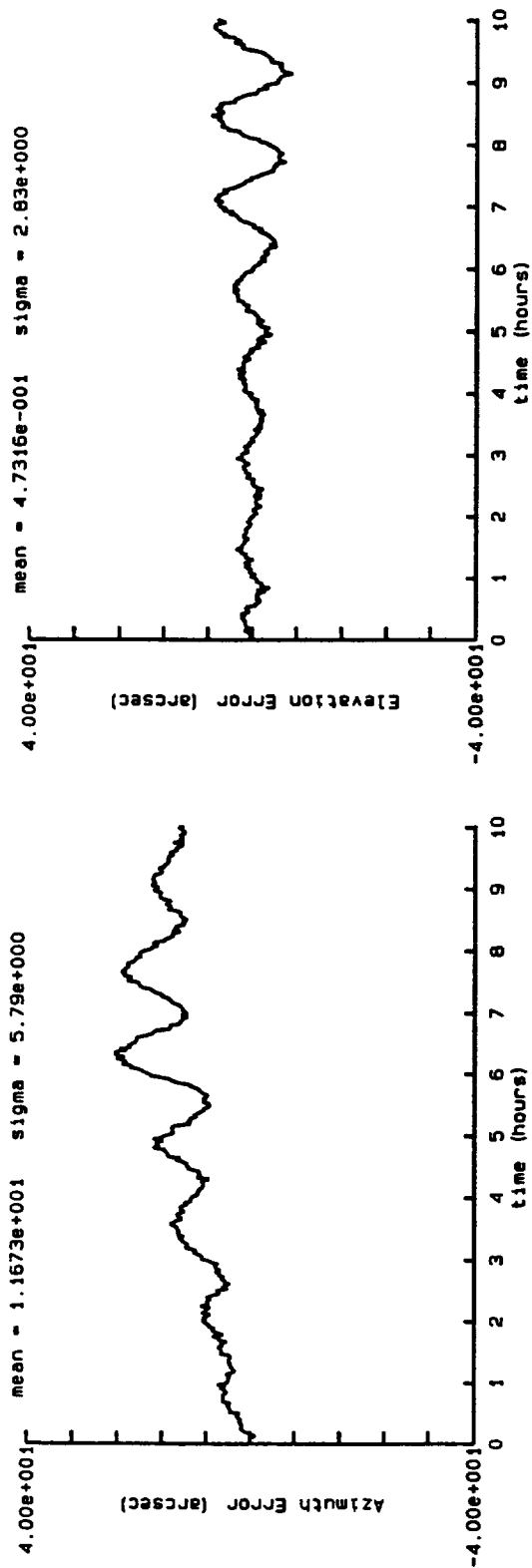| Data File | Table Azimuth Degrees | Table Azimuth Mils | System Output Mean Mils | Standard Deviation Mils | Number of Aligns |
|---|---|---|---|---|---|
| 100491e.dat | 180 | 3200 | 3199.86725 | 0.03291 | 17 |
| | 360 | 6400 | 6399.70531 | 0.04676 | 16 |
| | 90 | 1600 | 1599.59889 | 0.18183 | 17 |
| | 270 | 4800 | 4799.99072 | 0.12124 | 16 |

From this data, the X and Y bias corrections were changed for the first time since the initialization testing. Also, the Z gyro bias was calculated by knowing that the RSS of all three gyros must equal Earth's rate. The changes are -.00219, -.00090, and -0.00124 deg/hr resulting in a final bias of 0.00468, 0.01385 and 0.01273 deg/hr for gyros X, Y and Z, respectively. A tracking test was performed and a small (0.00036 deg/hr) bias error was still present for the Z gyro. This was corrected by changing the Z gyro bias to 0.01309 deg/hr. The last six tracking tests all had the same bias values.

Tracking Test Results

A total of 12 tracking tests were performed to evaluate the system's performance. After the first 6 tests, the system was re-calibrated as described above. Figure 16 shows a typical test and figure 17 is the best of the 12 tests (after re-calibration). These plots show the azimuth, elevation and pointing errors versus time and azimuth error versus elevation error. The pointing error was calculated by taking the RSS of the azimuth error and elevation error. The overall performance of each test was determined by taking the RMS of the pointing error. The plots of the other 10 tests are included in Appendix C.

Table XV summarizes the results for all 12 tracking tests. The first 8 tests were performed at 0 deg azimuth and 0 deg elevation. The ninth test performed incorporated all three phases of testing for the DSN application. An initialization was done (340 deg azimuth and 0 deg elevation) and was followed by a blind target acquisition

page 1

mean = 1.1673e+001     sigma = 5.79e+000

Azimuth Error (arcsec)

4.00e+001

-4.00e+001

0    1    2    3    4    5    6    7    8    9    10
time (hours)

mean = 4.7316e-001     sigma = 2.83e+000

Elevation Error (arcsec)

4.00e+001

-4.00e+001

0    1    2    3    4    5    6    7    8    9    10
time (hours)

mean y = 4.7316e-001     mean x = 1.1673e+001

Elevation Error (arcsec)

4.00e+001

-4.00e+001

-4.000e+001                    4.000e+001
Azimuth Error (arcsec)

mean = 1.2008e+001     sigma = 5.82e+000

RMS = 13.2

Pointing Error (arcsec)

4.00e+001

0.00e+000

0    1    2    3    4    5    6    7    8    9    10
time (hours)

DATA FILE: 092091a.1          Tracking Data with a RMS Pointing Error of 13.2 arc-sec

Figure 16     Tracking Test (typical)

47

page 1
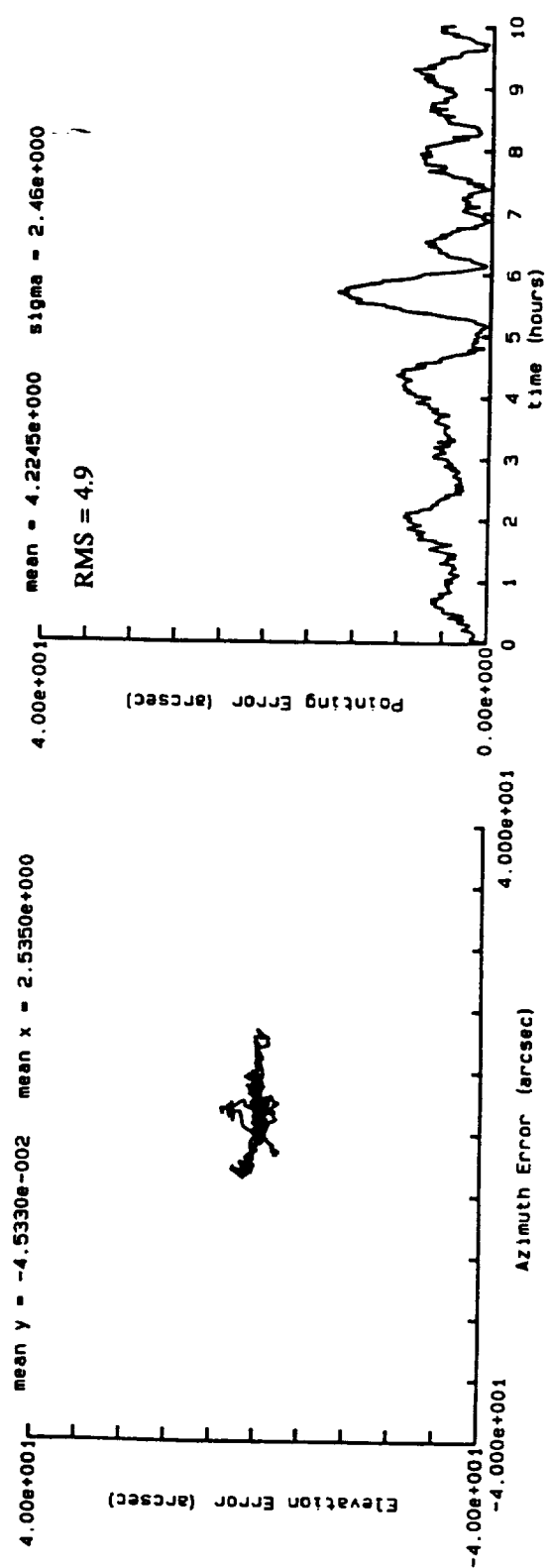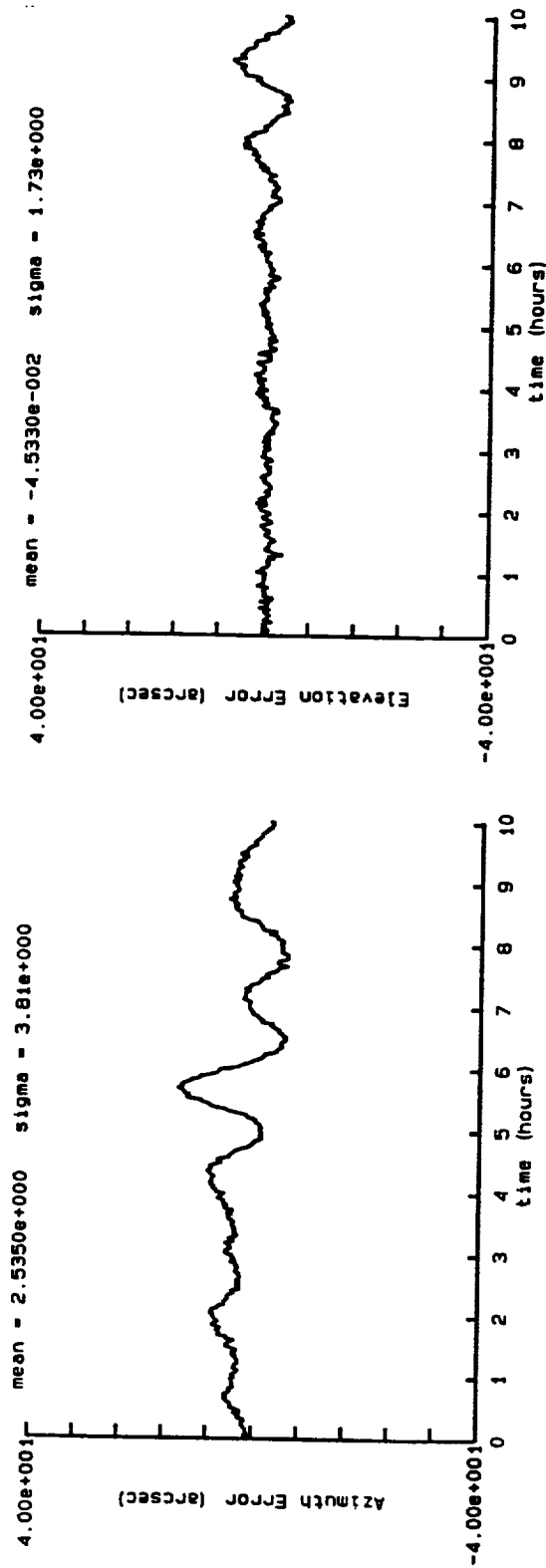
Best Tracking Data after Re-calibration with a
RMS Pointing Error of 4.9 arc-sec

Figure 17    Tracking Test (best)
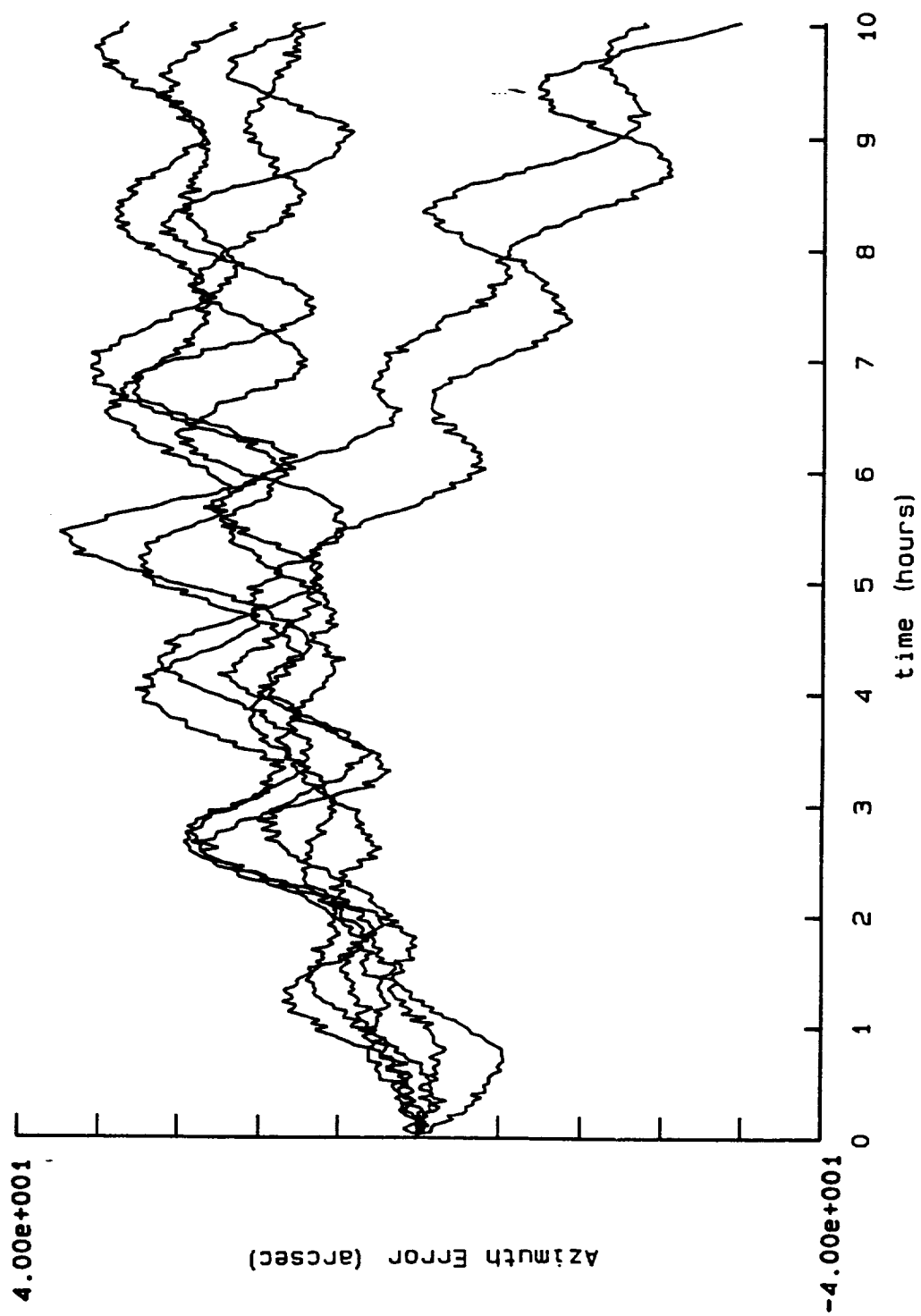
DATA FILE: 100891b.2

48

(20 deg. rotation & 60 deg. elevation change), which was followed by a 10 hr tracking test. The last 3 tests were initialized at 60 deg elevation followed by a 10 hour tracking test.

Table XV

| Tracking Error RMS Values (arcsec) | | | | |
|---|---|---|---|---|
| All value in arc-sec | | | | |
| Datafile | RMS of | RMS of | RMS of | Test  Description |
| | Azimuth Error (arc-sec) | Elevation Error (arc-sec) | Pointing Error (arc-sec) | |
| 092091a.dat | 13.0 | 2.9 | 13.2 | Aligned and tracked at 0 deg heading/0 deg elevation |
| | 17.6 | 4.4 | 17.8 | " |
| | 20.1 | 1.7 | 19.9 | " |
| | 12.4 | 4.0 | 12.8 | " |
| | 18.7 | 3.6 | 18.8 | " |
| 092591b.dat | 13.6 | 2.1 | 13.6 | " |
| | | | | Recalibrated |
| 100891b.dat | 10.8 | 2.7 | 11.2 | Aligned and tracked at 0 deg heading/0 deg elevation |
| | 4.6 | 1.7 | 4.9 | " |
| 100991b.dat | 11.2 | 3.8 | 11.8 | Aligned at 340 deg heading, 0 deg elevation, tracked at 0 deg heading, 60 deg elevation |
| | 17.2 | 3.0 | 17.4 | Aligned and tracked at 0 deg heading, 60 deg elevation |
| 101091a.dat | 10.4 | 3.7 | 11.0 | Aligned and tracked at 0 deg heading, 60 deg elevation |
| | 12.9 | 3.9 | 13.5 | Aligned and tracked at 0 deg heading, 60 deg elevation |
| Average | 13.5 | 3.1 | 13.8 | |
| Minimum | 4.6 | 1.7 | 4.9 | |
| Maximum | 20.1 | 4.4 | 19.9 | |

The first 6 tracking tests displayed characteristics of the consistent azimuth gyro (Z gyro) bias error. Figure 18 shows an overlay of the azimuth errors for the first 6 tests. Note that for the first 6 hrs all the azimuth errors increased, indicating an uncorrected gyro bias (about 0.0009 deg/hr). After this time other errors start to appear (coupled variables) and the error analysis is not straightforward. Computer analysis and modeling could be performed to model the cause of these longer time period errors.

As described earlier, the system was recalibrated before the last 6 tests. The next two tests showed that the calibration was successful and the dominant Z gyro bias error was removed. Figure 19 shows an overlay of azimuth errors for these two tests. Note that there is no initial increase in the azimuth error as previously evident in Figure 18 These two tests showed lower RMS values compared to the previous 6 tests that had a Z gyro bias error. The first 6 tests had a mean RMS pointing error of 16 arc-sec while the latter two tests had a mean RMS pointing error of 8 arc-sec. Though this is

49

page 1



DATA FILE: 092591b, 092091a

Figure 18    Overlay of Azimuth Tracking Errors for 1st 6 tests

50

page 1

Azimuth Error (arcsec)

4.00e+001

-4.00e+001

time (hours)

0 1 2 3 4 5 6 7 8 9 10
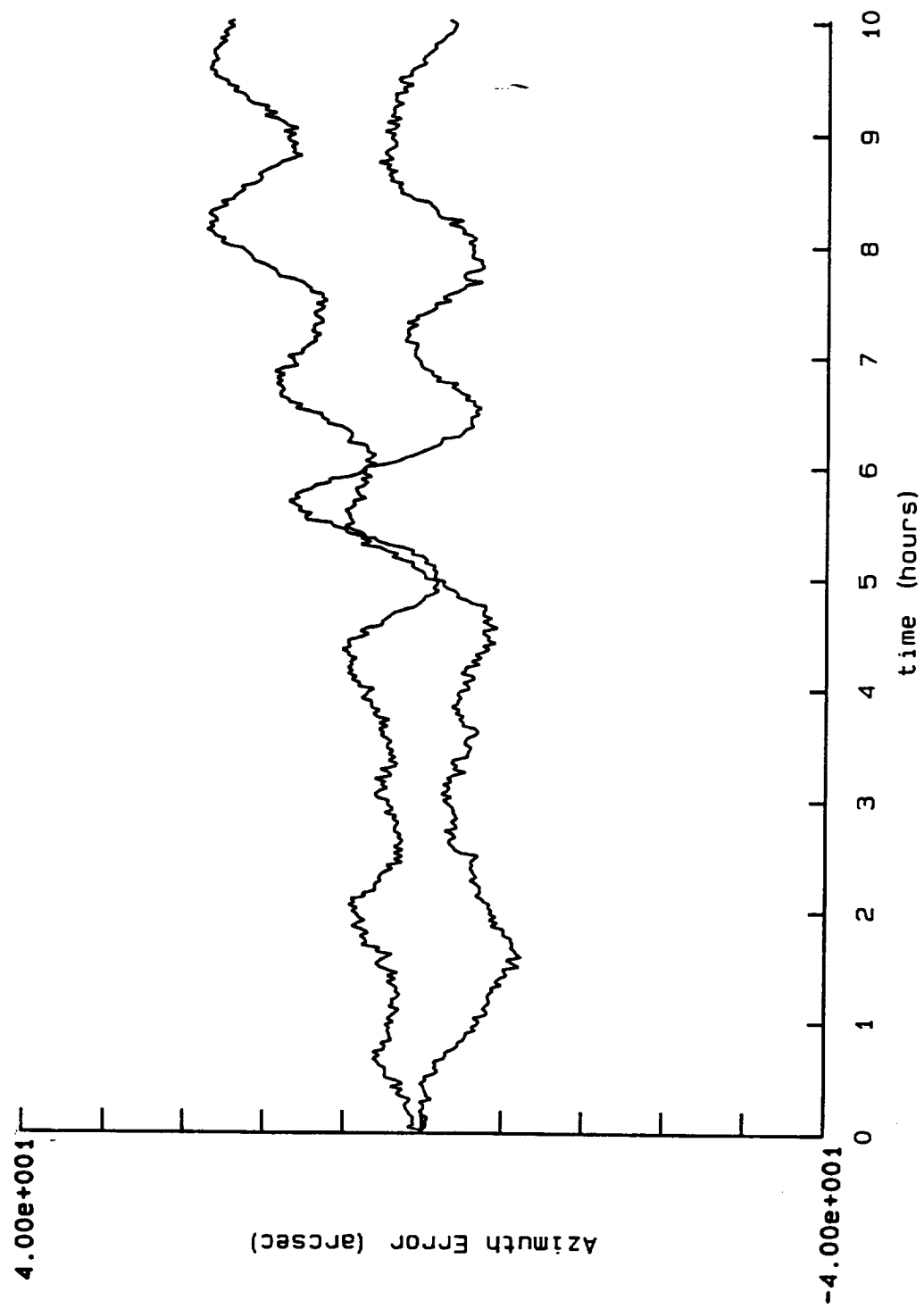
DATA FILE: 100891b.2

Figure 19    Azimuth Tracking Errors post Recalibration

51

based on only two tracking runs (20 hours of data), this 8 arc-sec RMS value is a better representation of the system's overall capability.

The last 4 tracking tests were all performed at 60 deg elevation. At a non-zero elevation, a combination of two gyro outputs ( X and Z) principally determine the azimuth reading. The 4 tests did not show any indications of gyro bias errors (the azimuth error did not drift consistently), but they did have accelerometer errors (large Schuler oscillations on the azimuth error). Figure 20 shows the azimuth errors for these 4 tests. Note the larger Schuler oscillations caused by accelerometer errors. The RMS error for these tests has a mean of 13.5 arc-sec. As will be discussed in the future recommendation section, pseudo-g computations should reduce the Schuler oscillations and the data should approach the expected 8 arc-sec value.

All of the previous tracking discussions were concerned with the azimuth error. The elevation error is consistently lower due to the stable Schuler oscillations that bound the error (see appendix B). The elevation RMS pointing error currently meets the goal of 3.6 arc-sec/10 hrs. Table XV also shows the distribution of pointing errors between azimuth and elevations.
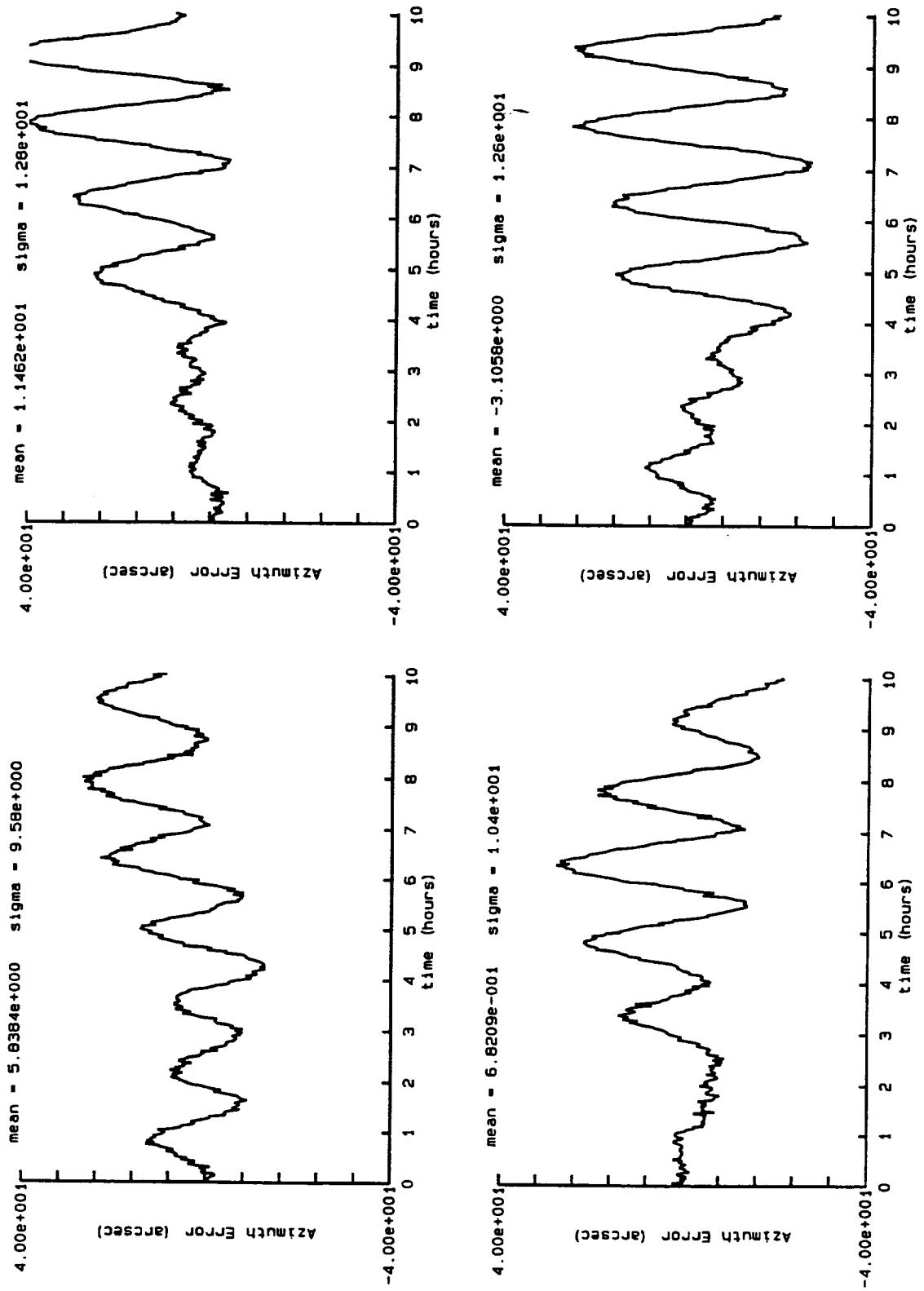
Error Analysis for Tracking

Given gyros that have 0.0003 deg/rt-hr RWC, and 0.0002 deg/hr bias stability, a noise limited prediction calculation can be made for the system. The NER and NEA for a 10 hour test will be 0.00022 dph and 7.9 arc-sec 1 sigma, respectively. The data obtained during the 2 tracking tests after calibration confirmed this with a mean RMS value of 8 arc-sec.

RMS Error vs Time

JPL personnel requested the test result be analyzed to show the RMS pointing error as a function of time. To do this, the n runs of m points each were applied to the following equation:

$$\text{RMS vs Time}_i = \sqrt{\frac{\sum_{j=1}^{n} (\text{Run } j)_i^2}{n}} \qquad \text{where } i = 1...m$$

52

page 1

mean = 5.8384e+000   sigma = 9.58e+000

mean = 6.8209e-001   sigma = 1.04e+001

mean = 1.1462e+001   sigma = 1.28e+001

mean = -3.1058e+000   sigma = 1.26e+001

Figure 20   Azimuth Tracking Errors at 60 deg Elevation

DATA FILE: 101091a.2

53

The 12 tracking tests were separated into four groups:

1) Figure 21 has runs 1-6 (datafile 092091a.dat - 092591b.dat), which are the tests prior to final, fine bias adjustments, showing the lesser performance of 0.006 degrees at 10 hours.

2) Figure 22 has runs 7-12 (datafile 100891b.dat), which are all tests after final, fine bias adjustments, including multiple motions. Note that the error for the first 4 hours was less than 0.002 degrees, and that this includes run #9 which had the entire worst case angular acquisition motion. With smaller accelerometer errors, the Schuler oscillations would decrease, resulting in this graph being near 0.003 degrees pointing error at 10 hours.

3) Figure 23 has runs 7-8 (datafile 100991b.dat - 101091a.dat), which are the two identical tracking tests after final, fine bias adjustments, indicating a 0.002 degree performance past 5 hours, and 0.00425 degrees error at 10 hours. With smaller accelerometer errors, the Schuler oscillations would decrease, changing this graph to nearly 0.003 degrees pointing error at 10 hours.

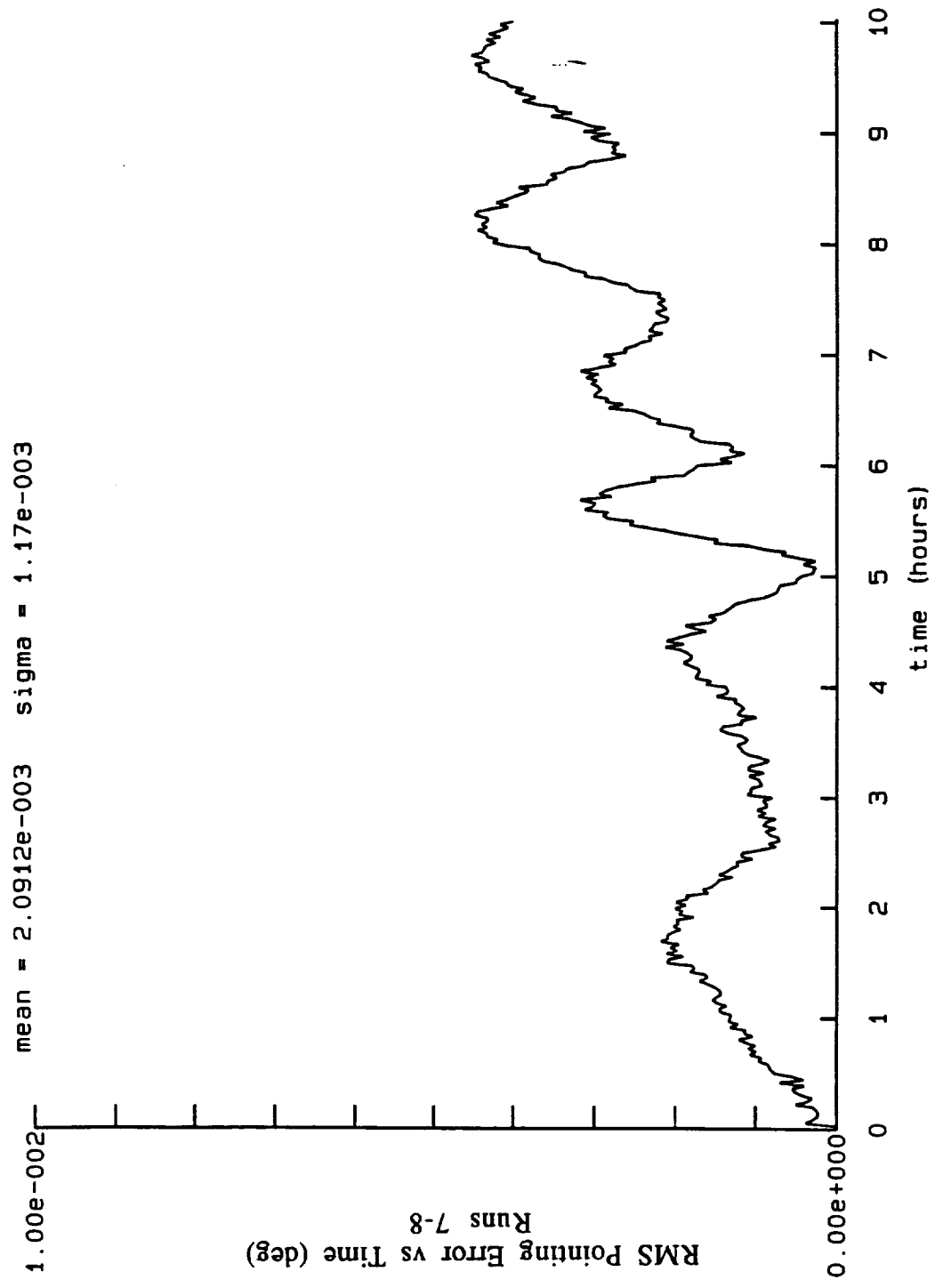4) Figure 24 has runs 1 -12 (all tracking tests), showing overall test results at about 0.006 degrees.
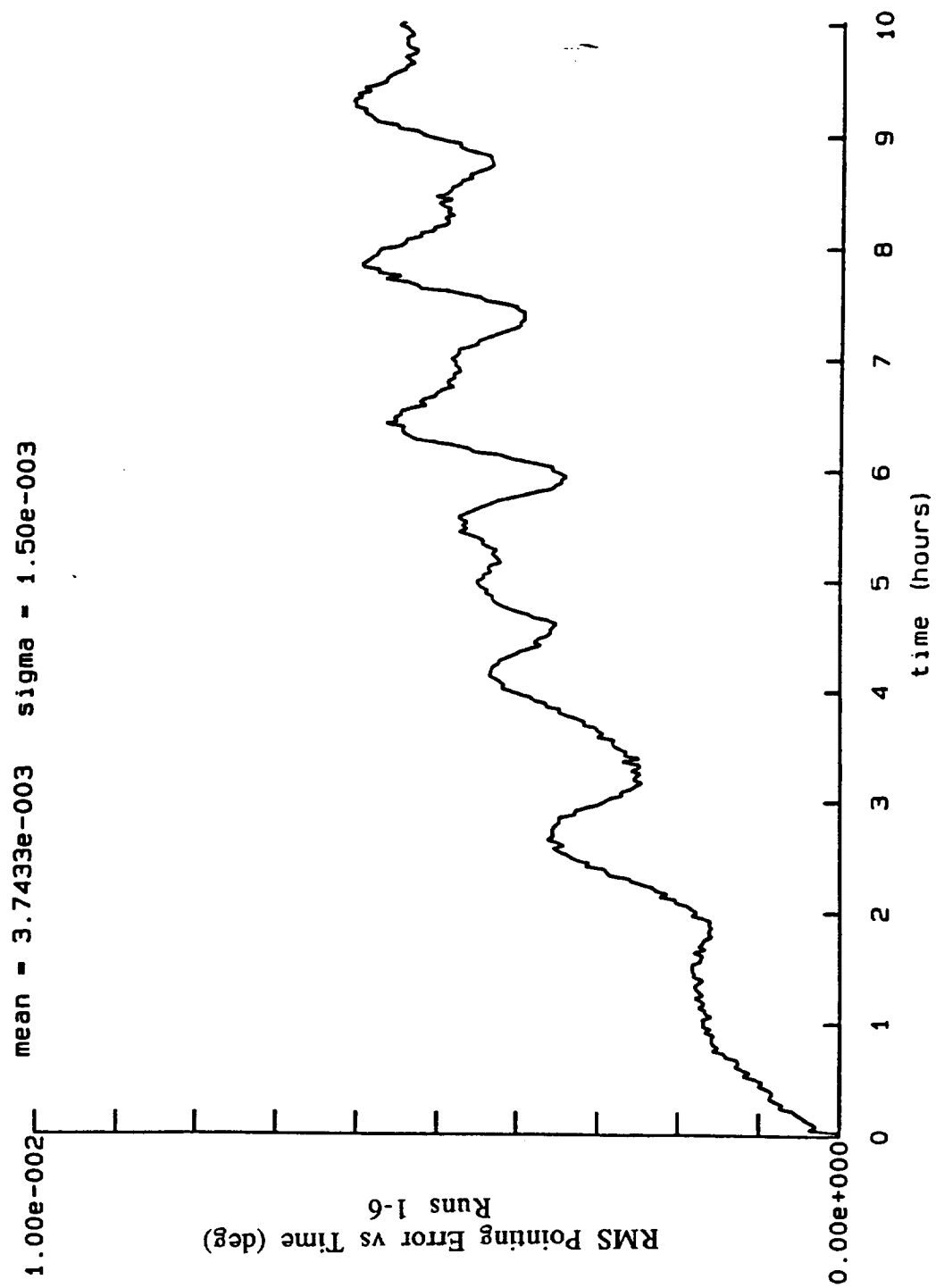
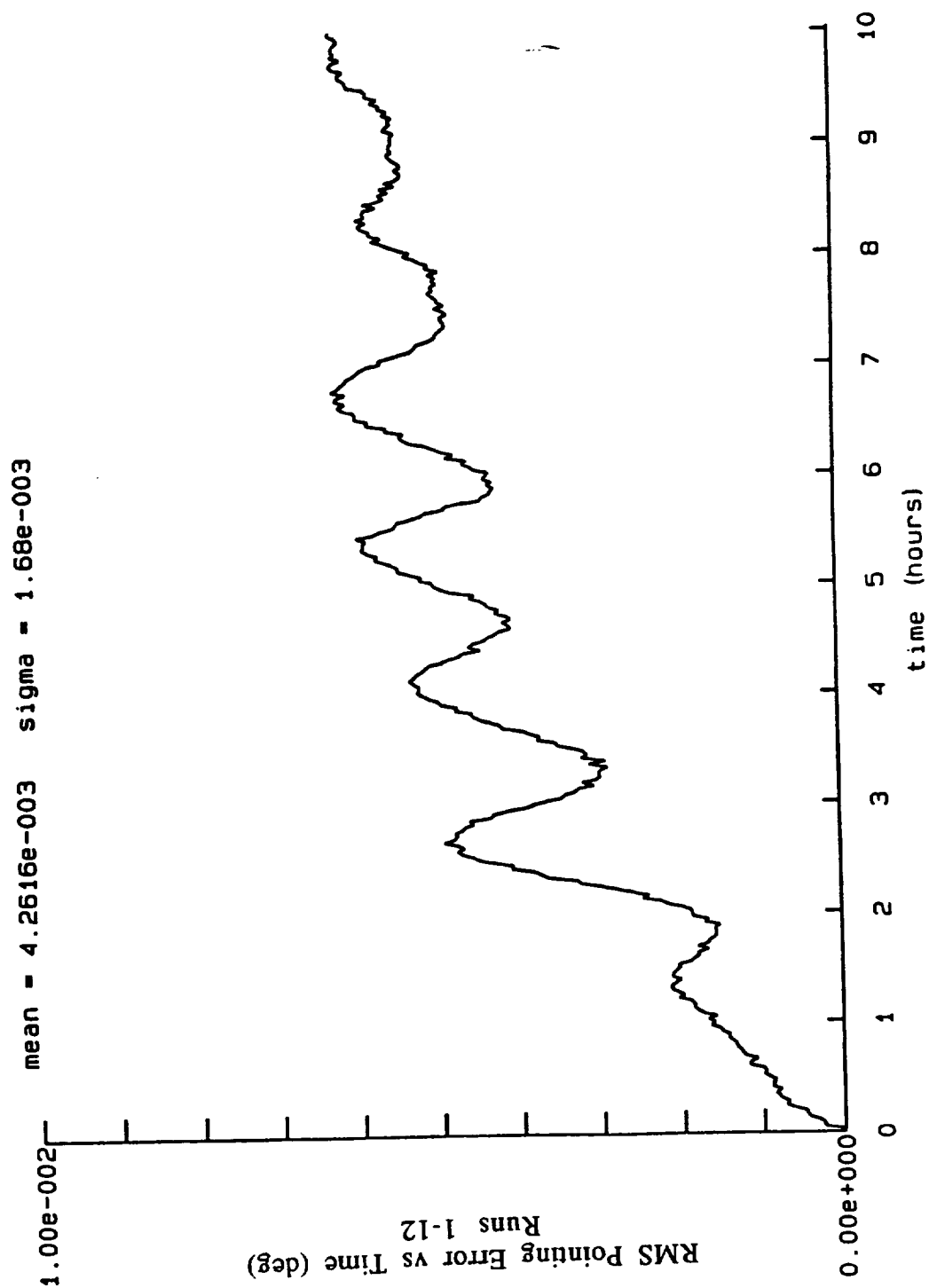Figure 21    RMS Pointing Error vs Time for Runs 1-6

11-07-91

55

mean = 3.0263e-003   sigma = 1.54e-003

RMS Pointing Error vs Time (deg)
Runs 7-12

time (hours)
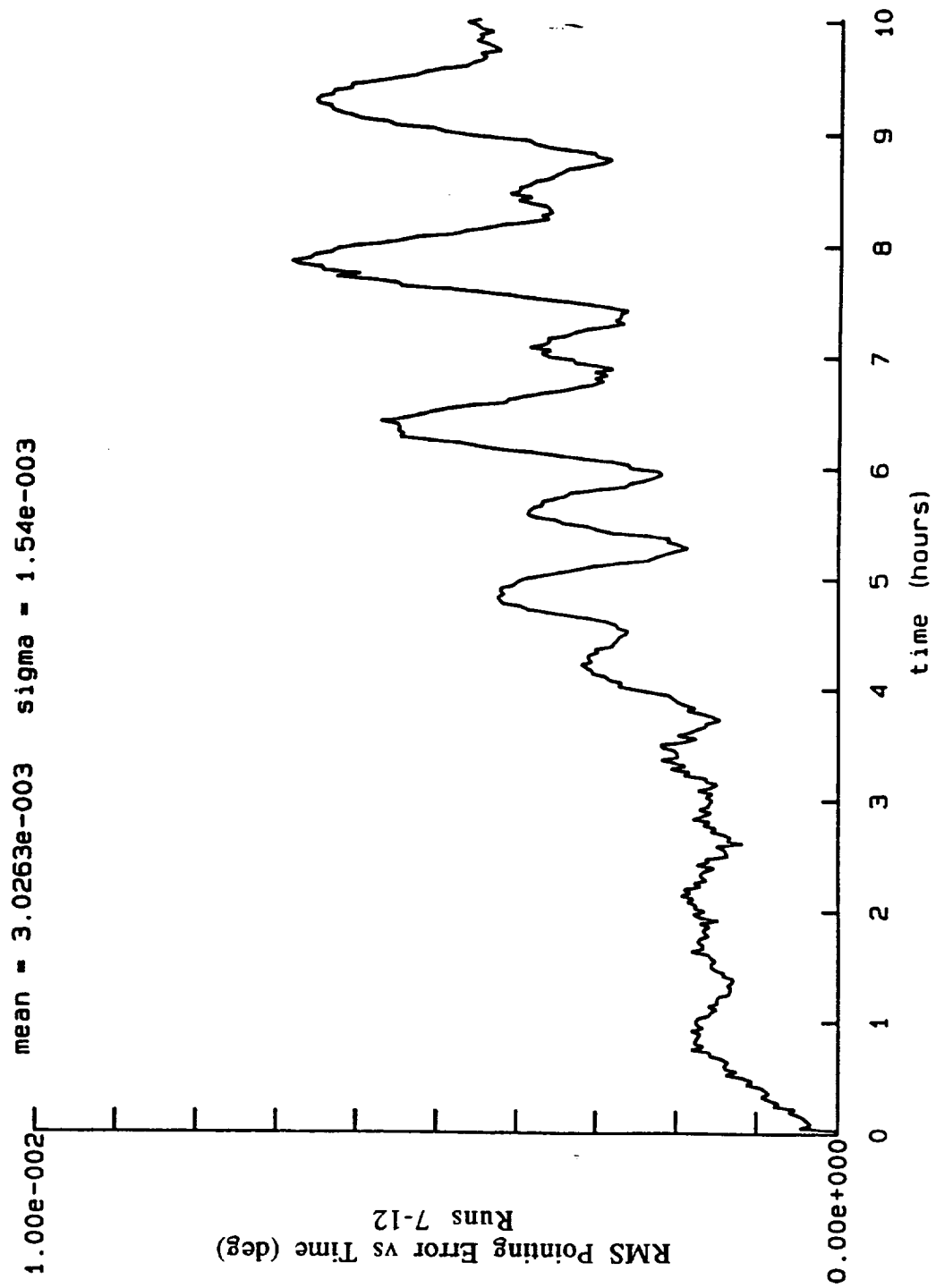
11-07-91

Figure 22    RMS Pointing Error vs Time for Runs 7-12

56

mean = 2.0912e-003   sigma = 1.17e-003

RMS Pointing Error vs Time (deg)
Runs 7-8

DATA FILE: 100891b.2          11-22-91

Figure 23    RMS Pointing Error vs Time for Runs 7-8

57

Figure 24    RMS Pointing Error vs Time for Runs 1-12

mean = 4.2616e-003    sigma = 1.68e-003

11-07-91

58

## VII. Parametric Error Model

The only parametric error model that is used to compensate the gyro's output is a thermal model of gyro bias. The coefficients for this model are first measured at the sensor level in gyro test. A temperature test is done from -55 to +70 deg C. with a temperature soak every 20 deg C. At each soak level, the gyro bias and random walk are calculated. A 4th order curve fit to temperature is then performed. The data sheets generated during this test are included in Appendix D

Once the gyros are installed into a system, the entire system is calibrated with a completely automated calibration test over temperature. The system is mounted on a 2 axis temperature controlled rate table. A multi-position test is performed which determines the gyro scale factor and bias, accelerometer scale factor and bias, and gyro and accelerometer misalignments. All (except gyro scale factor) are fitted to a second order equation of temperature. The gyro scale factor is less then 1 ppm uncompensated and does not need to be modeled.

Additionally we have included in Appendix E the differential equation based gyro model used in our systems modeling of RLG behavior.

# VIII.    Error allocation and overall system performance

The Ring Laser Gyro has only a few well understood error sources that have been briefly mentioned in this report, specifically quantization noise, angle random walk, and bias instability. At this point we would like to expand somewhat on bias instability and quantization as they specifically relate to the RL-34 gyro and this application.
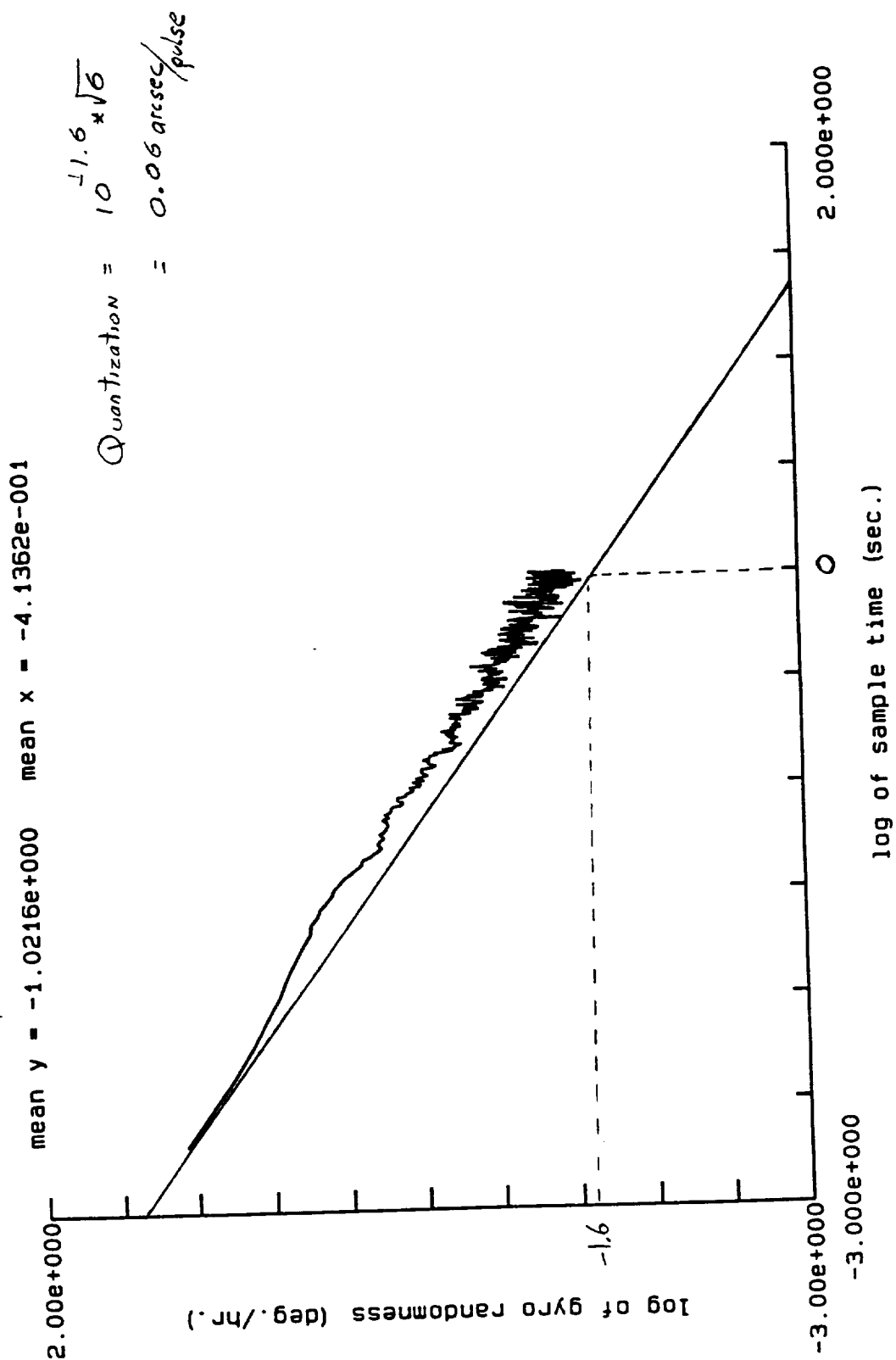
The bias instability can be thought of as small motions of the gyro's optical axis due to residual effects of pathlength control. The pathlength controllers impart some out-of plane motion of the optical axis, and these small, slowly changing motions will fluctuate in a non-deterministic manner with time resembling an AC signal component. The degree that they repeat from turn-on to turn-on was previously a limiting factor that severely degraded bias repeatability(DC component) of the RLG. The RL-34 gyro has state-of-the-art pathlength controllers that have reduced the repeatability from turn-on to turn-on to less than the small in-run fluctuations(AC component) of the bias. In the DSN application, this has very little impact on performance as the system and gyros can remain powered on at all times with no adverse lifetime impact.

The quantization of the gyros in this system is 0.38 arc-sec/pulse. The Allan Variance of the output signals indicate an effective quantization of about 1.2 arc-sec, indicating a lack of single pulse processing in gyro output. This aspect of the quantization is referred to as spillover pulses, which are due to the dither zero-crossing strobe being slightly imperfect. Several improvements are currently pending, and we are in the process of patent applications so we cannot completely describe how to solve this. The data in Figure 25 does however show one pulse resolution down to 0.05 arc-sec, indicating that we have solved the problem.
Quantization & spillover; base motion

In Appendix B we have included for informative purposes, a complete and thorough explanation of a strapdown navigator systems implementation, including the evolution of the Schuler oscillations on the navigation outputs.

60

page 1

mean y = -1.0216e+000    mean x = -4.1362e-001

$Quantization = 10^{\perp 1.6} * \sqrt{6}$

$= 0.06 \frac{arcsec}{pulse}$



log of gyro randomness (deg./hr.)

log of sample time (sec.)

-1.6

0

2.00e+000

-3.00e+000

2.000e+000

-3.000e+000

DATA FILE: 07-09-91.i04

Figure 25    X32 Reduced Quantization Allan Variance Plot

61

# IX. Recommended alternatives to improve performance

The azimuth stability was limited in this contract in part due to RLG S/N Z2002, which had slightly higher random walk coefficient and drift stability than the other level axis gyro. Incorporation of this gyro into a position other than azimuth may improve overall azimuth performance by approximately 30%. We also recommend potentially replacing the least accurate gyro with one of our newer 4500 series gyros, which will require new calibration, but should improve that axis random walk performance by 50%.

We recommend incorporation of the BGSD 32:1 quantization reduction circuitry on all gyro axes to reduce the noise equivalent angle during the initialization test sequencing. This is equally important in biasing the gyros as the time to roughly calibrate the bias is quantization limited. Fine calibration of the gyro bias is still random walk coefficient limited. Acquisition performance of the RL-34 based pointing system is greatly enhanced with a lower quantization value, due to the short times involved in the acquisition phase. An RL-34 has a nominal scale factor of 1.535 arc-sec/pulse. When the 32:1 logic is used, this is reduced to 0.05 arc-sec/pulse. Figure 19 shows initial 32:1 logic data during a proof of concept evaluation. The Allan variance quantization value for this data is 0.06 arc-sec/pulse, indicating that true single pulse limited noise has been attained.

We recommend moving to incorporate position damping into our Kalman filter to project known position and velocity states onto attitude to improve azimuth accuracy during tracking. This is applicable to the DSN application(tracking) because the position of the antenna is fixed in Earth coordinates(i.e. it cannot be moving on the surface at 2 ft/sec).

As an alternative to using the accelerometers to keep track of local level during elevation operations, a pseudo-g calculation could be modeled and implemented which would rely solely on the gyro rotational outputs, thus reducing the Schuler oscillation amplitudes during tracking operation.

We also recommend investigating increased dither (lowers the RWC) of the gyros in the system, which has the risk of potentially causing increased coning motion.

# X.  Summary

## Summary

The overall results of this laboratory evaluation are quite encouraging.  The gyro data is in good agreement with the system's overall pointing performance, which is quite close to the technical objectives for the DSN application.

The system can be calibrated to the levels required for millidegree levels of pointing performance, and initialization performance is within the required 0.001 degree objective.

The blind target acquisition performance is within a factor of two of the 0.0001 degree objective, limited only by a combination of the slow rate (0.5 deg/sec) and the existing production quantization logic(0.38 arc-sec/pulse).  Logic circuitry exists to better this performance such that it will better the objective by 50%.  Representative data with this circuitry has been provided for illustration.

Target tracking performance is about twice the one millidegree objective, with several factors contributing.  The first factor is the bias stability of the gyros, which is exceptional, but will limit performance to the 0.001 to 0.002 degree range for long tracking periods.  The second contributing factor is the accelerometer contributions when the system is elevated.  These degrade performance into the 0.003 to 0.004 degree range, which could be improved upon with some additional changes.

Finally, we have provided a set of recommendations to improve performance closer to the technical objectives.  These recommendations include gyro, electronics, and system configurational changes that form the basis for additional work to achieve the desired performance.

In conclusion, we believe that the RL-34 based advanced navigation system has demonstrated performance consistent with expectations and technical objectives, and it has the potential for even further enhancement for the DSN application.

# Appendix A

<u>Copy of letter sent to Noble Nerheim with the raw data records</u>

In this appendix a copy of the July 10th, 1991 letter to Noble Nerheim is enclosed. It contains a description of the ring laser gyro data provided at that time along with plots of the data.

The data is provided in 5 different plot formats for each ring laser gyro. The first four formats are contained on one page, with the fifth format on the following page. These are standard plots generated by our gyro test software used in BGSD's RLG production testing.

In the first graph(top left) are plotted the 100 second gyro count sums with the gyro input axis approximately perpendicular to local level (9.841 deg/hr Earth's input rate component). A mean value of the data and standard deviation are provided at the top of each graph.

The second graph (top right) shows the count sums multiplied by the 1.535 arc-sec/count gyro scale factor, and divided by 100 seconds to obtain scaled count sum units of deg/hr. The mean at the top of this graph shows the gyro mean output with the 9.841 deg/hr input. The standard deviation includes all gyro noise terms and also represents the first point on the sigma plot shown in the fifth graph.

The third graph (lower left) shows the scaled count sums filtered by an 18 point (half hour) triangular filter, with the 9.841 deg/hr input previously subtracted. The mean at the top of this graph shows the mean gyro bias for this test, but please note that gyro input axis misalignment does not get removed until final system calibration. The standard deviation for this graph is a rough approximation to the gyro bias instability.

The fourth plot (lower right) is just the data in the third plot subtracted from the data in the second plot. Here it only confirms that the mean gyro bias subtracted brought the data to near zero mean.

The fifth plot is a standard sigma plot of the data set for the RLG under test. Graphical analyses were done to estimate the RWC and Bias Instability for the gyro test.

The last set of data is of the three axes of the ISA tested with S/N Z2002's input axis vertical. This data set was obtained with 0.38 arc-sec/count test electronics.

A-1

July 10, 1991
Allied Signal Aerospace
BGSD
M/S 2/13
Teterboro, NJ 07608

Mr. Noble Nerheim
JPL
M/S 185105
4800 Oak Grove Drive
Pasadena, CA 91109

Dear Noble Nerheim:

Enclosed is the gyro data as discussed during the kick off meeting and telephone conference call. The raw data is on a 3.5" Apple Macintosh formatted disk as standard text files. The names of the four files are listed below.

| Filename | # of points | Gyro SN |
|---|---|---|
| BGSD file 09-15-89.f01 | 2300 | B2003 |
| BGSD file 10-27-90.d01 | 864 | Z2002 |
| BGSD file 12-14-90.b01 | 2300 | B4500 |
| BGSD file 06-30-91.g01 | 2300 | B2003, Z2002, B4500 |

The first three tests were in our standard static test stations and are the basis for some of the data included in the proposal. The last test is a recently performed test with the gyros installed in the Inertial Sensor Assembly (ISA).
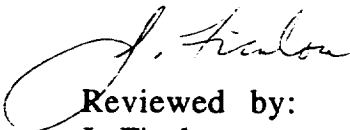
Also enclosed are the plots of the above data. The plots show the gyro output in counts and deg/hr (the scale factor for the RL34 is 1.535 arcsec/count). The plots of the first three tests also calculate the gyro bias (gyro output - local vertical Earth's rate).

Sigma plots are also included. The usefulness of these plots are in their graphical representation of the gyro's noise terms. The random walk coefficient (RWC) and in-run bias stability are shown on each plot. Note that some of the tests were not long enough to determine the limit of the gyro's in-run bias stability.

We look forward to you review of this data and welcome any comments or questions that you may have.

Sincerely,
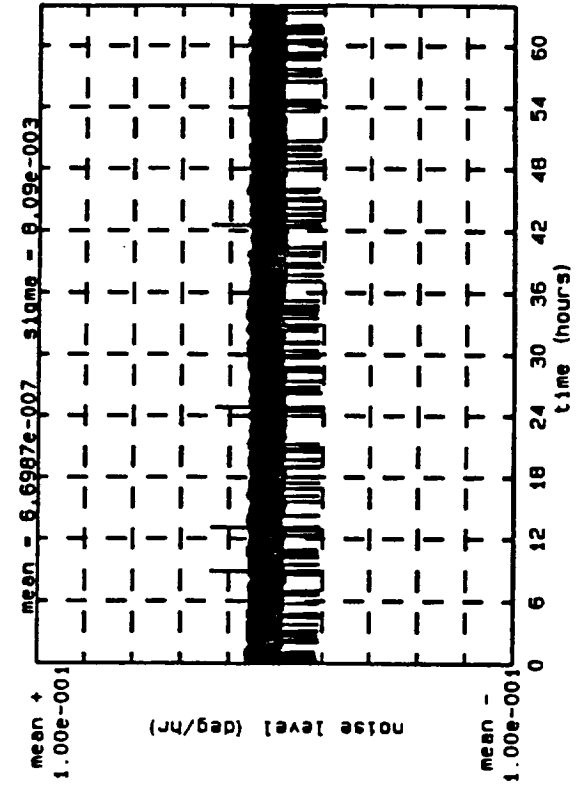
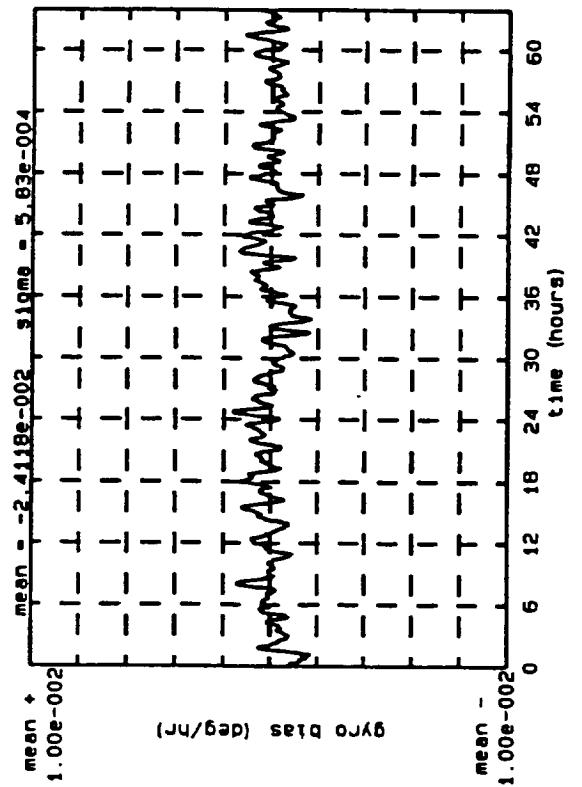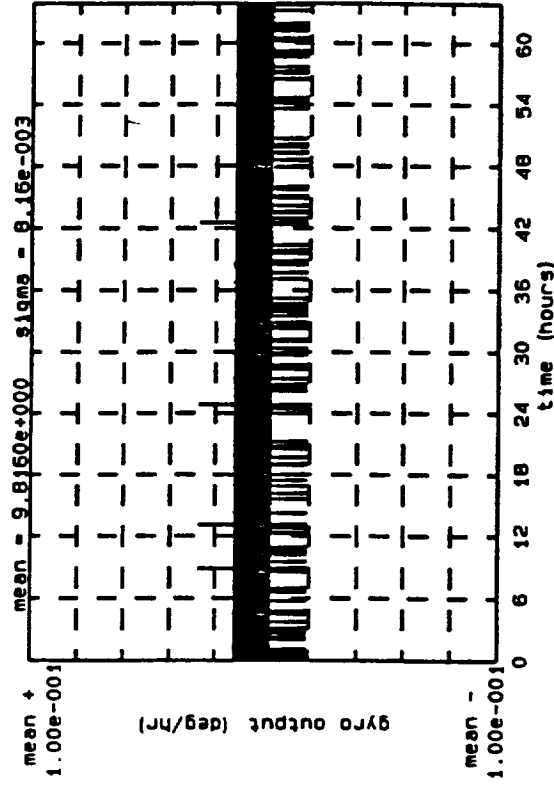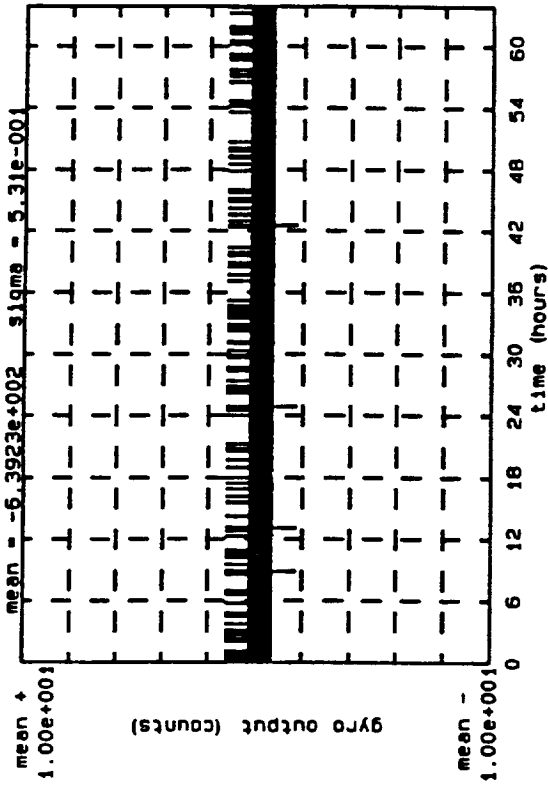Mark Grasso

Reviewed by:
J. Ficalora

cc:        W. Mitchell
           E. Luxford
           E. Mazurkiewicz

Enclosed:   12 data plots
           one 3.5" diskette

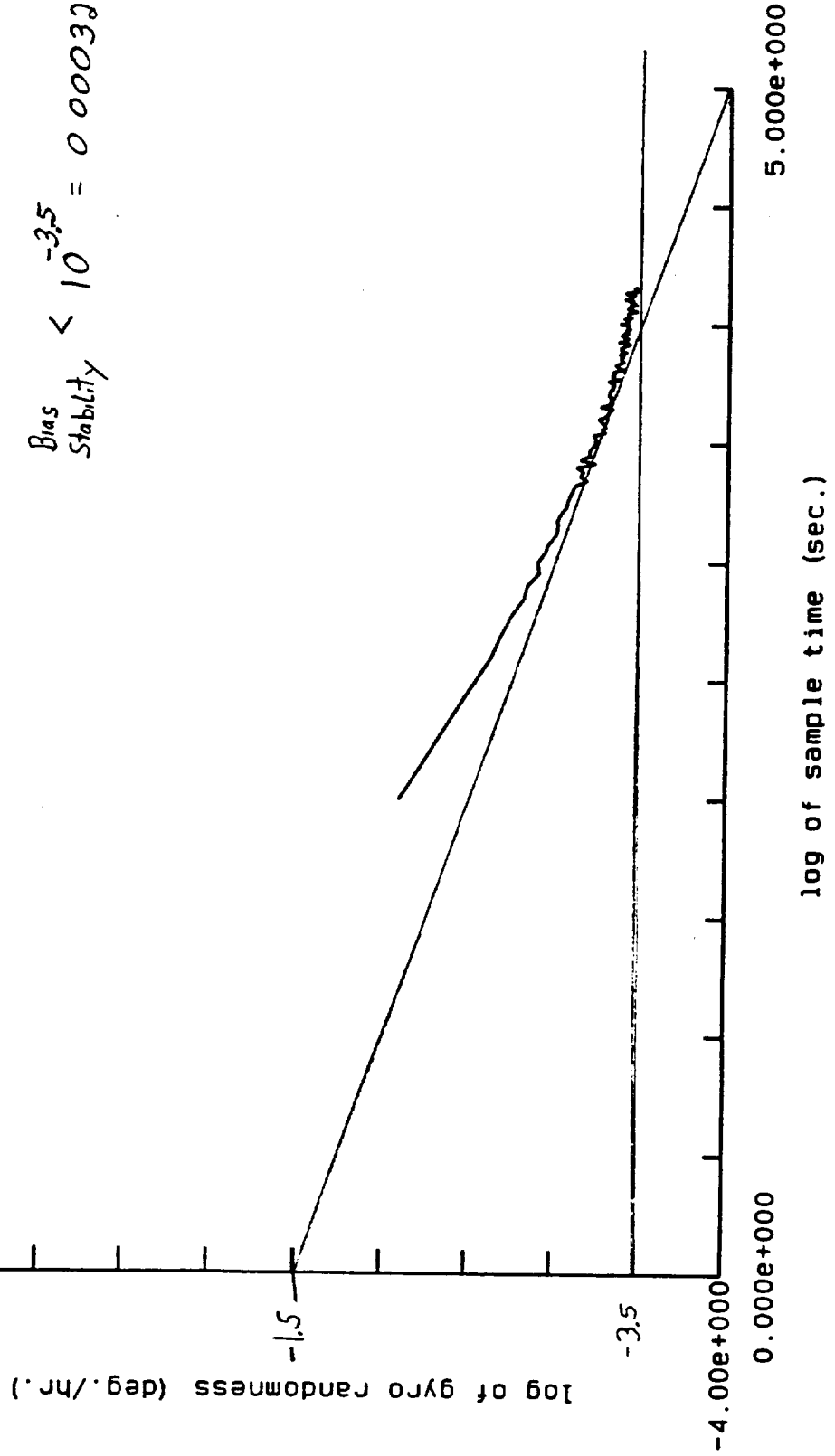page 1    B2003: weekend drift test at 46 dps dither

mean = 9.8160e+000  sigma = 8.16e-003

mean + 1.00e-001
gyro output (deg/hr)
mean - 1.00e-001

time (hours)

mean = 6.6987e-007  sigma = 8.09e-003

mean + 1.00e-001
noise level (deg/hr)
mean - 1.00e-001

time (hours)

mean = -6.3923e+002  sigma = 5.31e-001

mean + 1.00e+001
gyro output (counts)
mean - 1.00e+001

time (hours)

mean = -2.4118e-002  sigma = 5.83e-004

mean + 1.00e-002
gyro bias (deg/hr)
mean - 1.00e-002

time (hours)

07-09-91

GYRO: B2003    DATA FILE: 09-15-89.f01

A-4

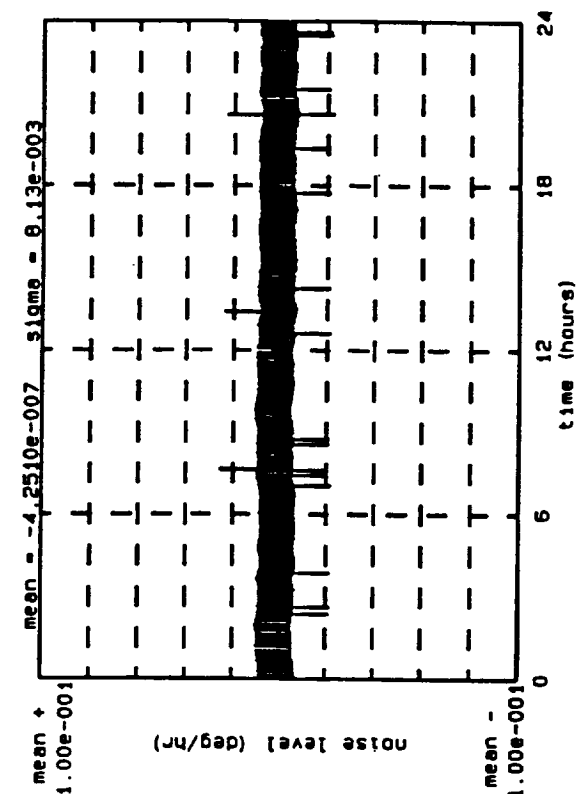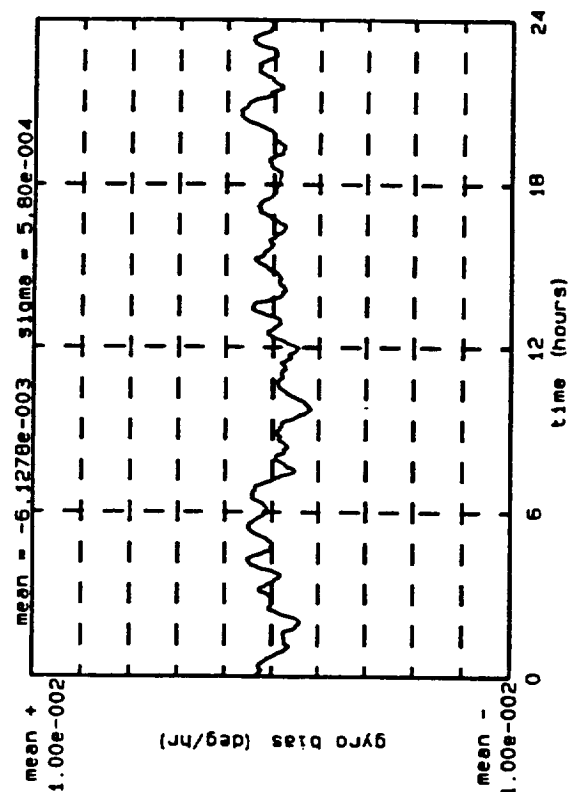page 1    B2003: weekend drift test at 46 dps dither

mean y = -3.2887e+000    mean x = 3.7314e+000

$$RWC = \frac{10^{-1.5}}{60} = 0.0005\ \%/\sqrt{hr}$$

$$\text{Bias Stability} < 10^{-3.5} = 0.00032\ \%/hr$$

log of gyro randomness (deg./hr.)

log of sample time (sec.)

1.00e+000

-1.5

-3.5

-4.00e+000

0.000e+000

5.000e+000

07-09-91

GYRO: B2003    DATA FILE: 09-15-89.f01

A-5

mean = -6.4040e+002    sigma = 5.33e-001

gyro output (counts)

mean + 1.00e+001

mean - 1.00e+001

time (hours)   0   6   12   18   24

mean = 9.8340e+000    sigma = 8.19e-003

gyro output (deg/hr)

mean + 1.00e-001

mean - 1.00e-001

time (hours)   0   6   12   18   24

mean = -6.1278e-003    sigma = 5.80e-004

gyro bias (deg/hr)

mean + 1.00e-002

mean - 1.00e-002

time (hours)   0   6   12   18   24

mean = -4.2510e-007    sigma = 8.13e-003

noise level (deg/hr)

mean + 1.00e-001

mean - 1.00e-001

time (hours)   0   6   12   18   24

GYRO: Z2002    DATA FILE: 10-27-90.d01

07-09-91
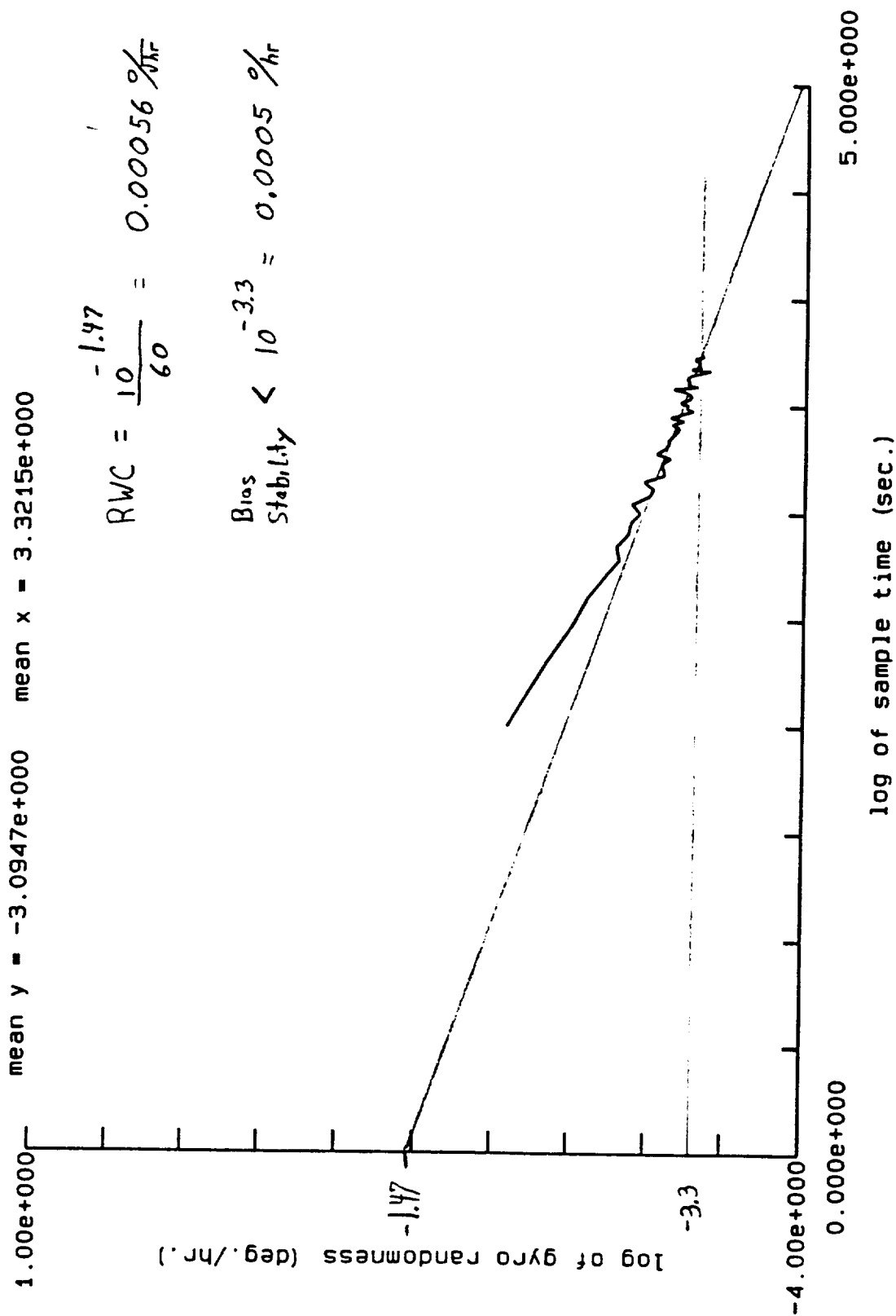
page 1    Z2002: weekend drift at 50 dps dither

mean y = -3.0947e+000    mean x = 3.3215e+000
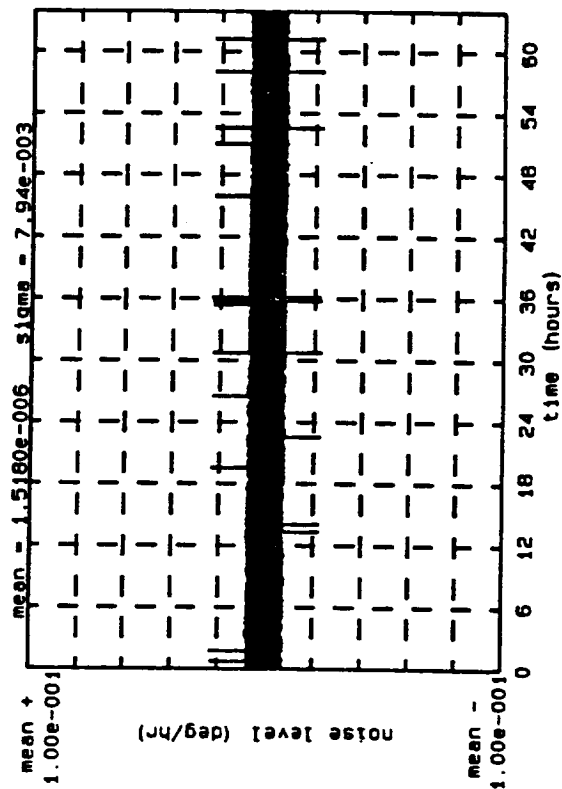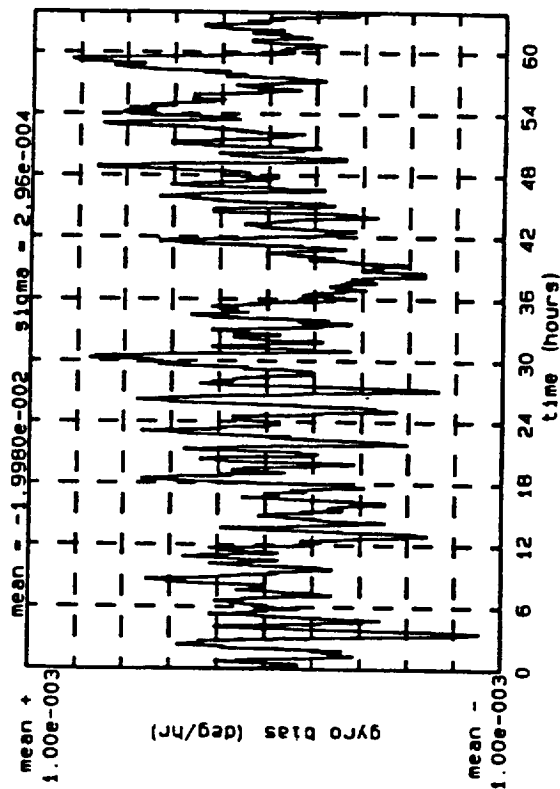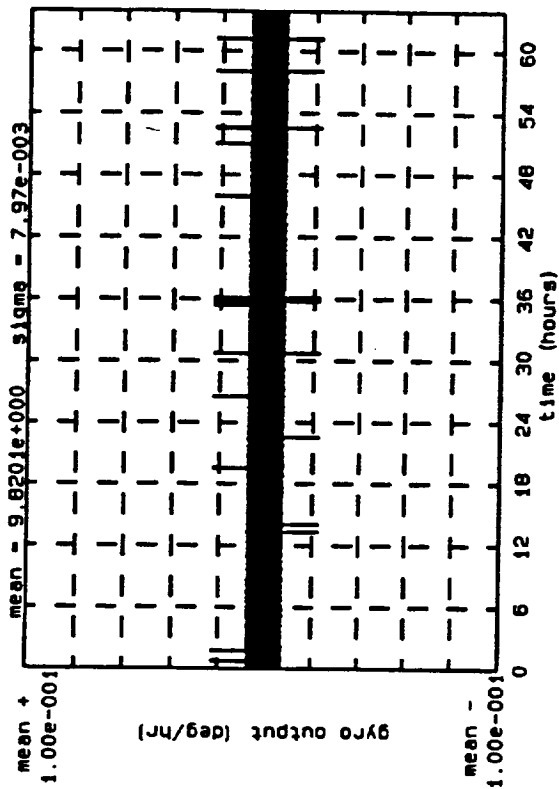
$$RWC = \frac{10^{-1.47}}{60} = 0.00056 \, \%/\sqrt{hr}$$

$$\text{Bias Stability} < 10^{-3.3} = 0.0005 \, \%/hr$$

log of gyro randomness (deg./hr.)

log of sample time (sec.)

-1.47

-3.3

1.00e+000

0.000e+000    5.000e+000

-4.00e+000

GYRO: Z2002    DATA FILE: 10-27-90.d01    07-09-91

A-7

B4500: weekend drift test @ 100 dps dither

GYRO: B4500    DATA FILE: 12-14-90.b01

07-09-91

A-8

page 1    B4500:  weekend drift test @ 100 dps dither

mean y = -3.5474e+000    mean x = 3.7314e+000

$$RWC = \frac{10^{-1.75}}{60} = 0.0003 \; \%/\sqrt{hr}$$

$$\begin{array}{l} B_{ias} \\ Stability \end{array} = 10^{-3.8} = 0.00016 \; \%/hr$$

log of gyro randomness (deg./hr.)

1.00e+000

-1.75

-3.8

-4.00e+000

0.000e+000

5.000e+000

log of sample time (sec.)

GYRO: B4500      DATA FILE: 12-14-90.b01

07-09-91

A-9

page 1

B2003, Z2002, B4500:  .1 NMPH ISA with new HVPS -weekend drift

mean = 1.4957e+003   sigma = 1.83e+000

gyro output (counts)

time (hours)

mean +
1.00e+001

mean -
1.00e+001

mean = -5.7421e+000   sigma = 7.04e-003

gyro output (deg/hr)

time (hours)

mean +
1.00e-001

mean -
1.00e-001

07-09-91

DATA FILE: 06-30-91.g01

GYRO: B2003

page 1    B2003.  Z2002.  B4500:  .1 NMPH ISA with new HVPS -weekend drift

mean y = -3.2494e+000    mean x = 3.7314e+000

$$RWC = \frac{10^{-1.45}}{60} = 0.00059 \, ^{\circ}/\sqrt{hr}$$

$$Bias\ Stability < 10^{-3.4} = 0.0004 \, ^{\circ}/hr$$

log of gyro randomness (deg./hr.)

log of sample time (sec.)

1.00e+000

-1.45

-3.4

-4.00e+000

0.000e+000

5.000e+000

GYRO: B2003    DATA FILE: 06-30-91.g01

07-08-91

A-11

page 1    B2003, Z2002, B4500:   .1 NMPH ISA with new HVPS -weekend drift



mean = 2.5515e+003   sigma = 1.41e+000

gyro output (counts)

time (hours)

mean = -9.7953e+000   sigma = 5.40e-003

gyro output (deg/hr)

time (hours)

A-12

page 1    B2003, Z2002, B4500: .1 NMPH ISA with new HVPS -weekend drift    mean x = 3.7314e+000

mean y = -3.4110e+000

$$RWC = \frac{10^{-1.6}}{60} = 0.00042 \; °/hr$$

$$Bias\; Stability < 10^{-3.7} = 0.0002 \; °/hr$$

log of gyro randomness (deg./hr.)

log of sample time (sec.)

07-08-91

GYRO: Z2002     DATA FILE: 06-30-91.g01

A-13

page 1    B2003, Z2002, B4500:   .1 NMPH ISA with new HVPS -weekend drift

4.3

gyro output (counts)

mean + 1.00e+001

mean - 1.00e+001

mean = 2.5584e+003   sigma = 1.85e+000

time (hours)

gyro output (deg/hr)

mean + 1.00e-001

mean - 1.00e-001

mean = -9.8600e+000   sigma = 7.09e-003

time (hours)

GYRO:  B4500        DATA FILE: 06-30-91.g01

page 1    B2003, Z2002, B4500:  .1 NMPH ISA with new HVPS -weekend drift

mean y = -3.5409e+000    mean x = 3.7314e+000

$$RWC = \frac{10^{-1.75}}{60} = 0.0003 \; \%/\sqrt{hr}$$

$$\begin{matrix} Bias \\ Stability \end{matrix} < 10^{-3.8} = 0.00016 \; \%/hr$$



log of gyro randomness (deg./hr.)

log of sample time (sec.)

1.00e+000

-1.75

-3.8

0.000e+000          5.000e+000

-4.00e+000

GYRO: B4500      DATA FILE: 06-30-91.g01      07-08-91

A-15

## Appendix B

### Explanation of Navigation Equations

Inertial navigation systems determine change in position from an initial reference location through double integration of acceleration measured along three orthogonal axes. The most commonly employed method of measuring acceleration is through electro-mechanical accelerometers. These devices are configured to electrically measure the amount of force required to restrain a proof-mass along their input axes. The electrical signal is then converted to a digital format for computer processing of the double integration to determine position.

Of course, one of the basic requirements is knowledge of the accelerometer input axes at all times while the system is in motion so that the direction of the change in position is determined correctly . Gyroscopes are employed in these systems for that purpose, maintaining an inertial reference for the accelerometers following an initial alignment. Two different mechanizations presently are employed in practice, which are gimballed and strapdown systems. The gimballed systems locate the accelerometers on the inner gimbal of sets of either three or four gimbals, with that inner gimbal stabilized by the gyroscopes and stabilization servos. The inner gimbal orientation is typically maintained such that one accelerometer input axis is located along each of three navigation axes (for example, North, East and Vertical).

With strapdown systems, the accelerometers are nominally located along three orthogonal vehicle axis (i.e., roll, pitch and yaw or roll, elevation and bearing) and the gyroscopes measure the orientation of the accelerometers (vehicle) relative to the navigation frame. The gyro measurements are employed in this case to continuously update a coordinate transformation matrix which takes the accelerometer measurements from the vehicle frame to the navigation frame. It is noted that in this strapdown case, it is necessary that the gyroscopes employed possess high bandwidth and accurate scale factor so that the accelerometer (vehicle) orientation relative to the navigation frame is instantaneously and accurately known. The basic navigation equations in the two mechanizations are therefore as follows:

$$\Delta V_N = \int_0^{\Delta t} a_N \, dt$$

$$\Delta V_E = \int_0^{\Delta t} a_E \, dt \qquad \text{gimballed}$$

$$\Delta V_v - g \, \Delta t = \int_0^{\Delta t} a_v \, dt$$

$$(1)$$

$$\begin{bmatrix} \Delta V_N \\ \Delta V_E \\ \Delta V_v - g\,\Delta t \end{bmatrix} = \begin{bmatrix} b_{11} & b_{12} & b_{13} \\ b_{21} & b_{22} & b_{23} \\ b_{31} & b_{32} & b_{33} \end{bmatrix} \cdot \begin{bmatrix} \int_0^{\Delta t} a_x \, dt \\ \int_0^{\Delta t} a_y \, dt \\ \int_0^{\Delta t} a_z \, dt \end{bmatrix}$$

strapdown

x = roll
y = pitch
z = yaw

As indicated in these equations, the gravitational field, as measured by the accelerometer proof-masses must be compensated so as not to impact the determination of position.

It is also noted that the orientation of the N, E, V navigation frame, referred to as a "local level" frame of reference is dependent on the position of the system at any given time. Maintaining this local level frame in the navigation mode is discussed in a later paragraph.

In addition to the navigation problem, there is also the problem of initializing the system (determining the initial orientation of the accelerometers). In fact, the system is capable of a self contained initialization (initial alignment mode) if the vehicle on which it is located remains stationary on the surface of the Earth for a few minutes. In this mode, the accelerometers are used to determine the system orientation with respect to vertical through the knowledge that gravity will be the only acceleration measured within a stationary vehicle. Similarly, the gyroscopes are used to determine the system orientation relative to East. Since no rotation exists around that axis to be measured by the gyros this null condition is determined computationally (gyrocompassing). With definition of the East and Vertical axes, the North axis is determined as the third orthogonal axis in the set. It is noted that any random vibration motion of the vehicle during this initialization averages to "zero" and therefore does not affect the alignment process.

To this point, the discussion has referred to a navigation frame of North, East and Vertical. This frame of reference is, of course, rotating relative to the inertial frame of reference established by the gyroscopes. There is the Earth's rotation rate, and if the vehicle is moving relative to the Earth, there is an additional rotation rate referred to as the transport rate or navigation frame rate.

Inertial system implementations must account for these rotations. A common implementation is to either rotate the gimbals physically or rotate the strapdown coordinate transformation matrix computationally at these same magnitudes. These rotations maintain the "system" level and pointing North and this mechanization is referred to as a North slaved, local level implementation.

In fact, employing this local level type of system implementation bounds the inertial reference errors due to accelerometer biases and/or gyro drifts due to a characteristic referred to as Schuler tuning. It is noted that in general the limits or bound on errors applies only to the inertial reference and cannot be extended to velocity and navigation position errors. In general, these errors may grow with time or time squared due to gyro drift (particularly azimuth gyro drift) for periods up to six hours for velocity and twelve hours for position. It is also noted that

the Schuler tuning mechanization is basically the same for both strapdown and gimballed systems since the computations are implemented in the navigation frame of reference (after the vehicle to navigation coordinate transformation in the strapdown case). Inertial component errors, propagate quite differently in the two systems however, and as a result a greater accuracy burden is generally placed on components in the strapdown mechanization.

Although this is a summary of the basis of inertial navigation, many complications arise in practice. The most common are accelerometer output biases which in general result in navigation errors and gyro drifts which destabilize the inertial reference (also resulting in navigation errors).

As previously indicated, in the presence of these errors, the Schuler tuning process bounds errors in the computed navigation frame relative to local level. The reason for this can be developed in a somewhat heuristic manner through the following exercise.

At any given location on the Earth, the transportation rotation rate is approximately the vehicle tangential velocity (East and North velocities) divided by the Earth's radius (plus altitude). Adding Earth's rotation rate, the following equations are correct to a first approximation.

$$\dot{\theta}_N = \frac{V_E}{R+h} + \omega_e \cos\lambda = \frac{\int a_E \, dt}{R+h} + \omega_e \cos\lambda$$

$$\dot{\theta}_E = \frac{V_N}{R+h} = \frac{\int a_N \, dt}{R+h}$$

$h = $ altitude $\qquad$ (2)
$\lambda = $ latitude
$\omega_e = $ earth's rate
$R = $ earth's radius

To gain the insight as to why the errors in the inertial reference are bounded, these equations are written as error equations. The error due to accelerometer measurement of gravity which results from any error in maintaining the inertial reference level is included in the $a_N$, $a_E$ terms.

For a high quality inertial system, the off level error is always small and the accelerometer measurement of gravity due to this error is therefore expressed as gravity multiplied by the orientation error.

Proceeding in this manner:

$$\dot{\theta}_{N_e} = \frac{\int a_{E_e} \, dt}{R+h}$$

$$\dot{\theta}_{E_E} = \frac{\int a_{N_E} \, dt}{R+h}$$

(3)

It has been assumed that the error in computing Earth's rate is negligible. This is a reasonable assumption particularly early in a navigation run before latitude errors become significant.

$$a_{E_\epsilon} = -g \cdot \theta_{N_\epsilon} \qquad a_{N_\epsilon} = -g \cdot \theta_{E_\epsilon} \qquad (4)$$

The negative sign in equation (4) is a result of the fact that tilt errors result in acceleration errors opposite in algebraic sign to the rotation rate computed by equation (2). In other words, the system in inherently stable.

Therefore

$$\dot{\theta}_{N_\epsilon} [R+h] = -g \int \theta_{N_\epsilon} \, dt$$

$$\dot{\theta}_{E_\epsilon} [R+h] = -g \int \theta_{E_\epsilon} \, dt \qquad (5)$$

Differentiating and rearranging

$$\ddot{\theta}_{N_\epsilon} + \frac{g}{R+h} \theta_{N_\epsilon} = 0$$

$$\ddot{\theta}_{E_\epsilon} + \frac{g}{R+h} \theta_{E_\epsilon} = 0 \qquad (6)$$

In fact, these equations are the equations of motion of a simple harmonic oscillator or undamped pendulum, expressed in polar coordinates, where the length of the pendulum is equal to the Earth's radius R plus the altitude H at the system location.

The frequency of this oscillator is:

$$f = \frac{1}{2\pi} \sqrt{\frac{g}{R+h}} \qquad (7)$$

This frequency is referred to as the Schuler frequency and the mechanization is referred to as Schuler tuned. Inserting nominal values for R, G and H in this equation, the period of oscillation computes to approximately 84.4 minutes in duration.
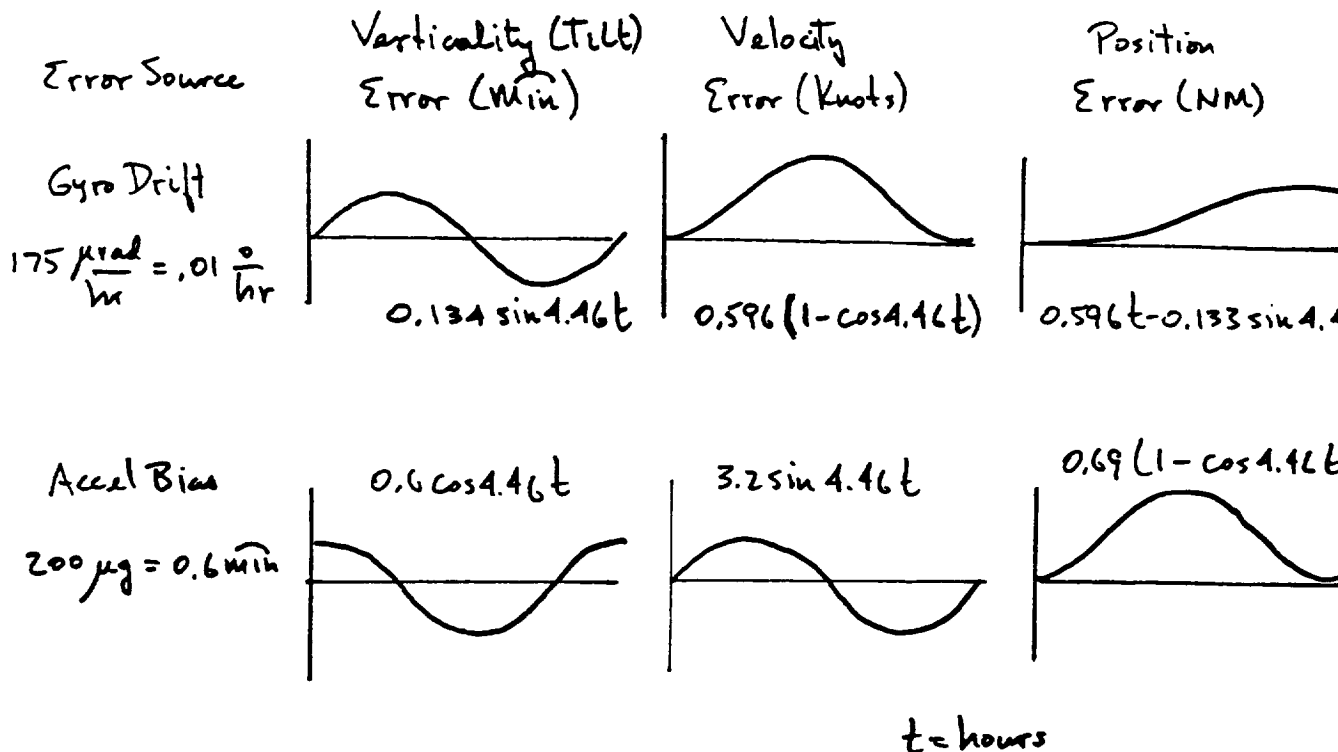
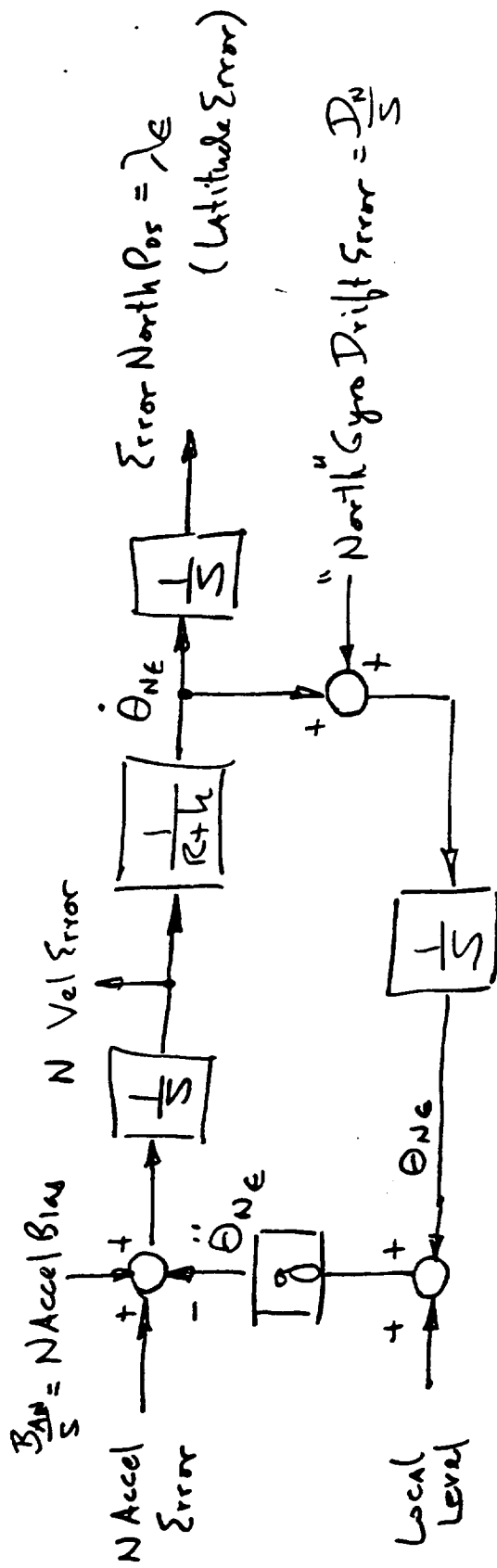It is also convenient to present these error equations using La Place transforms.

They are then written:

$$s^2 \theta_{N_\epsilon}(s) + \omega_s^2 \theta_{N_\epsilon}(s) = 0$$

$$s^2 \theta_{\epsilon_\epsilon}(s) + \omega_s^2 \theta_{\epsilon_\epsilon}(s) = 0 \qquad (8)$$

Examining these equations leads to a representation by two single axis block diagrams of undamped oscillators as shown in Figure 1. A complete block diagram error representation is significantly more complicated than Figure 1 (due to coupling errors that develop such as latitude error), but these diagrams allow predicting certain errors with reasonable accuracy. For example, propagation of accelerometer bias and/or gyro drift errors for periods up to one Schuler period are predicted with reasonable accuracy.

The results for step function errors in accelerometer bias and/or gyro drift are shown graphically as follows. It is noted by inspection that the tilt errors, which are the errors in computation of the inertial reference, are always bounded in this stable oscillator. It is also noted, however, that since the oscillator is undamped, the errors remain indefinitely once the oscillator is disturbed.

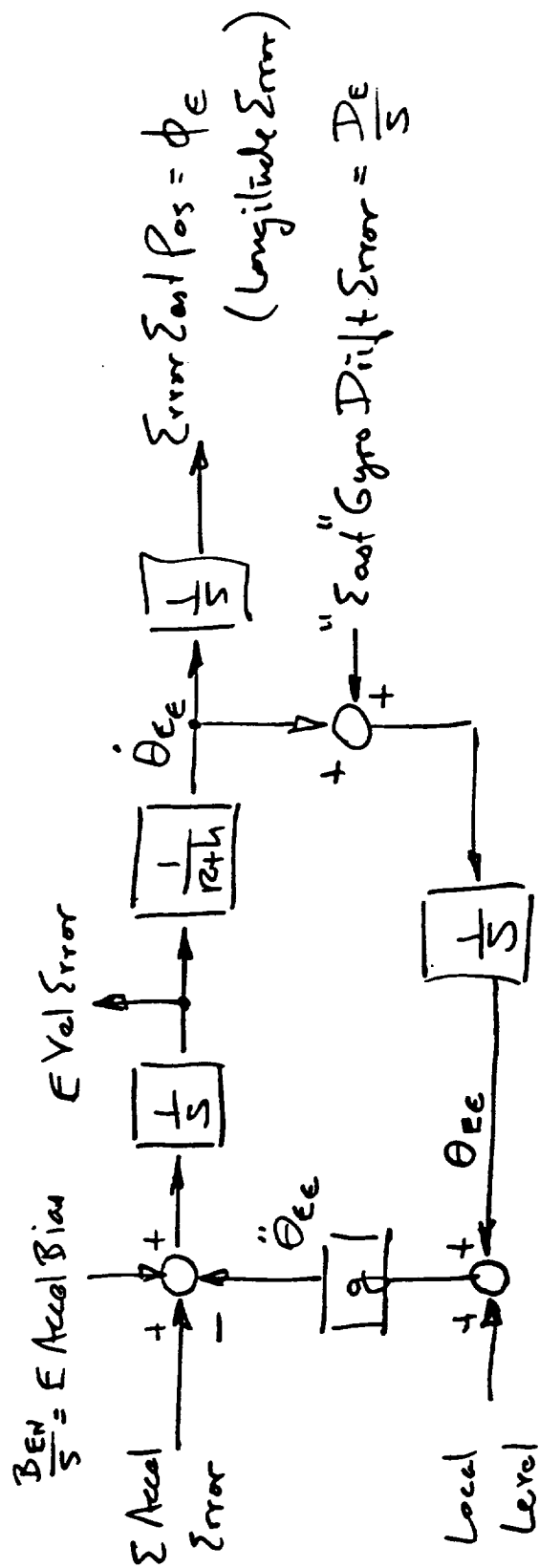| Error Source | Verticality (Tilt) Error (Min) | Velocity Error (Knots) | Position Error (NM) |
|---|---|---|---|
| Gyro Drift $175\,\mu\text{rad}/\text{hr} = .01\,°/\text{hr}$ | $0.134 \sin 4.46t$ | $0.596(1-\cos 4.46t)$ | $0.596t - 0.133 \sin 4.4$ |
| Accel Bias $200\,\mu g = 0.6\,\text{min}$ | $0.6 \cos 4.46t$ | $3.2 \sin 4.46t$ | $0.69(1-\cos 4.46t$ |

$t = \text{hours}$

B-5

Figure 2  N/E Schuler Oscillators

Development of the navigation equations is closely related to equations (1) and (2) and Figure 1. In fact, the equations for latitude and longitude rate are as follows:

$$\dot{\lambda} = \frac{V_N}{R+h} \qquad\qquad \lambda = \text{latitude} \qquad\qquad (9)$$

$$\dot{\phi} = \frac{V_{GE}}{[R+h]\cos\lambda} \qquad\qquad \phi = \text{longitude}$$

Where R is the local corrected value of Earth's radius.

The $A_N$ and $A_E$ accelerometer measurement terms are measurements in an

inertial frame of reference and therefore must be corrected for Coriolis effects to determine acceleration relative to the Earth.

In other words

$$\dot{V}_N = A_N - \text{Coriolis Terms} \qquad\qquad (10)$$

$$\dot{V}_{GE} = A_E - \text{Coriolis Terms}$$

Assuming a spherical Earth as a first order approximation

$$\dot{V}_N = A_N - \left[ \frac{V_N}{R+h}\dot{h} + \left( 2\omega_E \sin\lambda + \frac{V_{GE}\tan\lambda}{R+h} \right) V_{GE} \right] \qquad (1$$

$$\dot{V}_{GE} = A_E - \left[ \left( 2\omega_E \cos\lambda + \frac{V_{GE}}{R+h} \right)\dot{h} - \left( 2\omega_E \sin\lambda + \frac{V_{GE}\tan\lambda}{R+h} \right) V_N \right]$$

These equations operating in conjunction with the "leveling" rotations and North slaving rotation define a North slaved, local level inertial navigation system.

Development of the navigation equations is closely related to equations (1) and (2) and Figure 1. In fact, the equations for latitude and longitude rate are as follows:

$$\dot{\lambda} = \frac{V_N}{R+h}$$

$$\dot{\phi} = \frac{V_{GE}}{[R+h]\cos\lambda}$$

$\lambda =$ latitude

$\phi =$ longitude

(9)

Where R is the local corrected value of Earth's radius.

The $A_N$ and $A_E$ accelerometer measurement terms are measurements in an

inertial frame of reference and therefore must be corrected for Coriolis effects to determine acceleration relative to the Earth.

In other words

$$\dot{V}_N = A_N - \text{Coriolis Terms}$$

$$\dot{V}_{GE} = A_E - \text{Coriolis Terms}$$

(10)

Assuming a spherical Earth as a first order approximation

$$\dot{V}_N = A_N - \left[ \frac{V_N}{R+h}\dot{h} + \left( 2\omega_E \sin\lambda + \frac{V_{GE}\tan\lambda}{R+h} \right) V_{GE} \right]$$

$$\dot{V}_{GE} = A_E - \left[ \left( 2\omega_E \cos\lambda + \frac{V_{GE}}{R+h} \right)\dot{h} - \left( 2\omega_E \sin\lambda + \frac{V_{GE}\tan\lambda}{R+h} \right) V_N \right]$$

These equations operating in conjunction with the "leveling" rotations and North slaving rotation define a North slaved, local level inertial navigation system.

Due to problems with navigation over a pole (convergence of longitude) these equations are modified to develop what is referred to as a unipolar, wander azimuth configuration. A "pole flag" is employed which changes sign automatically at the equator to prevent divergence in the navigation equations at the single pole in the mechanization. One development of this mechanization is as follows:

Modify the North slaving rotation rate as follows:

$$\omega_V = (\omega_E + \dot{\phi}) \sin\lambda \qquad \text{North slaved}$$

(12)

to

$$\omega_V = (\omega_E + \dot{\phi}) \sin\lambda \pm \dot{\phi} \qquad \text{Unipolar}$$

The plus or minus sign is selected at the equator depending on hemisphere.

In the Northern hemisphere

$$\omega_V = \omega_E \sin\lambda + \dot{\phi}(\sin\lambda - 1)$$

In the Southern hemisphere

$$\omega_V = \omega_E \sin\lambda - \dot{\phi}(\sin\lambda - 1)$$

A second definition is that longitude rate is equal to minus the wander azimuth rate.

$$-\dot{\phi} = +\dot{\alpha}$$

(13)

In the Northern hemisphere

$$\omega_V = (\omega_E + \dot{\phi}) \sin\lambda + \dot{\alpha}$$

It is seen that a difference will develop in the "location" of accelerometer measurement reference axes (X-Y axes) relative to the Earth's N/E axes.

$$\int_{t=0}^{T} \dot{\alpha} \, dt = \alpha(T) - \alpha(0)$$
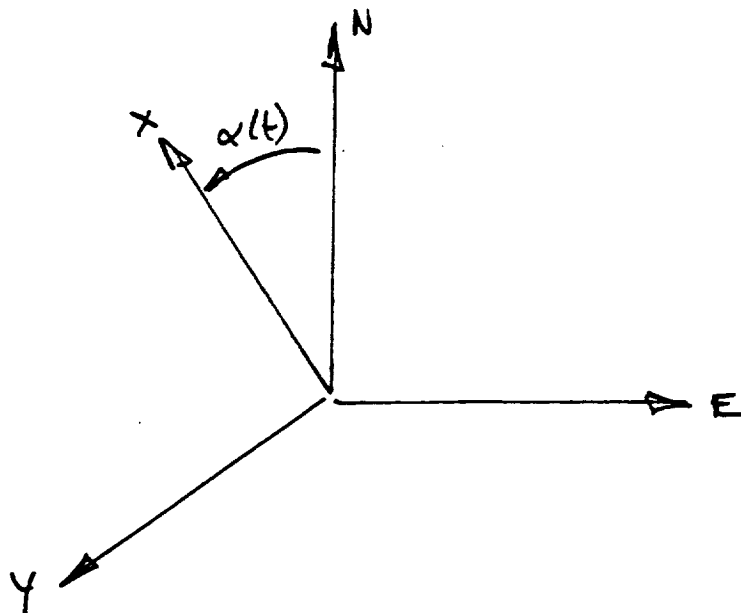
(14)

Figure 2 illustrates this situation

Fig 2

Wander Azimuth Coordinates

Velocity and acceleration in the X-Y coordinate frame is therefore

$$A_x = \cos\alpha \cdot A_N - \sin\alpha \cdot A_E$$

$$A_y = -\sin\alpha \cdot A_N - \cos\alpha \cdot A_E$$

$$(15)$$

$$V_x = \cos\alpha \cdot V_N - \sin\alpha \cdot V_{GE}$$

$$V_y = -\sin\alpha \cdot V_N - \cos\alpha \cdot V_{GE}$$

Differentiating

$$\dot{V}_x = \cos\alpha \dot{V}_N - \sin\alpha \dot{V}_{GE} - \dot{\alpha}\sin\alpha V_N - \dot{\alpha}\cos\alpha V_{GE}$$

$$(16)$$

$$\dot{V}_y = -\sin\alpha \dot{V}_N - \cos\alpha \dot{V}_{GE} - \dot{\alpha}\cos\alpha V_N + \dot{\alpha}\sin\alpha V_{GE}$$

Combining the last two equations

$$\dot{V}_x = \cos\alpha \cdot \dot{V}_N - \sin\alpha \cdot \dot{V}_{GE} + \dot{\alpha} \cdot V_y$$

$$(17)$$

$$\dot{V}_y = -\sin\alpha \cdot \dot{V}_N - \cos\alpha \cdot \dot{V}_{GE} - \dot{\alpha} \cdot V_x$$

Substitution of equation (11) in (17) and simplifying with (15)

$$\dot{V}_x = A_x - \left[\frac{V_x}{R+h} - 2\omega_E\cos\lambda\sin\alpha\right]\dot{h} + \left[2\omega_E\sin\lambda + \frac{V_{GE}}{R+h}\tan\lambda + \dot{\alpha}\right]$$

$$\dot{V}_y = A_y - \left[2\omega_E\cos\lambda\cos\alpha - \frac{V_y}{R+h}\right]\dot{h} - \left(2\omega_E\sin\lambda + \frac{V_{CE}}{R+h}\tan\lambda + \dot{\alpha}\right]$$

Define rotation rates

$$(18)$$

$$\rho_x \approx -\frac{V_y}{R+h}$$

$$\rho_y \approx \frac{V_x}{R+h}$$

$$(19)$$

$$\rho_z = \dot{\phi}\sin\lambda + \dot{\alpha}$$

$$\omega_{Ex} = \omega_E \cos\lambda \cdot \cos\alpha = \omega_{EN} \cos\alpha$$

$$\omega_{Ey} = -\omega_E \cos\lambda \cdot \sin\alpha = -\omega_{EN} \sin\alpha \qquad (19)$$

$$\omega_{Ez} = \omega_E \sin\lambda = \omega_{EV}$$

Substituting of (19) into (18)

$$\dot{V}_x = A_x - \left[ \rho_y + 2\omega_{Ey} \right] V_z + \left[ 2\omega_{Ez} + \rho_z \right] V_y$$

$$\dot{V}_y = A_y + \left[ \rho_x + 2\omega_{Ex} \right] V_z - \left[ 2\omega_{Ez} + \rho_z \right] V_x \qquad (20)$$

Which are the basic unipolar navigation equations.

In order to navigate in this mechanization, a set of direction cosines (and direction cosine rates) are developed using the terms in equation (20). The initial value of the direction cosines are determined during the gyro-compassing alignment and updated during vehicle motion through solution of the direction cosine rate equations. Latitude and longitude are determined from the latest values of three direction cosines.

Proceed as follows:

By definition

$$C_{11} = \cos\lambda \cos\alpha$$

$$C_{12} = -\cos\lambda \sin\alpha \qquad (21)$$

$$C_{13} = \sin\lambda$$

Differentiating

$$\dot{C}_{11} = -\dot{\lambda} \sin\lambda \cos\alpha - \dot{\alpha} \cos\lambda \sin\alpha$$

$$\dot{C}_{12} = \dot{\lambda} \sin\lambda \sin\alpha - \dot{\alpha} \cos\lambda \cos\alpha \qquad (22)$$

$$\dot{C}_{13} = \dot{\lambda} \cos\lambda$$

But

$$\rho_x = -\frac{V_Y}{R+h} = \dot{\lambda} \sin\alpha + \dot{\phi} \cos\alpha \cos\lambda$$

$$\rho_Y = \frac{V_X}{R+h} = \dot{\lambda} \cos\alpha - \dot{\phi} \sin\alpha \sin\lambda \qquad (23)$$

$$\rho_z = \dot{\phi} \sin\lambda + \dot{\alpha}$$

Therefore

$$\dot{C}_{11} = C_{12} \rho_z - C_{13} \rho_Y$$

$$\dot{C}_{12} = C_{13} \rho_x - C_{11} \rho_z \qquad (24)$$

$$\dot{C}_{13} = C_{11} \rho_Y - C_{12} \rho_x$$

These are the necessary relationships for updating the direction cosines during vehicle motion in order to compute values of latitude and longitude.

These are computed as follows:

$$\frac{C_{12}}{C_{11}} = -\tan \alpha(t)$$

$$\alpha(t) = -\tan^{-1} \frac{C_{12}}{C_{11}} = \alpha(0) - \phi(t) - \phi_0 \qquad (25)$$

Which is easily solved for longitude.

In addition

$$\frac{C_{13}}{(C_{11}^2 + C_{12}^2)^{1/2}} = \frac{\sin \lambda}{(\cos^2\alpha \cos^2\lambda + \sin^2\alpha \cos^2\lambda)^{1/2}} = \frac{\sin \lambda}{\cos \lambda} = \tan \lambda(t) \qquad ($$

Which is solved for latitude

$$\lambda(t) = \tan^{-1} \frac{C_{13}}{(C_{11}^2 + C_{12}^2)^{1/2}} \qquad (27)$$

A block diagram of this unipolar mechanization is shown in Figure 3.
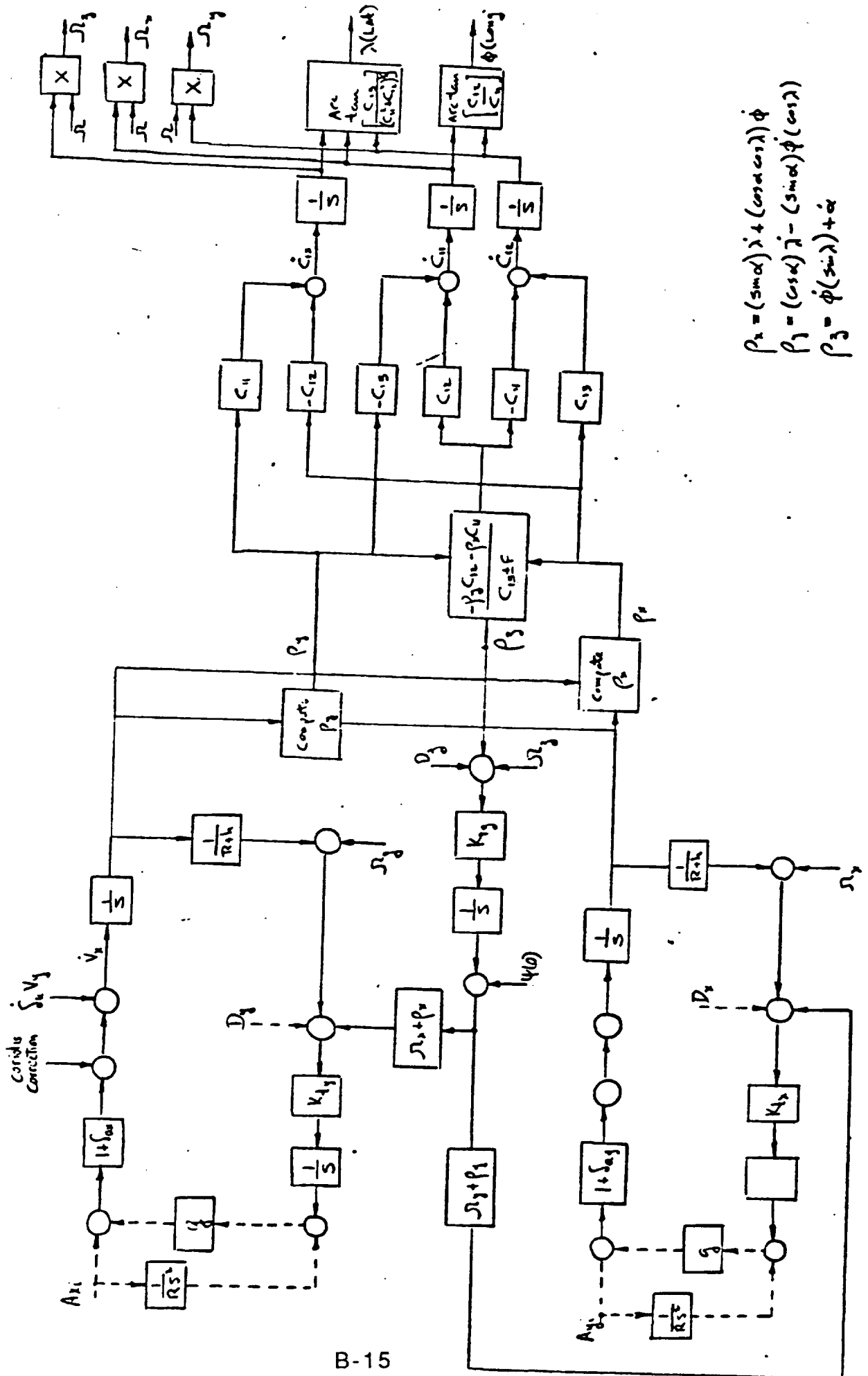
Figure 3.

$\rho_2 = (\sin\alpha)\dot{\lambda} + (\cos\alpha\cos\lambda)\dot{\phi}$

$\rho_1 = (\cos\alpha)\dot{\lambda} - (\sin\alpha)\dot{\phi}(\cos\lambda)$

$\rho_3 = \dot{\phi}(\sin\lambda) + \dot{\alpha}$

B-15
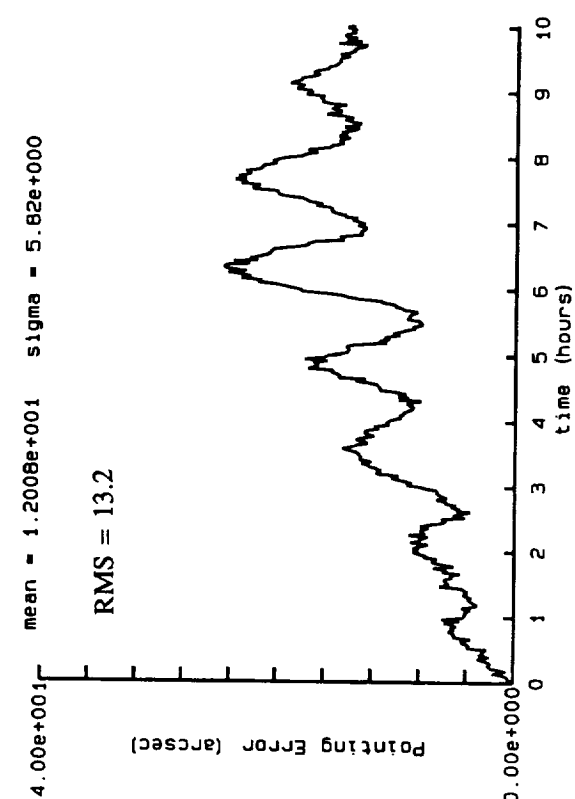
Tracking Data with an RMS Pointing Error of 13.2 arc-sec

page 1
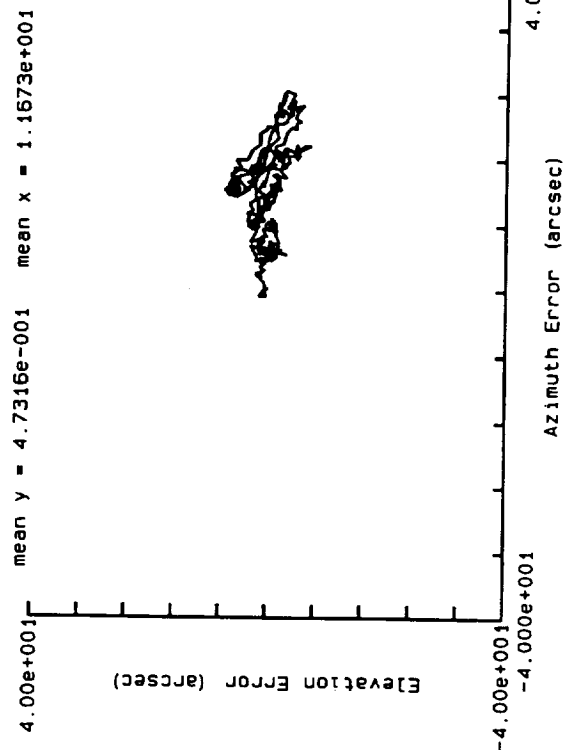
DATA FILE: 092091a.1

11-07-91

## Tracking Data with an RMS Pointing Error of 17.8 arc-sec

page 1

mean = 1.5299e+001    sigma = 8.53e+000

Azimuth Error (arcsec)
4.00e+001
-4.00e+001
0   1   2   3   4   5   6   7   8   9   10
time (hours)

mean = 8.3098e-002    sigma = 4.36e+000

Elevation Error (arcsec)
4.00e+001
-4.00e+001
0   1   2   3   4   5   6   7   8   9   10
time (hours)

mean y = 8.3098e-002    mean x = 1.5299e+001

Elevation Error (arcsec)
4.00e+001
-4.00e+001
-4.000e+001                4.000e+001
Azimuth Error (arcsec)

mean = 1.5798e+001    sigma = 8.73e+000

RMS = 17.8

Pointing Error (arcsec)
4.00e+001
0.00e+000
0   1   2   3   4   5   6   7   8   9   10
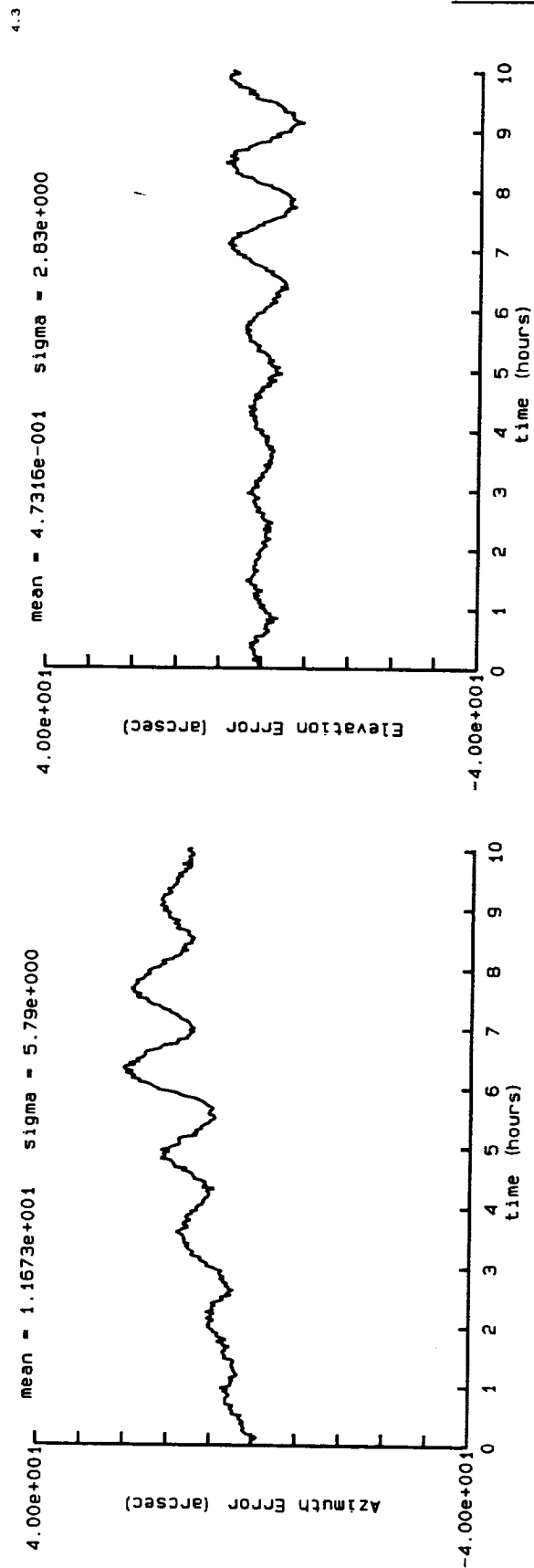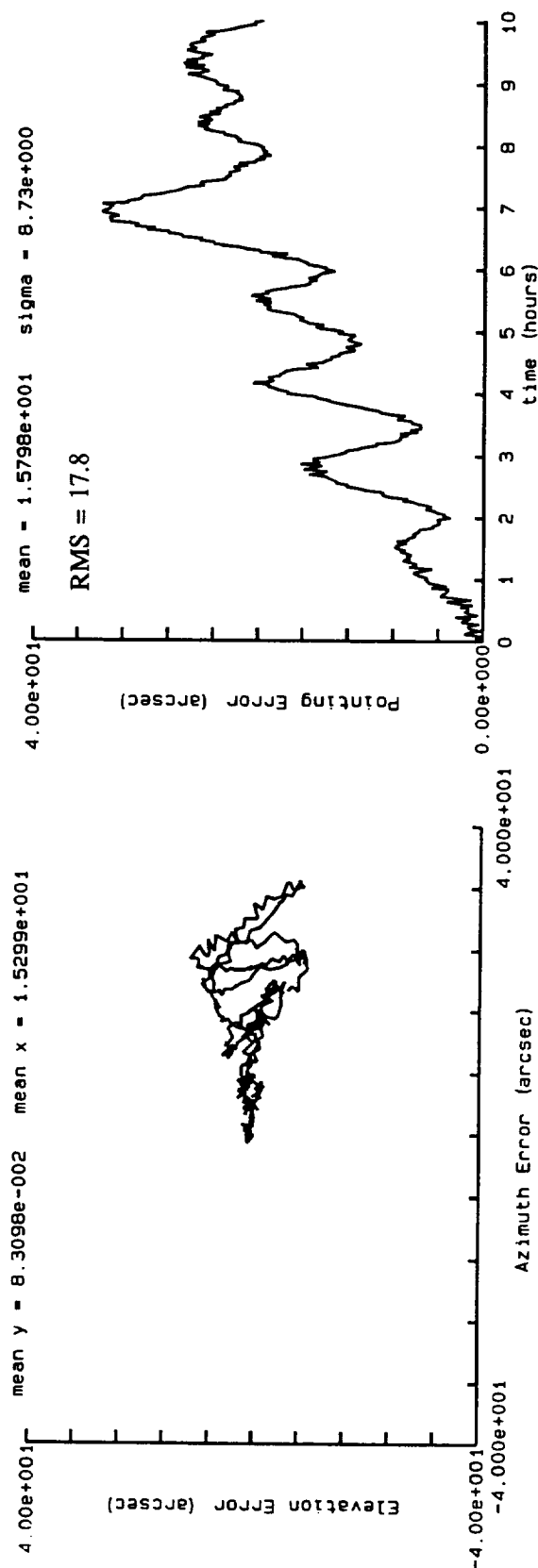time (hours)

DATA FILE: 092091a.2                                11-07-91

4.3

## Tracking Data with an RMS Pointing Error of 19.9 arc-sec

page 1

mean = 1.7220e+001    sigma = 1.04e+001

mean = 4.5272e-001    sigma = 1.62e+000

mean = 1.7569e+001    sigma = 9.94e+000

RMS = 19.9

mean y = 4.5272e-001    mean x = 1.7220e+001

Azimuth Error (arcsec)

Elevation Error (arcsec)

Pointing Error (arcsec)

Elevation Error (arcsec)

time (hours)

time (hours)

time (hours)

4.00e+001

-4.00e+001

4.00e+001

-4.00e+001

4.00e+001

0.00e+000

4.00e+001
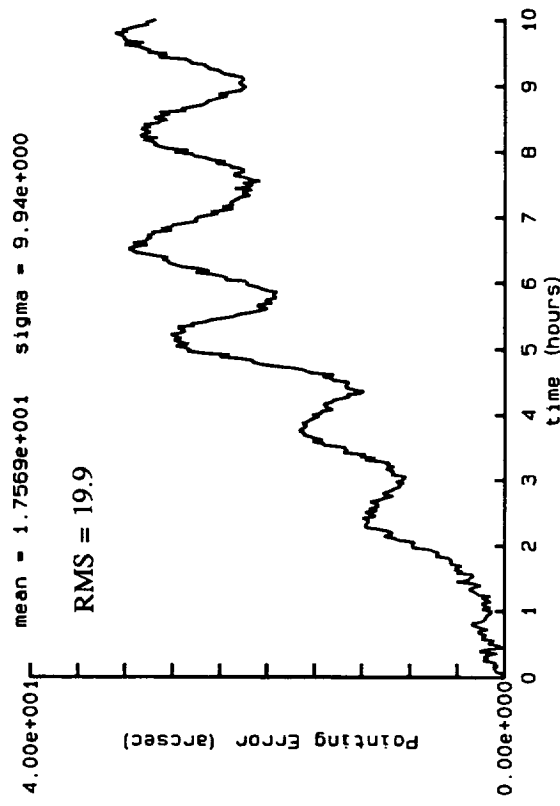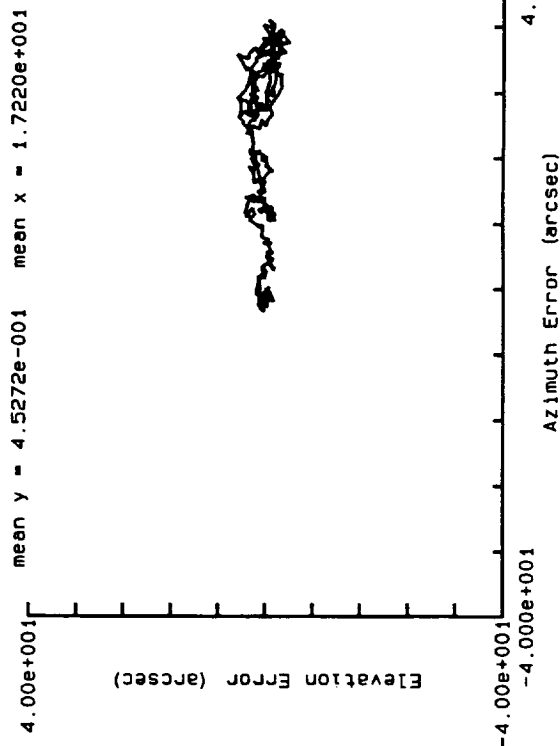
-4.00e+001

4.000e+001

-4.000e+001

DATA FILE: 092091a.3

11-07-91

4.3

C-3

# Tracking Data with an RMS Pointing Error of 12.8 arc-sec

page 1

mean = -7.6729e-002    sigma = 1.24e+001

Azimuth Error (arcsec)

time (hours)

mean = -9.0138e-001    sigma = 3.85e+000

Elevation Error (arcsec)

time (hours)

mean y = -9.0138e-001    mean x = -7.6729e-002

Elevation Error (arcsec)

Azimuth Error (arcsec)

mean = 1.1302e+001    sigma = 6.39e+000

RMS = 12.8

Pointing Error (arcsec)

time (hours)

C-4

DATA FILE: 092091a.4
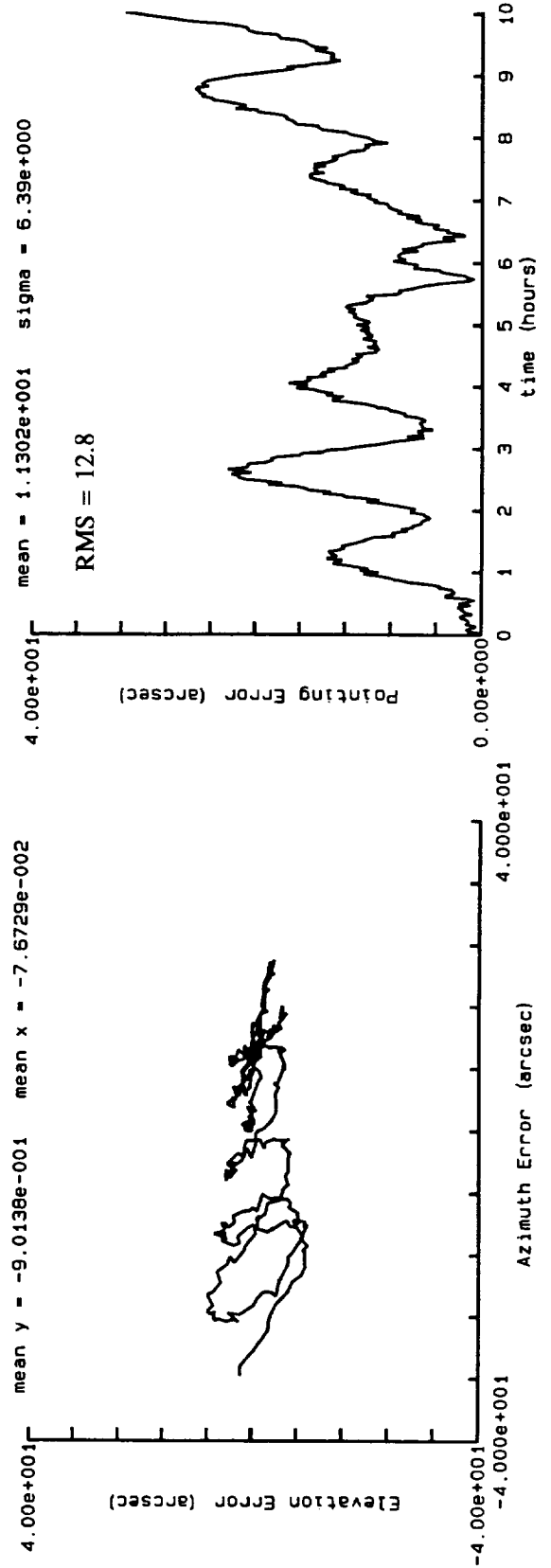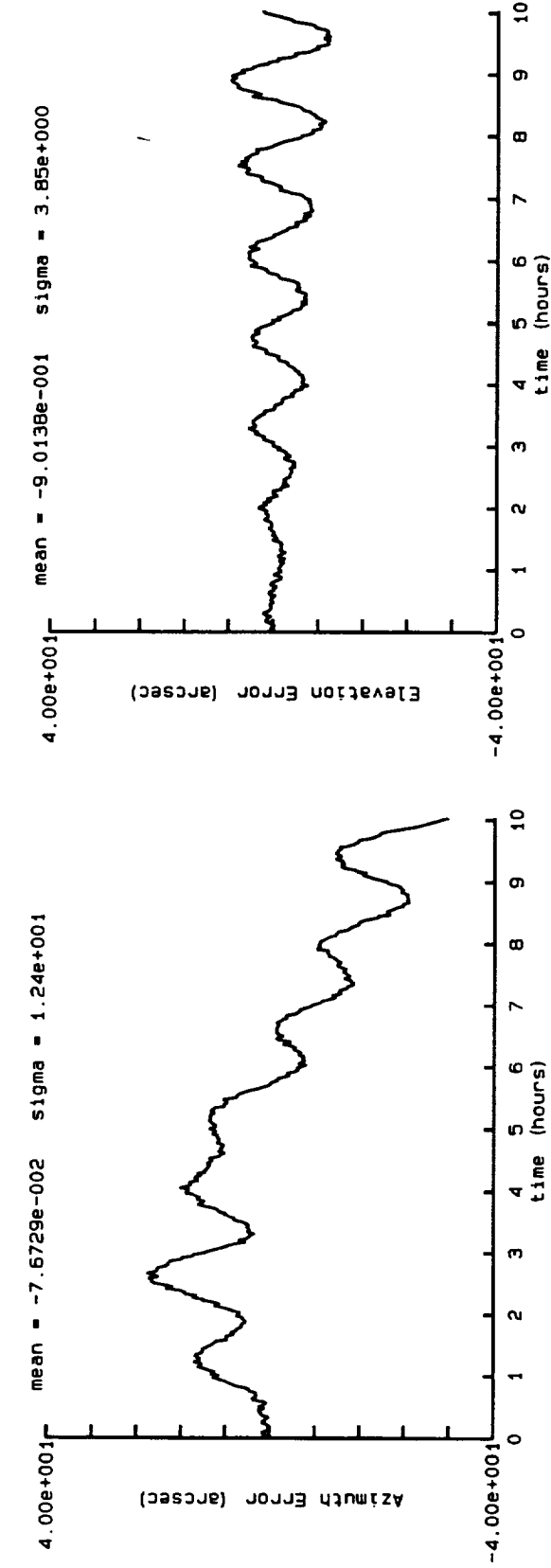
11-07-91

# Tracking Data with an RMS Pointing Error of 18.8 arc-sec

page 1

mean = 1.6596e+001    sigma = 8.58e+000

Azimuth Error (arcsec)

time (hours)

mean = 6.1818e-001    sigma = 3.57e+000

Elevation Error (arcsec)

time (hours)

mean y = 6.1818e-001    mean x = 1.6596e+001

Elevation Error (arcsec)

Azimuth Error (arcsec)

mean = 1.7217e+001    sigma = 8.10e+000

RMS = 18.8

Pointing Error (arcsec)

time (hours)

C-5

DATA FILE: 092091a.5
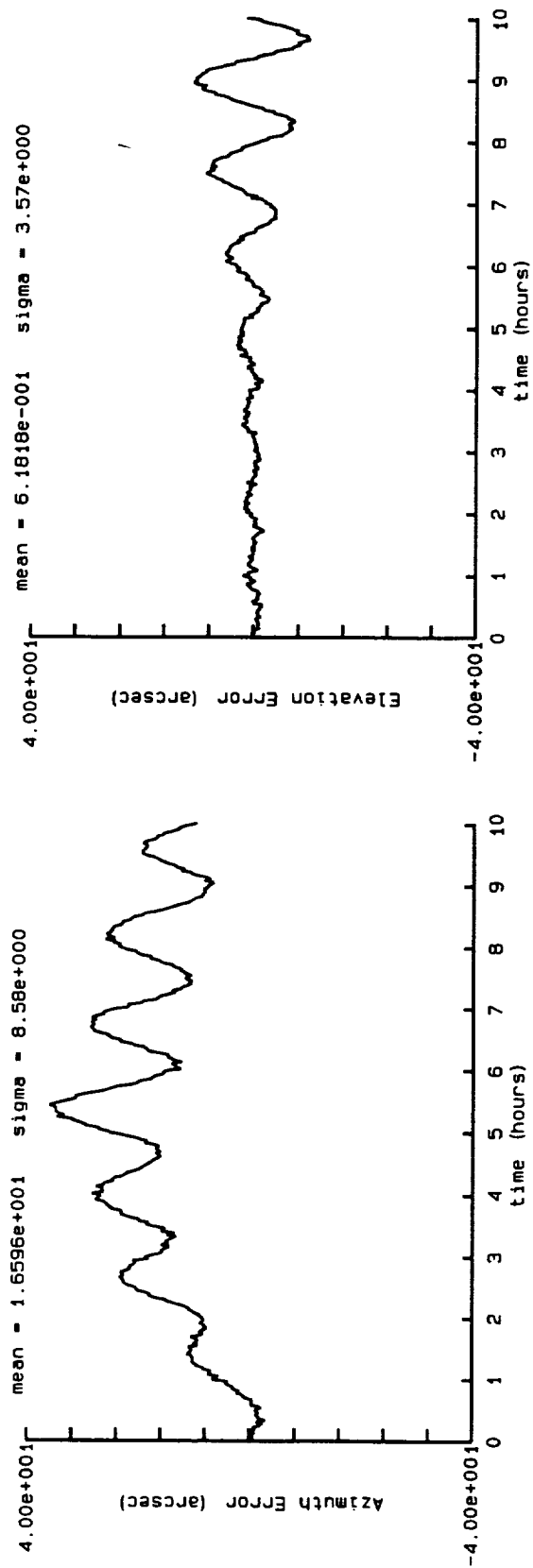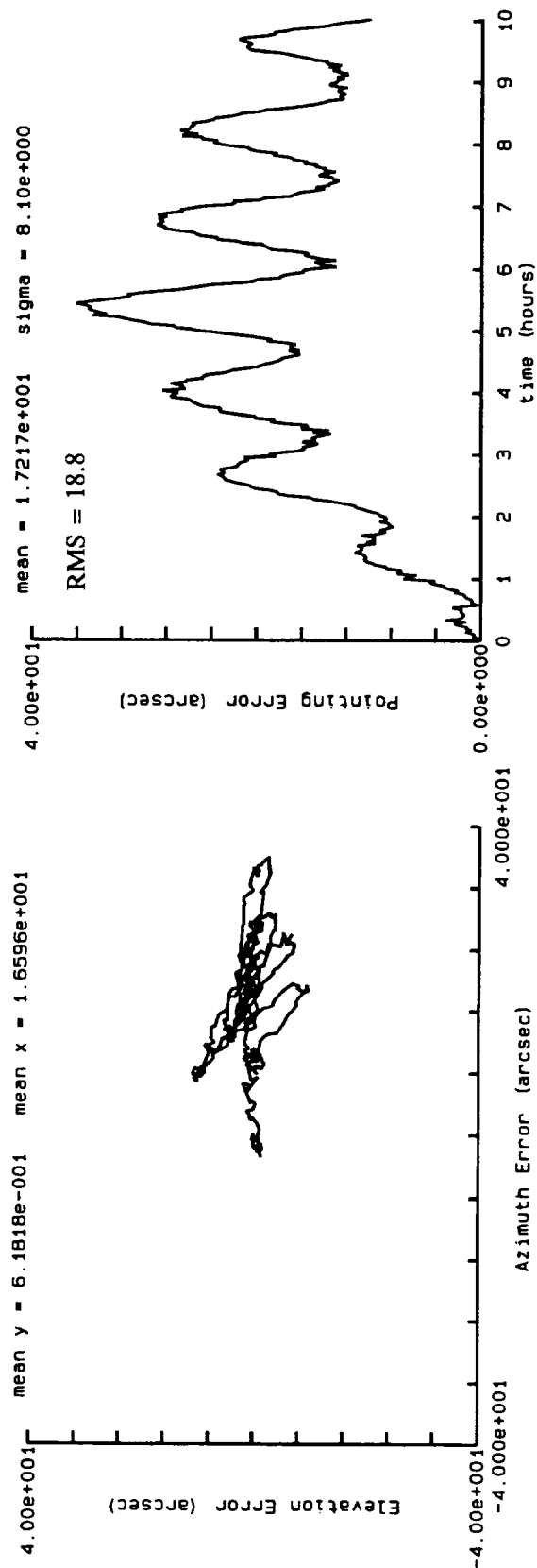
11-07-91

# Tracking Data with an RMS Pointing Error of 13.6 arc-sec

page 1

mean = 3.6110e+000    sigma = 1.31e+001

Azimuth Error (arcsec)

time (hours)

mean = 3.1390e-001    sigma = 2.10e+000

Elevation Error (arcsec)

time (hours)

mean x = 3.6110e+000

mean y = 3.1390e-001

Elevation Error (arcsec)

Azimuth Error (arcsec)

mean = 1.1581e+001    sigma = 7.43e+000

RMS = 13.6

Pointing Error (arcsec)

time (hours)
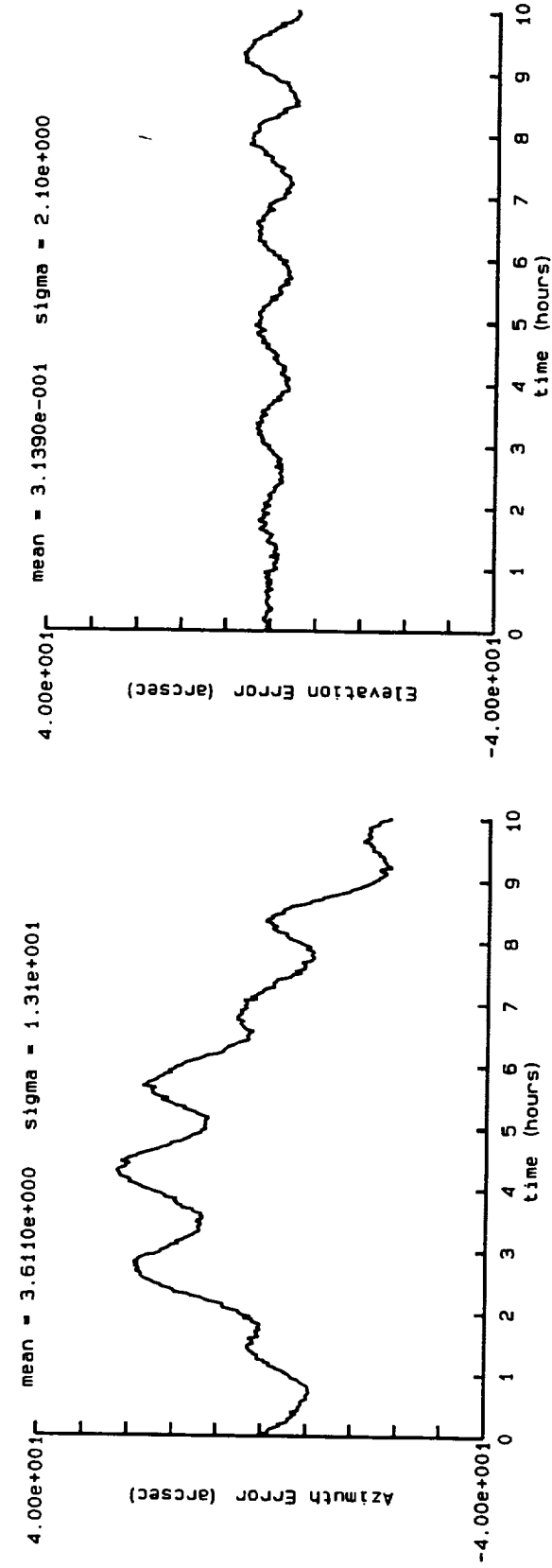
C-6
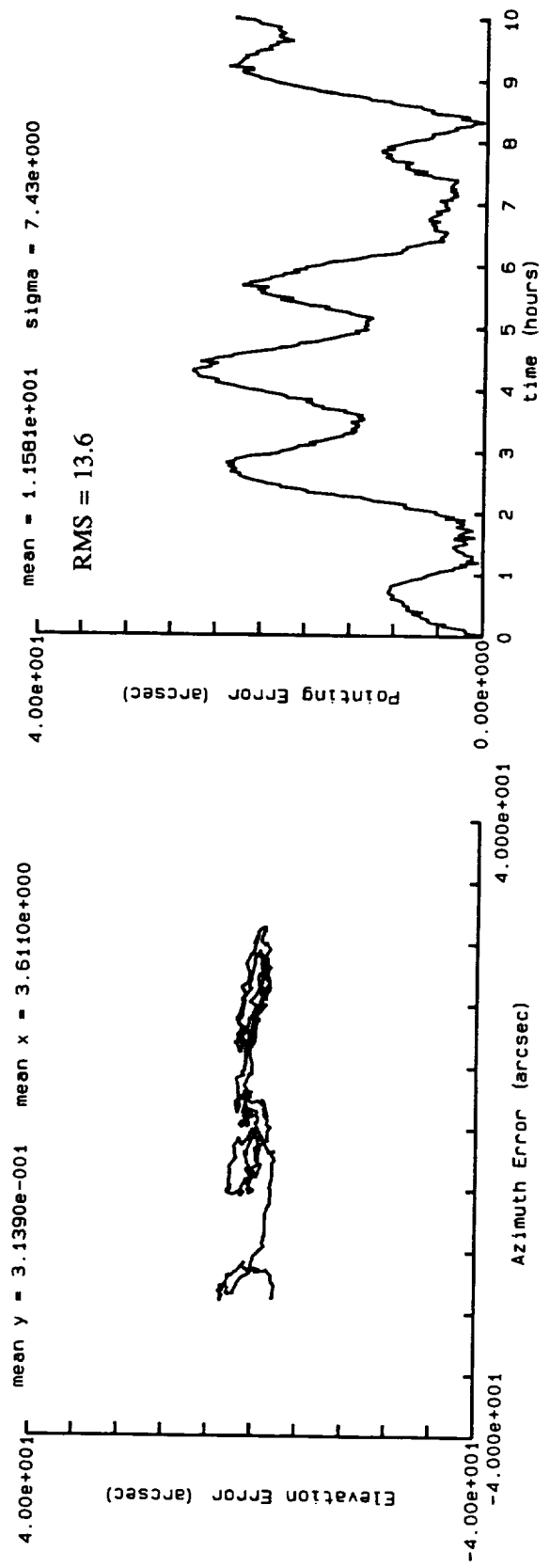
DATA FILE: 092591b.1

11-07-91

## Tracking Data after Re-calibration
## RMS Pointing Error of 11.2 arc-sec

page 1

mean = 4.4580e+000    sigma = 9.89e+000

4.00e+001

Azimuth Error (arcsec)

-4.00e+001

0  1  2  3  4  5  6  7  8  9  10
time (hours)

mean = -4.0698e-001    sigma = 2.67e+000

4.00e+001

Elevation Error (arcsec)

-4.00e+001

0  1  2  3  4  5  6  7  8  9  10
time (hours)

mean y = -4.0698e-001    mean x = 4.4580e+000

4.00e+001

Elevation Error (arcsec)

-4.000e+001

-4.000e+001          Azimuth Error (arcsec)          4.000e+001

mean = 9.1904e+000    sigma = 6.35e+000

RMS = 11.2

4.00e+000

Pointing Error (arcsec)

0.00e+000

0  1  2  3  4  5  6  7  8  9  10
time (hours)

C-7

DATA FILE: 100891b.1

11-07-91

# Best Tracking Data after Re-calibration
## RMS Pointing Error of 4.9 arc-sec

page 1

mean = 2.5350e+000    sigma = 3.81e+000

4.00e+001

Azimuth Error (arcsec)

-4.00e+001

0  1  2  3  4  5  6  7  8  9  10
time (hours)

mean = -4.5330e-002    sigma = 1.73e+000

4.00e+001

Elevation Error (arcsec)

-4.00e+001

0  1  2  3  4  5  6  7  8  9  10
time (hours)

mean y = -4.5330e-002    mean x = 2.5350e+000

4.00e+001

Elevation Error (arcsec)

-4.00e+001

-4.000e+001    Azimuth Error (arcsec)    4.000e+001

mean = 4.2245e+000    sigma = 2.46e+000

RMS = 4.9

4.00e+001

Pointing Error (arcsec)

0.00e+000

0  1  2  3  4  5  6  7  8  9  10
time (hours)
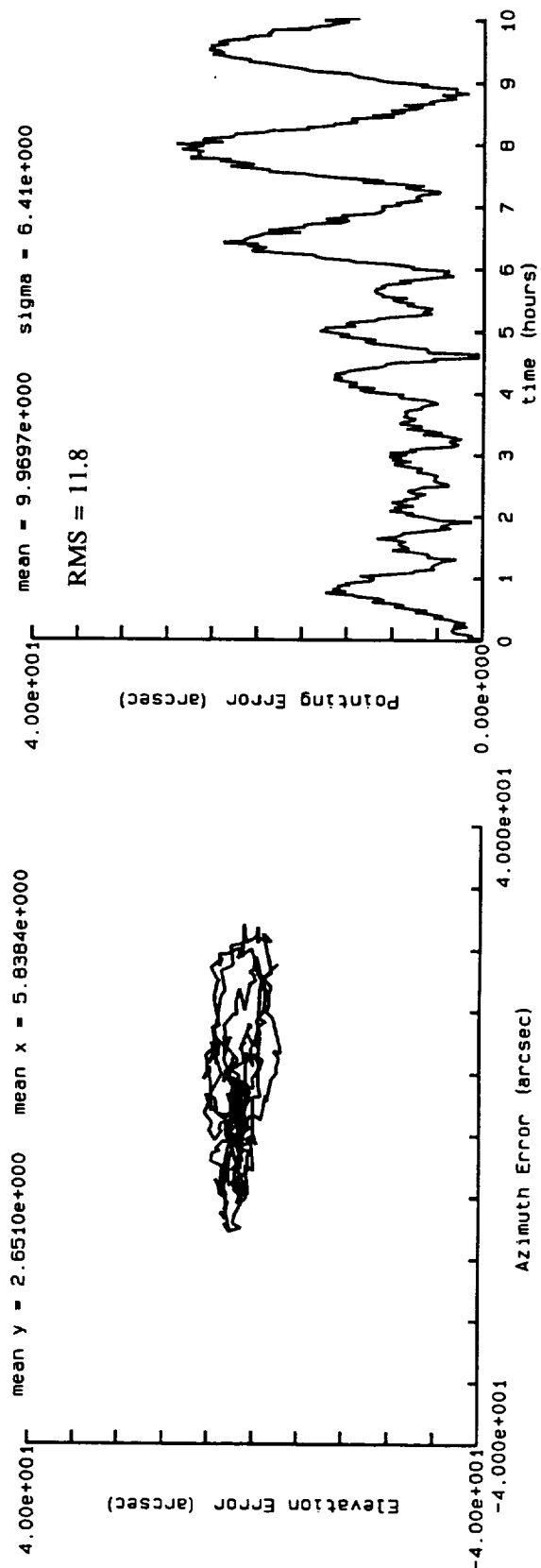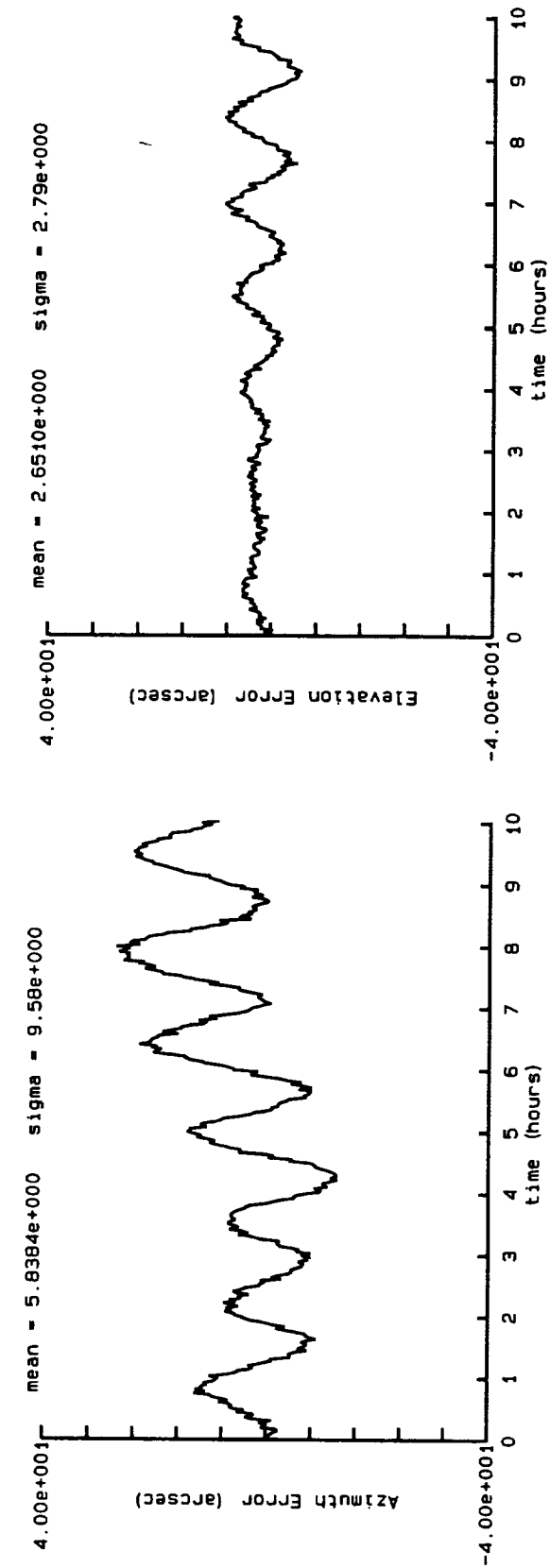
C-8

DATA FILE: 100891b.2

11-07-91

4.3

# Tracking data at 60 deg Elevation
## Following Acquisition of 20 azimuth and 60 Elevation
### RMS Pointing Error of 11.8 arc-sec

page 1

mean = 5.8384e+000    sigma = 9.58e+000



Azimuth Error (arcsec)

time (hours)

mean = 2.6510e+000    sigma = 2.79e+000



Elevation Error (arcsec)

time (hours)

mean y = 2.6510e+000    mean x = 5.8384e+000



Elevation Error (arcsec)

Azimuth Error (arcsec)

mean = 9.9697e+000    sigma = 6.41e+000

RMS = 11.8



Pointing Error (arcsec)

time (hours)

C-9

DATA FILE: 100991b.1

11-07-91
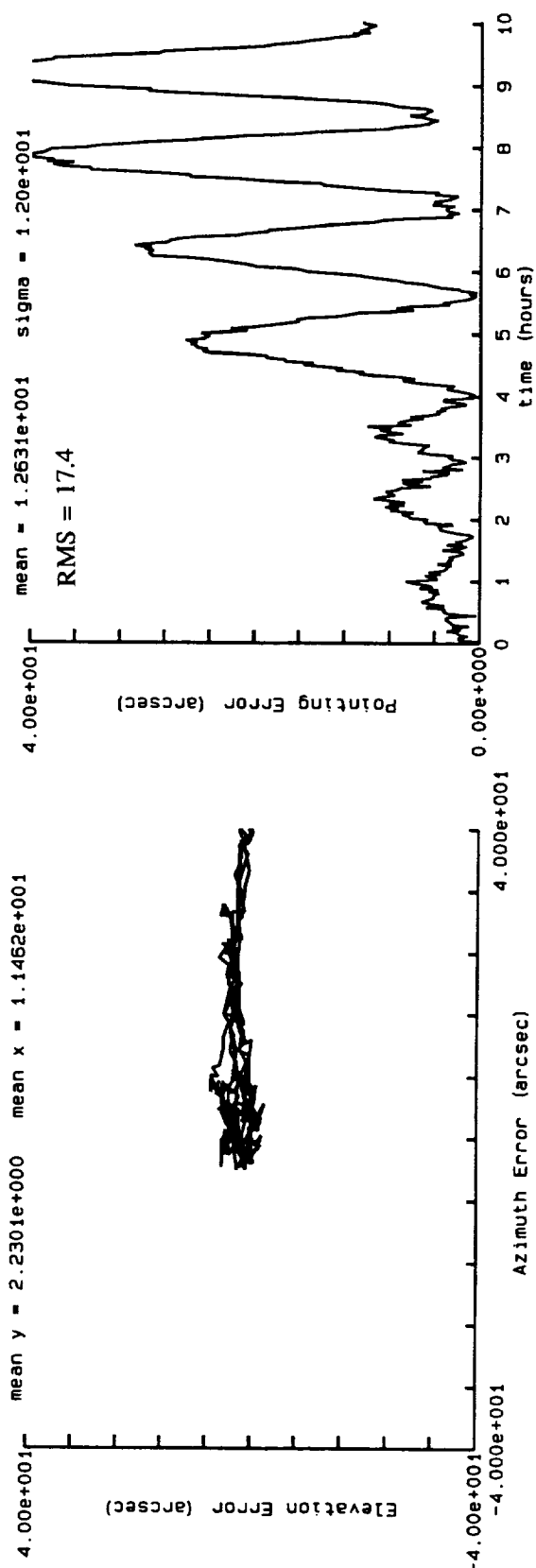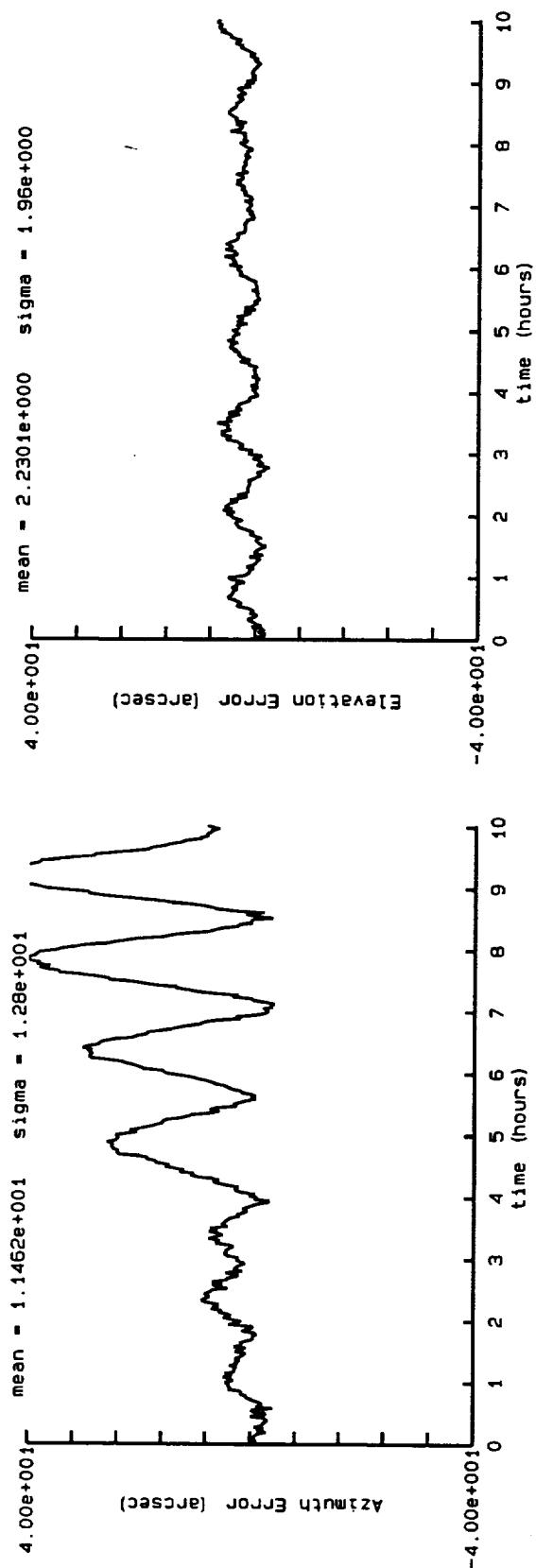
Tracking data at 60 deg Elevation
RMS Pointing Error of 17.4 arc-sec

page 1

DATA FILE: 100991b.2

11-07-91

C-10
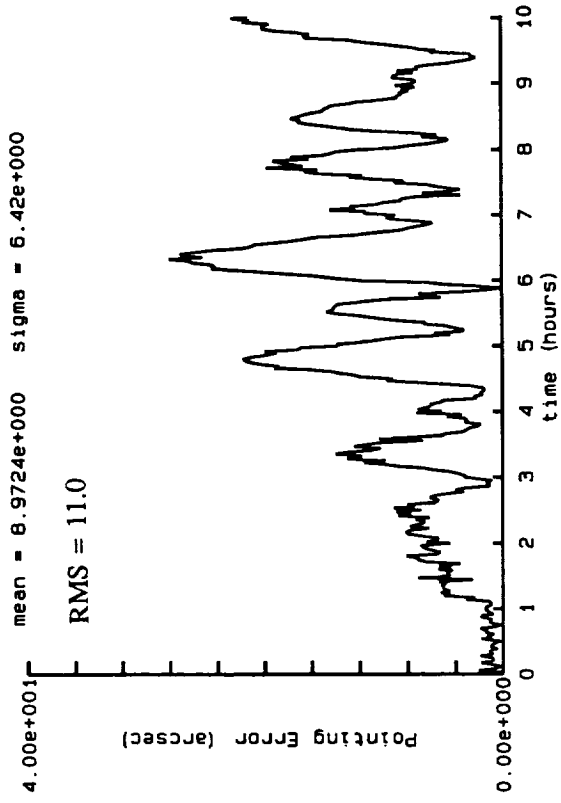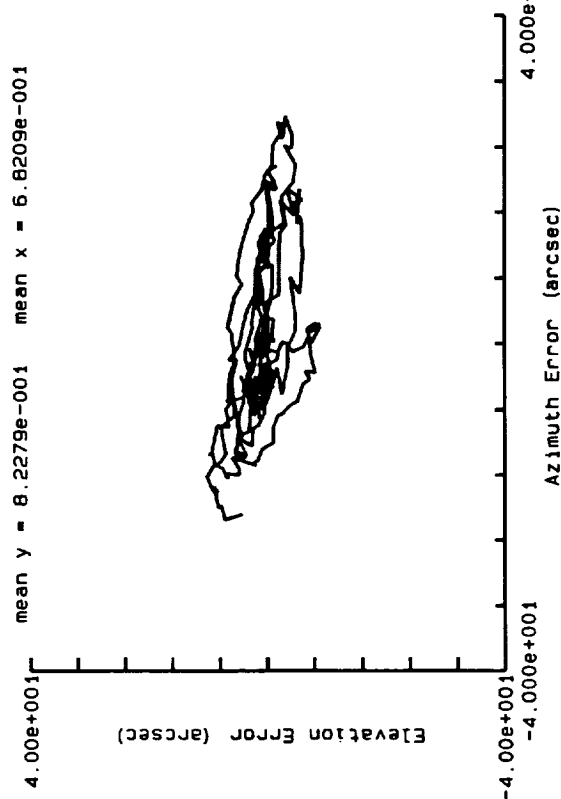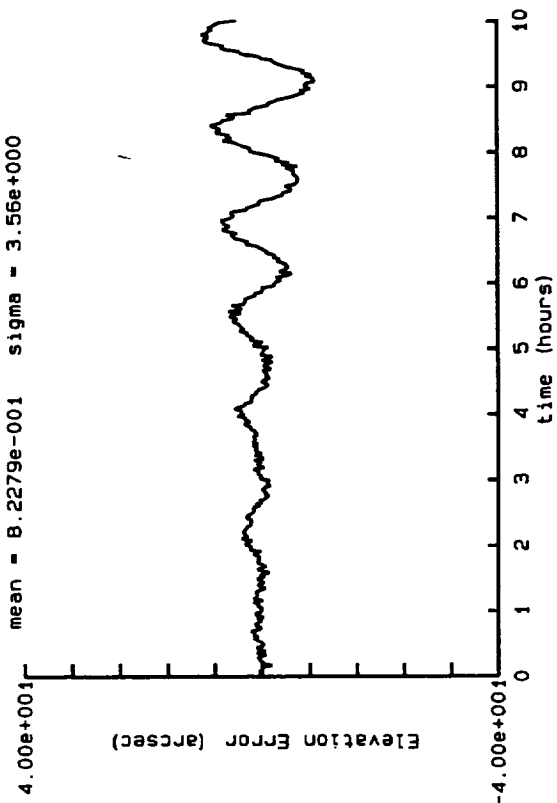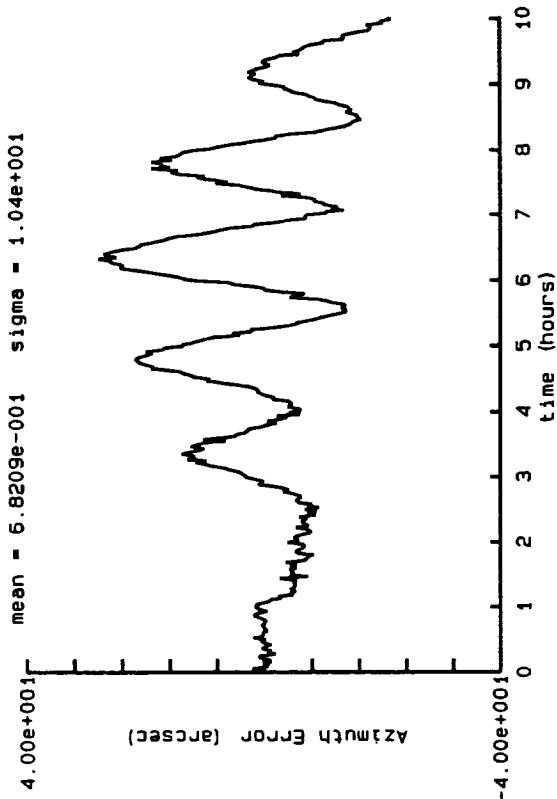
Tracking data at 60 deg Elevation
RMS Pointing Error of 11.0 arc-sec

page 1

mean = 6.8209e-001    sigma = 1.04e+001

mean = 8.2279e-001    sigma = 3.55e+000

mean = 8.9724e+000    sigma = 6.42e+000

RMS = 11.0

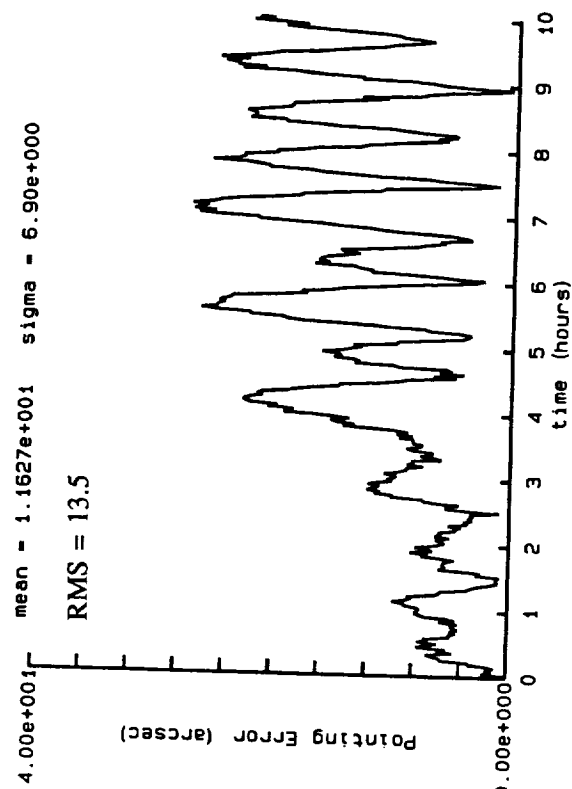mean y = 8.2279e-001    mean x = 6.8209e-001

DATA FILE: 101091a.1

11-07-91

C-11

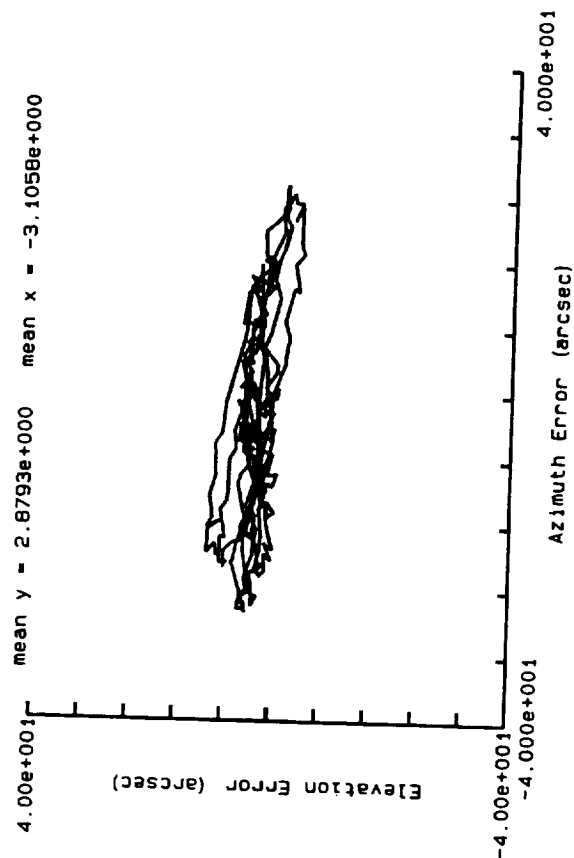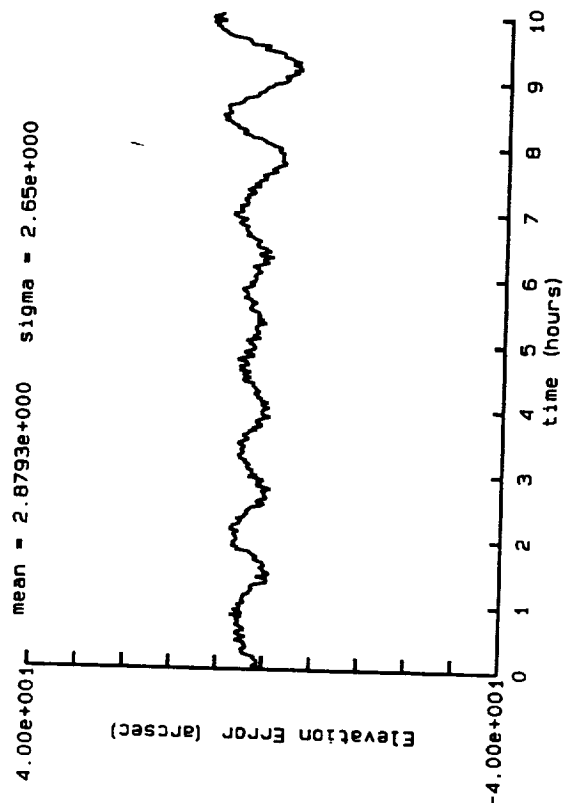# Tracking data at 60 deg Elevation
## RMS Pointing Error of 13.5 arc-sec

page 1

mean = -3.1058e+000    sigma = 1.26e+001

Azimuth Error (arcsec)

-4.00e+001    4.00e+001

0  1  2  3  4  5  6  7  8  9  10
time (hours)

mean = 2.8793e+000    sigma = 2.65e+000

Elevation Error (arcsec)

-4.00e+001    4.00e+001

0  1  2  3  4  5  6  7  8  9  10
time (hours)

4.3

mean y = 2.8793e+000    mean x = -3.1058e+000

Elevation Error (arcsec)

-4.000e+001    4.00e+001

-4.000e+001    4.000e+001
Azimuth Error (arcsec)

mean = 1.1627e+001    sigma = 6.90e+000

RMS = 13.5

Pointing Error (arcsec)

0.00e+000    4.00e+001

0  1  2  3  4  5  6  7  8  9  10
time (hours)

11-07-91

DATA FILE: 101091a.2

C-12

# Appendix D

## Gyro Data over Temperature and Thermal Model

### STATIC TEMPERATURE DATA

Gyro: Z2002
Data file: 06-07-90.b01

| chamber temp. (deg.C) | output (deg/hr) | random walk (deg/rt-hr) | gyro T. (deg.C) | T. dev. (deg.C) | delta T (deg.C) | dT dev. (deg.C) |
|---|---|---|---|---|---|---|
| 25 | 9.8246 | 0.0003 | 26.24 | 0.20 | -0.18 | 0.01 |
| 45 | 9.8235 | 0.0011 | 44.59 | 0.19 | -0.11 | 0.01 |
| 70 | 9.8233 | 0.0008 | 66.88 | 0.19 | -0.06 | 0.01 |
| 45 | 9.8255 | 0.0006 | 42.12 | 0.31 | -0.66 | 0.02 |
| 25 | 9.8238 | 0.0007 | 27.08 | 0.13 | -0.09 | 0.00 |
| 5 | 9.8239 | 0.0005 | 8.21 | 0.20 | -0.16 | 0.01 |
| -15 | 9.8230 | 0.0008 | -10.30 | 0.30 | -0.23 | 0.01 |
| -35 | 9.8238 | 0.0004 | -26.70 | 1.61 | -0.24 | 0.01 |
| -55 | 9.8230 | 0.0011 | -47.87 | 0.41 | -0.33 | 0.01 |
| -35 | 9.8240 | 0.0008 | -29.73 | 0.41 | -0.32 | 0.01 |

summary
   peak to peak variation of 25 degree points = 0.0008 (deg/hr)
   average random walk = 0.0007 (deg/rt-hr)

thermal model
output = bias + local vertical earth rate + k0*dt +
   k1*T + k2*T^2 + k3*T^3 + k4*T^4
      where T = gyro temperature - 25

   bias = 2.3160e-001 (deg/hr),
    k0  = -5.000e-003 (deg/hr/deg.C)
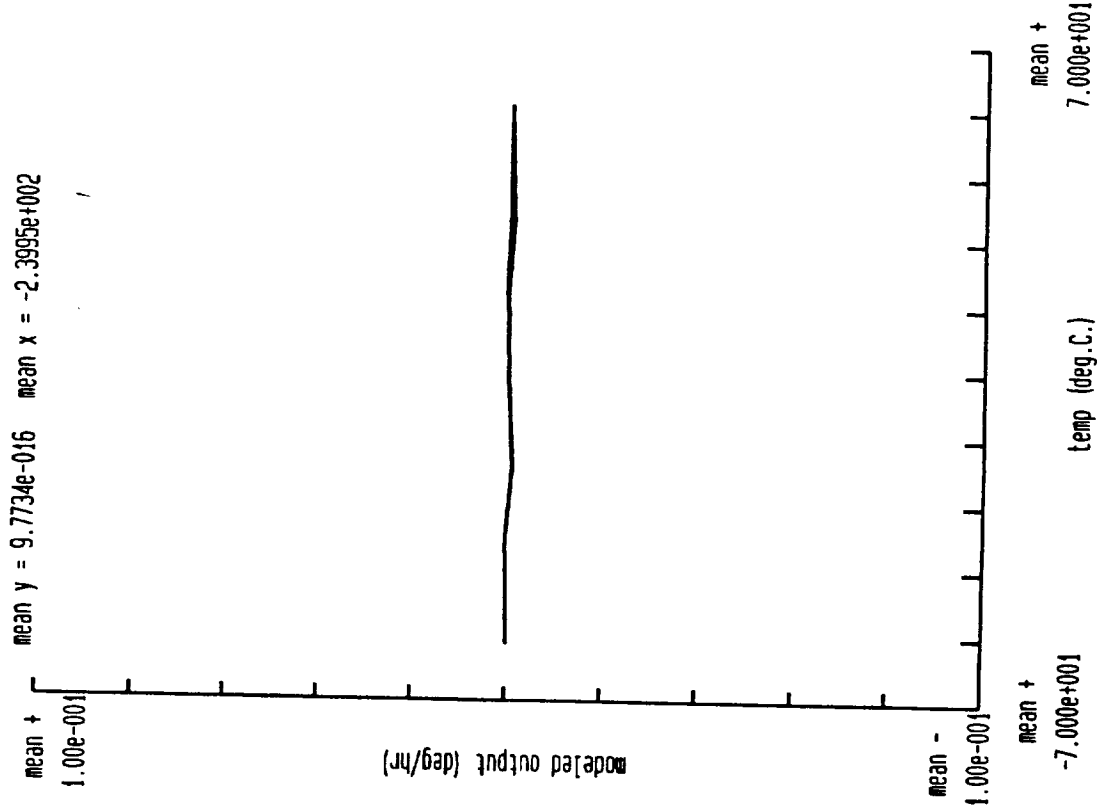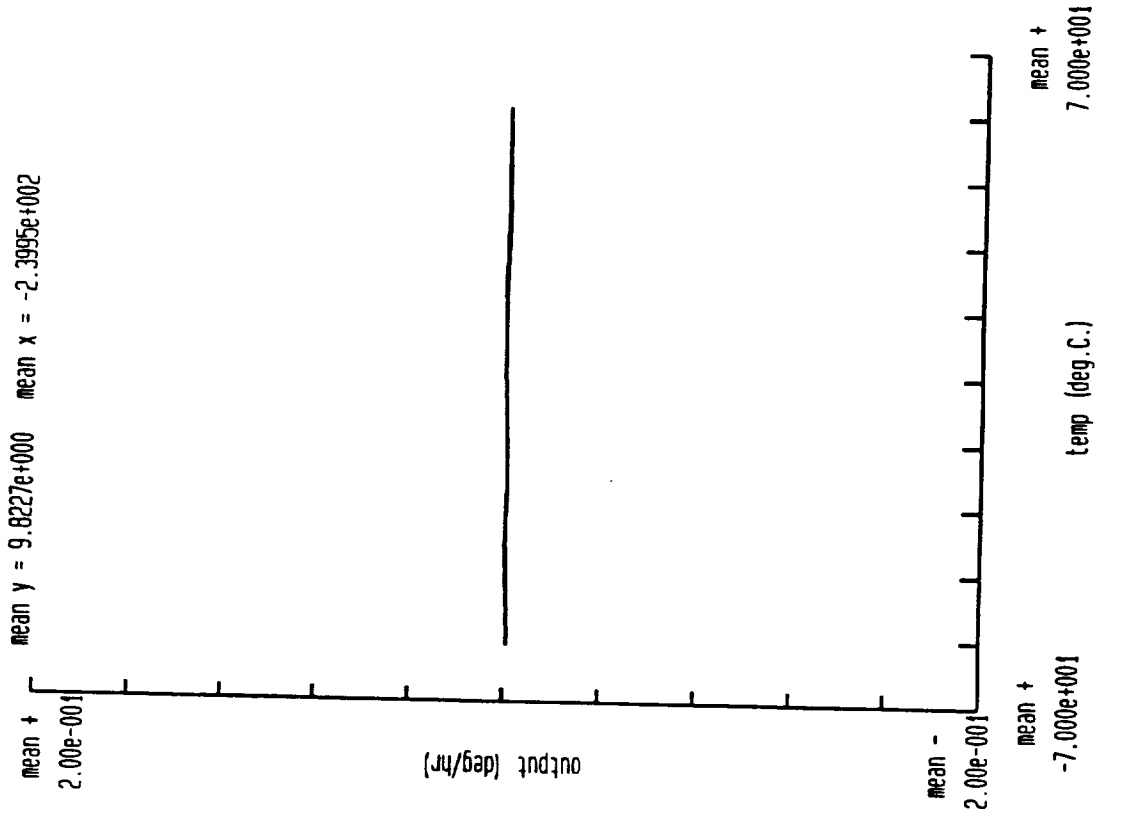    k1  = 4.278e-003 (deg/hr/deg.C)
    k2  = 2.713e-005 (deg/hr/deg.C^2)
    k3  = 7.511e-008 (deg/hr/deg.C^3)
    k4  = 7.643e-011 (deg/hr/deg.C^4)


bias repeatability = 0.0005 (deg/hr 1 sigma)

page 1    Z2002: 5 day bias repeatability test

mean y = 9.8227e+000    mean x = -2.3995e+002



mean y = 9.7734e-016    mean x = -2.3995e+002



GYRO: Z2002    DATA FILE: 06-07-90.b01

11-08-91

D-2

page 1    Z2002: 5 day bias repeatability test

GYRO: Z2002    DATA FILE: 06-07-90.b01

11-08-91

D-3
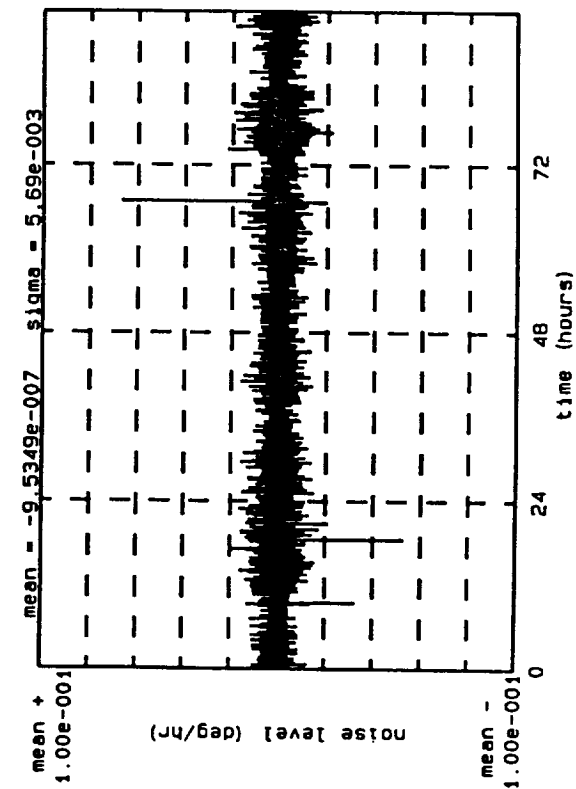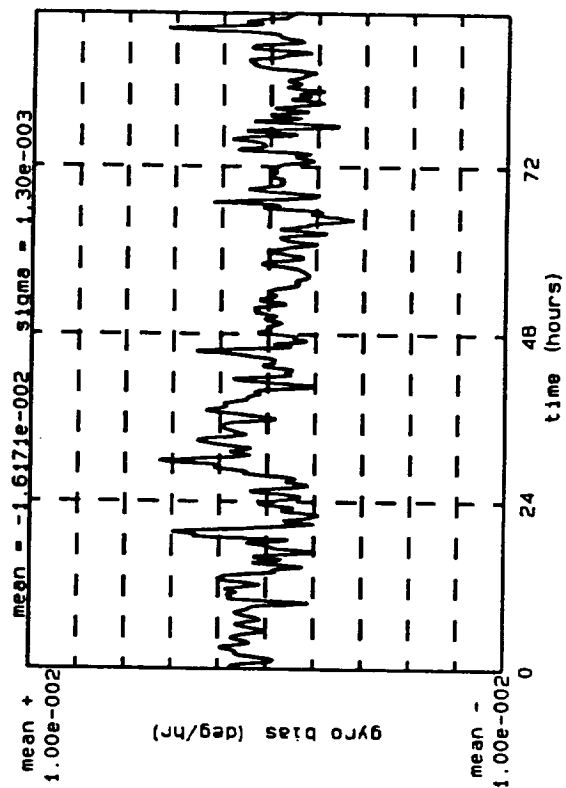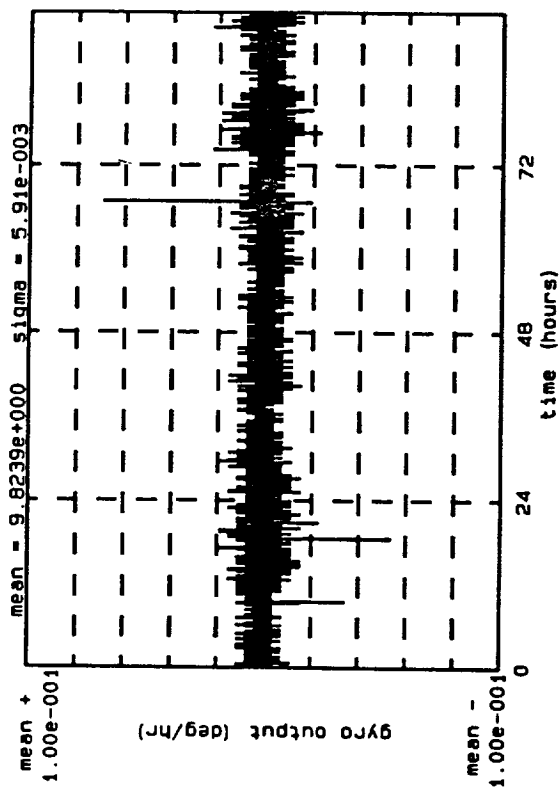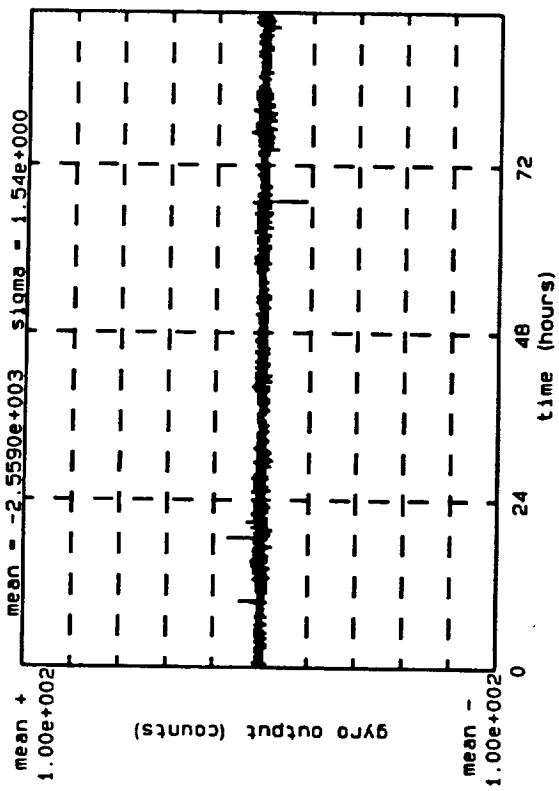
page 2    Z2002:  5 day bias repeatability test

mean = 1.0140e+001    sigma = 3.45e+001

mean = -2.5834e-001    sigma = 1.64e-001

gyro temp (deg C.)

delta temp (deg C.)

mean = 1.4453e+000    sigma = 4.78e+000

mean = 1.7944e+000    sigma = 8.42e-002

clc integrator (v dc)

dcint

time (hours)

GYRO:  Z2002    DATA FILE: 06-07-90.b01

11-08-91

D-4

page 3    Z2002: 5 day bias repeatability test

mean = -1.0485e+000   sigma = 8.79e-004

total current (mAmp)
mean +
1.00e-002
mean -
1.00e-002

0    24    48    72
time (hours)

mean = 1.3092e-005   sigma = 3.63e-005

delta current (mAmp)
mean +
1.00e-003
mean -
1.00e-003

0    24    48    72
time (hours)
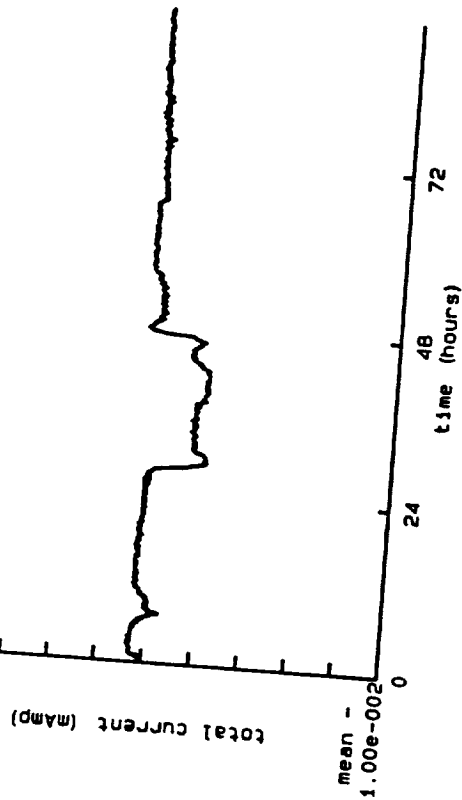
mean = 7.0999e-001   sigma = 3.23e-003

pickoff (rms V)
mean +
1.00e-001
mean -
1.00e-001

0    24    48    72
time (hours)
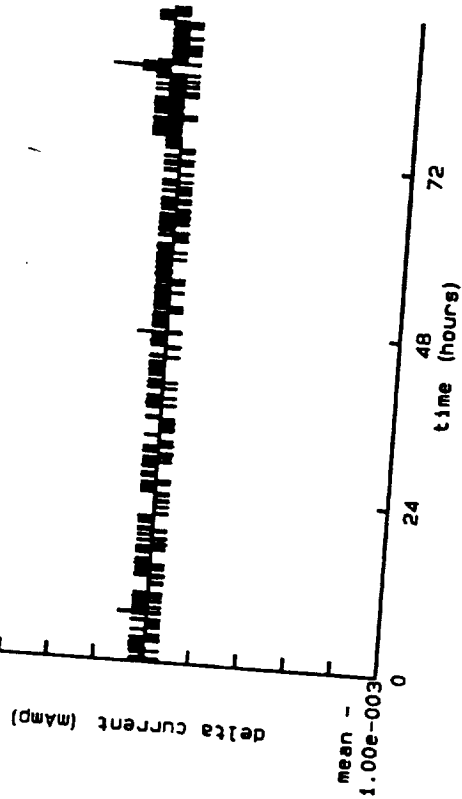
mean = 7.4522e+000   sigma = 3.79e+001

chamber temp (deg. c.)
mean +
1.00e+002
mean -
1.00e+002

0    24    48    72
time (hours)

GYRO: Z2002    DATA FILE: 06-07-90.b01

11-08-91

D-5
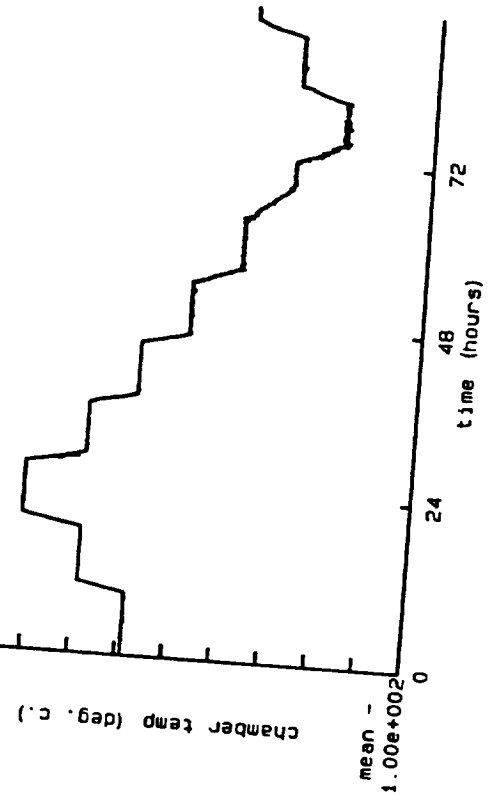
## STATIC TEMPERATURE DATA

Gyro: B2003
Data file: 09-29-89.a01

| chamber temp. (deg.C) | output (deg/hr) | random walk (deg/rt-hr) | gyro T. (deg.C) | T. dev. (deg.C) | delta T (deg.C) | dT dev. (deg.C) |
|---|---|---|---|---|---|---|
| 25 | 9.7887 | 0.0005 | 26.04 | 0.09 | 0.00 | 0.00 |
| 45 | 9.7872 | 0.0006 | 44.45 | 0.21 | 0.00 | 0.00 |
| 70 | 9.7849 | 0.0005 | 67.80 | 0.21 | -0.00 | 0.00 |
| 45 | 9.7877 | 0.0005 | 45.37 | 0.23 | 0.00 | 0.00 |
| 25 | 9.7896 | 0.0005 | 26.82 | 0.17 | 0.00 | 0.00 |
| 5 | 9.7897 | 0.0006 | 7.94 | 0.15 | 0.00 | 0.00 |
| -15 | 9.7923 | 0.0006 | -10.74 | 0.07 | 0.00 | 0.00 |
| -35 | 9.7933 | 0.0008 | -28.83 | 0.41 | 0.01 | 0.01 |
| -55 | 9.7960 | 0.0006 | -47.15 | 0.38 | -0.00 | 0.00 |
| -35 | 9.7939 | 0.0008 | -30.44 | 0.37 | 0.00 | 0.00 |
| -15 | 9.7924 | 0.0005 | -11.67 | 0.30 | 0.00 | 0.00 |
| 5 | 9.7906 | 0.0006 | 7.22 | 0.26 | 0.01 | 0.00 |
| 25 | 9.7899 | 0.0006 | 25.88 | 0.28 | 0.01 | 0.00 |

summary
  peak to peak variation of 25 degree points = 0.0012 (deg/hr)
  average random walk = 0.0006 (deg/rt-hr)

thermal model
output = bias + local vertical earth rate + k0*dt +
      k1*T + k2*T^2 + k3*T^3 + k4*T^4
          where T = gyro temperature - 25

  bias = -1.3823e-001 (deg/hr),
  k0  = 0.000e+000 (deg/hr/deg.C)
  k1  = -8.686e-004 (deg/hr/deg.C)
  k2  = -2.561e-006 (deg/hr/deg.C^2)
  k3  = -4.281e-010 (deg/hr/deg.C^3)
  k4  = 6.516e-012 (deg/hr/deg.C^4)

bias repeatability = 0.0004 (deg/hr 1 sigma)

D-6

page 1     B2003: re-run 5 day bias repeatability test

mean y = 9.7905e+000    mean x = -2.4056e+002

mean +
2.00e-001

output (deg/hr)

mean -
2.00e-001

mean +
-7.000e+001

temp (deg.C.)

mean +
7.000e+001

mean y = 1.4780e-016    mean x = -2.4056e+002

mean +
1.00e-001

modeled output (deg/hr)

mean -
1.00e-001

mean +
-7.000e+001

temp (deg.C.)

mean +
7.000e+001

GYRO:  B2003    DATA FILE: 09-29-89.a01

11-08-91

4.3

page 1     B2003: re-run 5 day bias repeatability test     4.3

mean = 9.7905e+000   sigma = 7.31e-003
gyro output (deg/hr)
mean + 1.00e-001
mean - 1.00e-001
time (hours)
0     24     48     72     96

mean = 4.9405e-008   sigma = 6.66e-003
noise level (deg/hr)
mean + 1.00e-001
mean - 1.00e-001
time (hours)
0     24     48     72     96

mean = -2.5502e+003   sigma = 6.38e+000
gyro output (counts)
mean + 1.00e+003
mean - 1.00e+003
time (hours)
0     24     48     72     96

mean = -4.9591e-002   sigma = 2.92e-003
gyro bias (deg/hr)
mean + 1.00e-002
mean - 1.00e-002
time (hours)
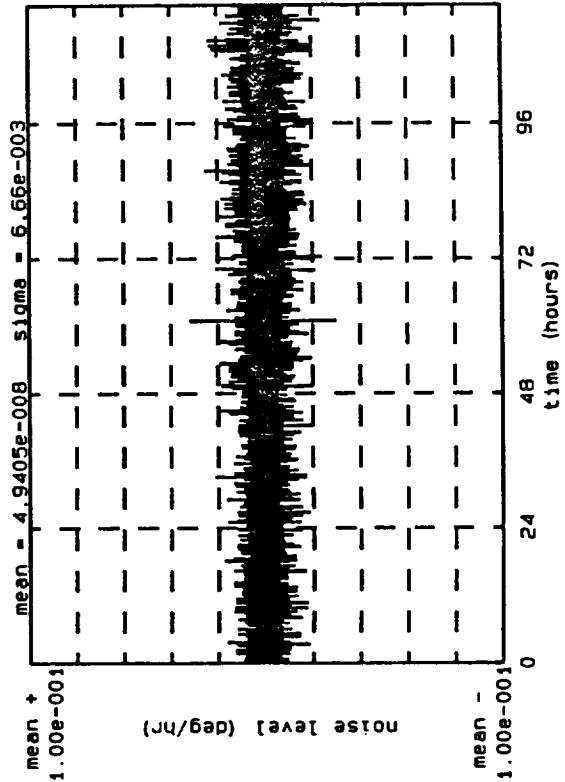0     24     48     72     96

11-08-91

GYRO: B2003     DATA FILE: 09-29-89.a01

page 2    B2003: re-run 5 day bias repeatability test

mean = 9.2781e+000    sigma = 3.23e+001

gyro temp (deg C.)

9.00e+001

-6.00e+001

mean = 2.4172e-003    sigma = 4.34e-003

delta temp (deg C.)

1.00e+000

-1.00e+000

mean = -1.6455e+000    sigma = 1.83e+000

clc integrator (V dc)

1.00e+001

-1.00e+001

mean = 2.8951e+000    sigma = 1.38e-001

dcint

mean +
1.00e+000

mean -
1.00e+000

time (hours)
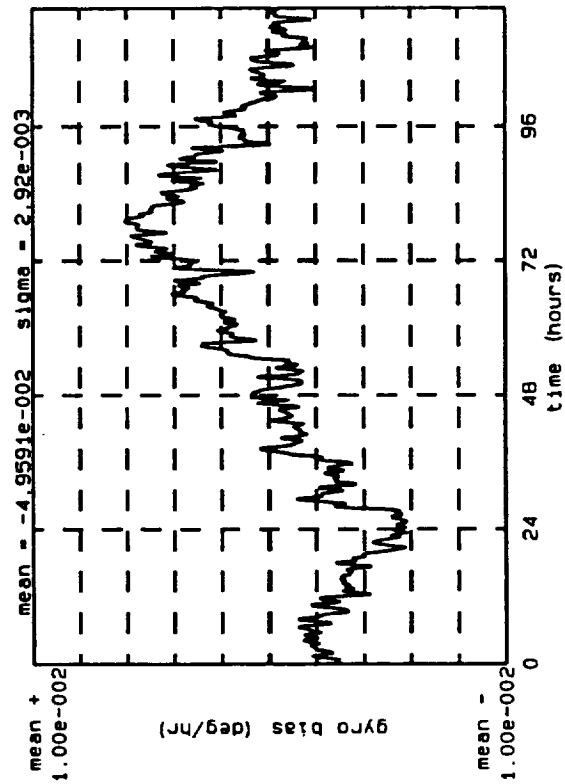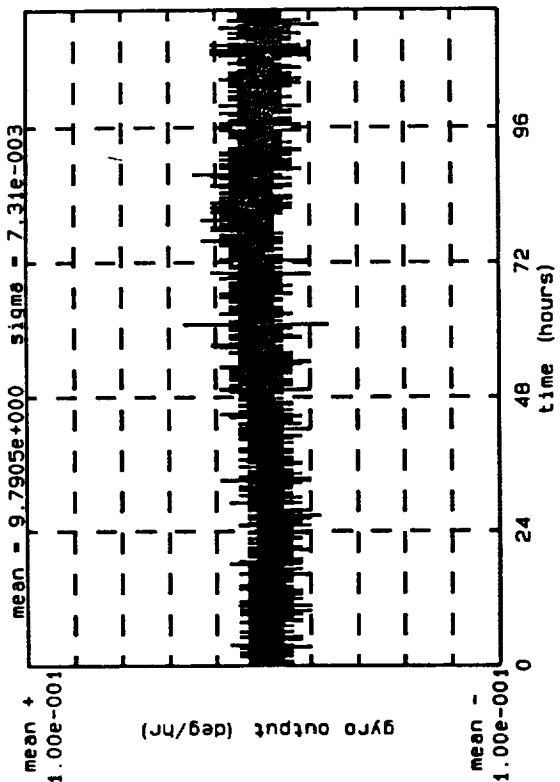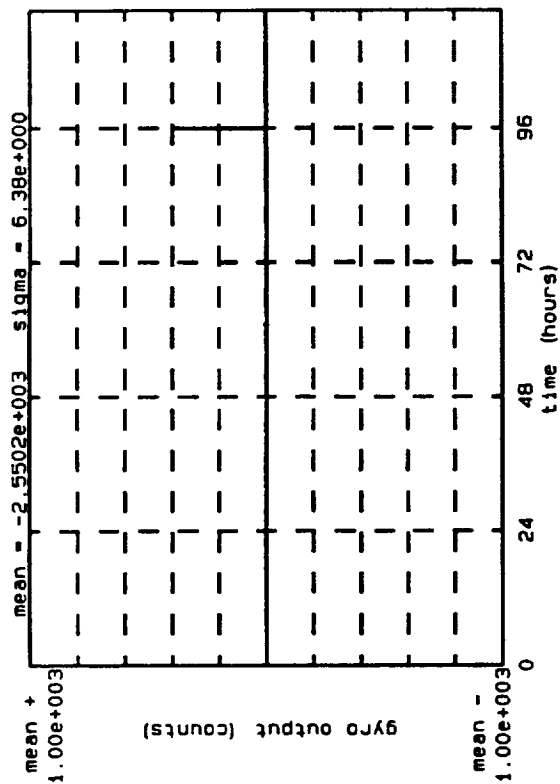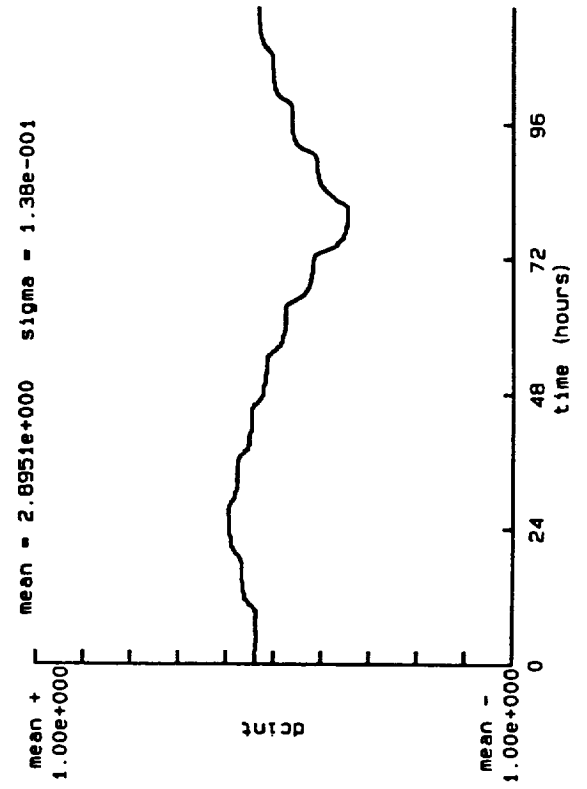
0    24    48    72    96

GYRO: B2003    DATA FILE: 09-29-89.a01

11-08-91
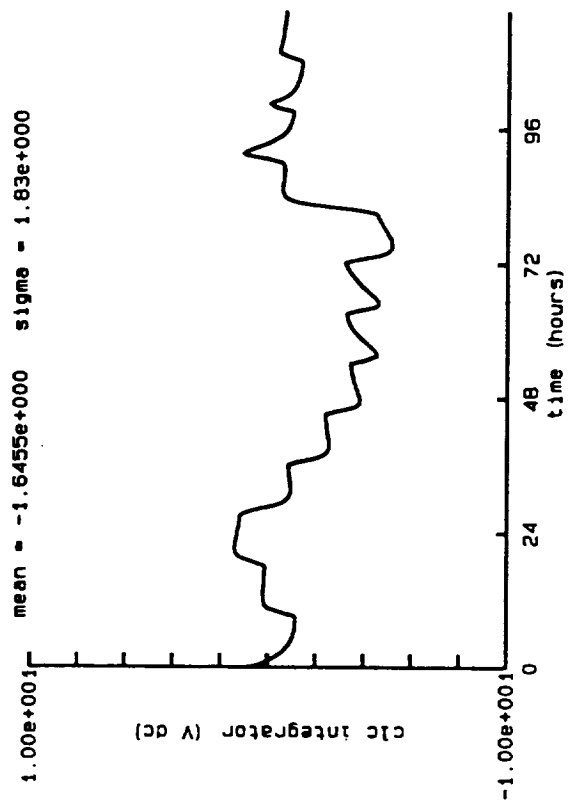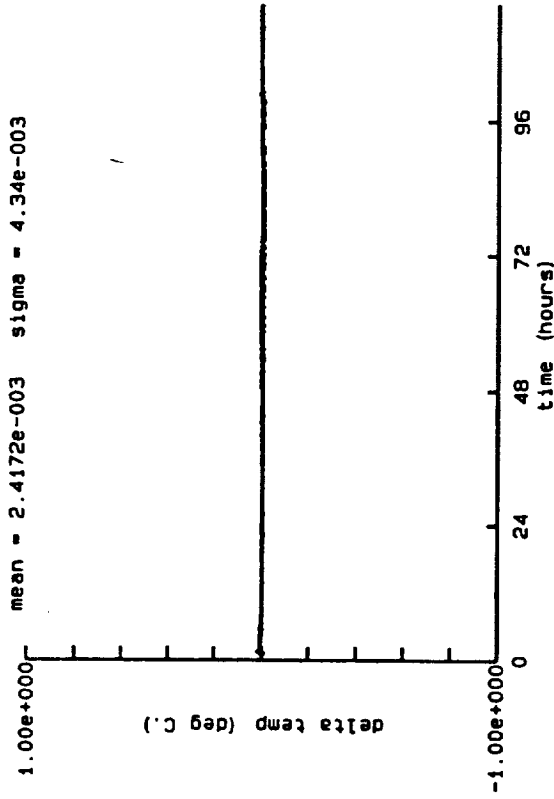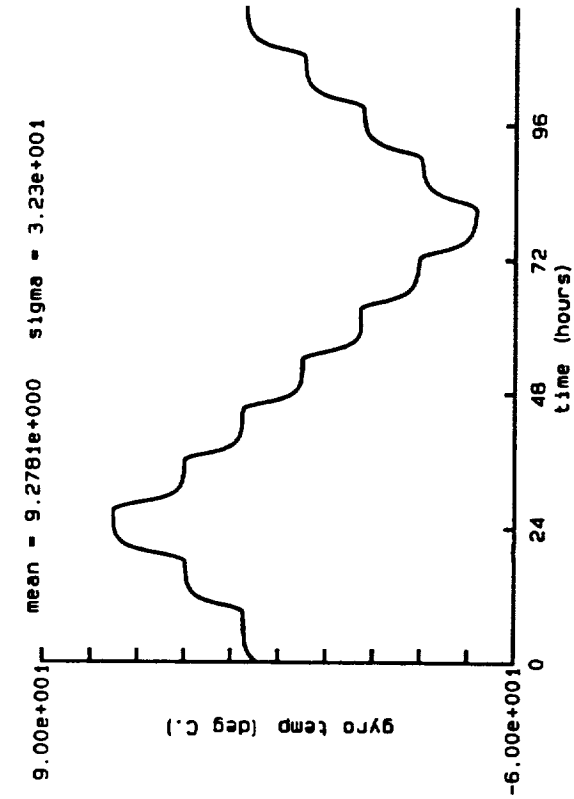
page 3    B2003: re-run 5 day bias repeatability test

mean = -1.0478e+000    sigma = 2.78e-004

mean = -2.2698e-004    sigma = 2.40e-004

total current (mAmp)

delta current (mAmp)

mean = 1.5962e+000    sigma = 7.11e-003

mean = 6.8551e+000    sigma = 3.52e+001

pickoff (rms V)

chamber temp (deg. c.)

time (hours)

GYRO: B2003    DATA FILE: 09-29-89.a01

11-08-91

D-10

# STATIC TEMPERATURE DATA

Gyro: B4500
Data file: 03-30-90.a01

| chamber temp. (deg.C) | output (deg/hr) | random walk (deg/rt-hr) | gyro T. (deg.C) | T. dev. (deg.C) | delta T (deg.C) | dT dev. (deg.C) |
|---|---|---|---|---|---|---|
| 25 | 9.8165 | 0.0004 | 26.39 | 0.04 | -0.48 | 0.00 |
| 45 | 9.8169 | 0.0005 | 43.90 | 0.22 | -0.48 | 0.00 |
| 70 | 9.8188 | 0.0005 | 66.64 | 0.16 | -0.54 | 0.00 |
| 45 | 9.8165 | 0.0005 | 44.72 | 0.45 | -0.46 | 0.00 |
| 25 | 9.8154 | 0.0005 | 26.39 | 0.33 | -0.44 | 0.00 |
| 5 | 9.8133 | 0.0004 | 8.00 | 0.19 | -0.44 | 0.00 |
| -15 | 9.8118 | 0.0007 | -10.71 | 0.20 | -0.46 | 0.00 |
| -35 | 9.8110 | 0.0006 | -29.20 | 0.29 | -0.50 | 0.01 |
| -55 | 9.8110 | 0.0004 | -48.14 | 0.40 | -0.48 | 0.01 |
| -35 | 9.8110 | 0.0005 | -30.08 | 0.31 | -0.50 | 0.02 |
| -15 | 9.8118 | 0.0005 | -11.40 | 0.32 | -0.51 | 0.00 |
| 5 | 9.8138 | 0.0005 | 7.27 | 0.27 | -0.53 | 0.01 |

summary
    peak to peak variation of 25 degree points = 0.0011 (deg/hr)
    average random walk = 0.0005 (deg/rt-hr)

thermal model
output = bias + local vertical earth rate + k0*dt +
        k1*T + k2*T^2 + k3*T^3 + k4*T^4
            where T = gyro temperature - 25

    bias = 2.0200e-001 (deg/hr),
    k0  = -5.000e-003 (deg/hr/deg.C)
    k1  = 4.249e-003 (deg/hr/deg.C)
    k2  = 3.024e-005 (deg/hr/deg.C^2)
    k3  = 9.561e-008 (deg/hr/deg.C^3)
    k4  = 1.113e-010 (deg/hr/deg.C^4)


bias repeatability = 0.0003 (deg/hr 1 sigma)

page 1     B4500: bias repeatability test

mean y = 9.8116e+000   mean x = -2.4218e+002

output (deg/hr)

mean +
2.00e-001

mean -
2.00e-001

mean +
-7.000e+001

mean +
7.000e+001

temp (deg.C.)

mean y = 3.5543e-016   mean x = -2.4218e+002

modeled output (deg/hr)

mean +
1.00e-001

mean -
1.00e-001

mean +
-7.000e+001

mean +
7.000e+001

temp (deg.C.)

GYRO: B4500     DATA FILE: 03-30-90.a01

11-08-91

page 1    B4500: bias repeatability test

GYRO: B4500    DATA FILE: 03-30-90.a01

11-08-91

D-13

page 3    B4500: bias repeatability test

mean = -1.2485e+000   sigma = 5.12e-004
total current (mAmp)

mean = 1.6215e-005   sigma = 4.04e-005
delta current (mAmp)

mean = 1.5081e+000   sigma = 3.72e-003
pickoff (rms V)

mean = 6.8355e+000   sigma = 3.52e+001
chamber temp (deg. c.)

time (hours)

GYRO: B4500    DATA FILE: 03-30-90.a01

11-08-91

# Appendix E

## Differential Equation Gyro Model

The following differential equation describes a model for RLG angle error:

$$\dot{\theta} = \mathcal{E}GB + \mathcal{E}GB_w + \mathcal{E}GB_{SF} + \mathcal{E}GBI + QN + \mathcal{E}GN$$

where:

$\mathcal{E}GB$ is the error in fixed gyro bias. It is modelled as a random, initial bias.

$$\frac{d(\mathcal{E}GB)}{dt} = 0$$

$\mathcal{E}GB_w$ is the gyro bias warm-up error, and is modelled as an exponentially decaying uncertainty in gyro bias. The uncertainty is reduced with time until a lower limit is reached after which it is modelled as a fixed random bias.

e.g.

if $E(\mathcal{E}GBw)^2 \geq \sigma^2$ limit

then model: $\dfrac{d(\mathcal{E}GBw)}{dt} = -\dfrac{\mathcal{E}GBw}{\tau}$

else model: $\dfrac{d(\mathcal{E}GBw)}{dt} = 0$

$\varepsilon GB_{SF}$ is an error in gyro rate produced by an error in gyro scale factor.

$$\varepsilon GB_{SF} = \varepsilon SF * \Omega$$

$$\varepsilon \frac{d(SF)}{dt} = 0$$

where:

$\Omega$ is the sensed gyro rate, and

$\varepsilon SF$ is the error in gyro scale factor. This error is modelled as an initial random scale factor error.

The next three terms are the major sources of noise that exist in the RL-34 gyro and are related to those variances typically used in gyro testing to compute/model the noise equivalent rate(NER).

$\varepsilon GBI$ is the random bias error. This error source is used to model gyro bias instability. This is modelled as a first order Markov process:

$$\frac{d(\varepsilon GBI)}{dt} = -\frac{\varepsilon GBI}{\tau_{bm}} + n_{bm}$$

where $n_{bm} = w(t) * \sqrt{\dfrac{2*\sigma_{bm}^2}{\tau_{bm}}}$

for long term stability, a random ramp model is used:

$$\frac{d(\varepsilon GBI)}{dt} = \alpha$$

$$\frac{d(\alpha)}{dt} = 0 \; ; \quad \alpha = \text{Random Ramp}$$

QN is the quantization noise due to gyro output angle quantization. It is modelled as an integral of gyro quantization(producing gyro angle error) by a white noise process with variance bounded(uniform distribution).

$$QN = \dot{\Theta}_{GQ}$$

$\varepsilon$GN is the gyro random walk in angle, which has a white rate noise distribution in power spectral density.

# Appendix  F

## Description of Raw Data Records

Four data files are included on a 3.5" Macintosh formatted disk as standard test files. The names of the four files are listed below:

| Filename | Description |
|---|---|
| BGSD file 090991a.dat | Example of an initialization test |
| BGSD file 100991b.dat | Example of two tracking tests |
| BGSD file 101191f.dat | Example of an acquisition test |
| BGSD file 700Hz | Example of 700 Hz data |

The first two files contain gyro X, Y and Z outputs in 'deg/hr', accelerometer outputs in 'Gs', system attitude (heading, roll, and pitch) in 'mils', and alignment/navigation time in 'seconds'. The last file only contains the system attitude and alignment/navigation time. The alignment/navigation time is a system variable that is used to either show the time left in alignment mode or the time in navigation mode. The 700 Hz data file only contains X,Y and Z gyro counts.

For example, Figure F-I shows the first 30 points of BGSD file 090991a.dat. During this test, multiple 15 minute alignments were performed. The alignment/navigation time starts at 900 (15 minutes = 900 sec) and counts down to zero, then counts up until commanded into align mode again (300 seconds later). Note, the data acquisition was performed asynchronous to the alignment/navigation time. The heading data recorded in table III (pg 24) of the report is the last data point while still in align mode. For example, the first value and second points in table III corresponds to data point 10 and 22. respectively.

Figure F-II shows the first 30 points of file BGSD file 100991b.dat. This datafile contains two tracking tests. Data points 3-11 show the alignment data. Data point 13 shows the acquisition data (20 azimuth and 60 deg elevation). Data points 14 though 388 show the 10 hrs of tracking data. After the 10 hrs of tracking was complete, the system was re-initialized and a second tracking test was performed. Data points 389 to 397 represent the second alignment and points 398 - 775 represent the second tracking test.

BGSD file 101191F. DAT contains the raw data records of a compound angle acquisition test (azimuth table rotation rate at 0.2 deg/sec from 350 deg azimuth and 0 deg elevation to 330 deg

azimuth and +60 deg elevation). Test data points 2 through 10 show the 15 alignment after which the system was switched to navigation mode for the target acquisition test. The first acquisition point was test data point 11 where the system was located at 330 azimuth and 0 deg elevation. The next test point was an intermediate point taken during the acquisition motion. At test point 13, the system completed the compound angle rotation and was located at 350 deg azimuth and +60 deg elevation. The reverse operation which moves the system back to the original position was recorded in test points: 14 and 15. This procedure was repeated 8 times. All the intermediate test points ( pts: 12, 14, 16, 18 ..etc.) were removed before processing the data. Please refer to the text where an example calculation was given on pg 36.

The 700 Hz data file only contains X,Y and Z gyro counts. The scale factor for this data is 0.3838 arcsec/pulse. The total length of the test is 6 seconds.

BGSD file 090991a.dat Excel

| Data Point | X Gyro (Deg/hr) | Y Gyro (Deg/hr) | Z Gyro (Deg/hr) | X Accel. (Gs) | Y Accel. (Gs) | Z Accel. (Gs) | Heading (mils) | Roll (mils) | Pitch (mils) | Alignment or Navigation time (Sec) |
|---|---|---|---|---|---|---|---|---|---|---|
| 1 | 11.42496 | 0.03317 | -9.78951 | 0.004208 | 0.000848 | -1.000035 | 0.9423 | -0.8434 | 4.2991 | 461 |
| 2 | 11.39761 | 0.00802 | -9.80416 | 0.004209 | 0.000848 | -1.000027 | 6398.6934 | -0.8607 | 4.2882 | 817 |
| 3 | 11.40081 | 0.02856 | -9.78117 | 0.004208 | 0.000848 | -1.000034 | 6398.9229 | -0.8661 | 4.2890 | 718 |
| 4 | 11.40338 | 0.02394 | -9.80206 | 0.004209 | 0.000848 | -1.000018 | 6398.7998 | -0.8724 | 4.2865 | 620 |
| 5 | 11.40830 | 0.02532 | -9.79936 | 0.004208 | 0.000848 | -1.000023 | 6398.6943 | -0.8687 | 4.2869 | 523 |
| 6 | 11.40858 | 0.02285 | -9.80490 | 0.004209 | 0.000849 | -1.000004 | 6398.7012 | -0.8629 | 4.2835 | 424 |
| 7 | 11.40725 | 0.02105 | -9.80007 | 0.004209 | 0.000848 | -1.000032 | 6398.7080 | -0.8643 | 4.2878 | 326 |
| 8 | 11.41952 | 0.02533 | -9.79872 | 0.004208 | 0.000848 | -1.000022 | 6398.7559 | -0.8621 | 4.2866 | 229 |
| 9 | 11.39979 | 0.01559 | -9.78868 | 0.004209 | 0.000848 | -1.000020 | 6398.7236 | -0.8626 | 4.2907 | 130 |
| 10 | 11.40657 | 0.02413 | -9.80615 | 0.004209 | 0.000847 | -1.000012 | 6398.7148 | -0.8653 | 4.2926 | 32 |
| 11 | 11.41266 | 0.03163 | -9.79158 | 0.004209 | 0.000849 | -1.000037 | 6398.7314 | -0.8708 | 4.2873 | 65 |
| 12 | 11.40582 | 0.01350 | -9.80364 | 0.004208 | 0.000848 | -1.000028 | 6398.7217 | -0.8806 | 4.2908 | 164 |
| 13 | 11.40251 | 0.01616 | -9.79237 | 0.004209 | 0.000848 | -1.000031 | 6398.7227 | -0.8741 | 4.2844 | 262 |
| 14 | 11.40704 | 0.02835 | -9.79983 | 0.004209 | 0.000848 | -1.000022 | 6399.3779 | -0.8655 | 4.2876 | 805 |
| 15 | 11.41760 | 0.02035 | -9.79296 | 0.004208 | 0.000849 | -1.000032 | 6399.0010 | -0.8643 | 4.2833 | 707 |
| 16 | 11.39992 | 0.02788 | -9.81151 | 0.004208 | 0.000848 | -1.000033 | 6399.0459 | -0.8682 | 4.2861 | 609 |
| 17 | 11.39992 | 0.02788 | -9.81151 | 0.004209 | 0.000849 | -1.000033 | 6398.9102 | -0.8662 | 4.2839 | 511 |
| 18 | 11.41128 | 0.01071 | -9.79631 | 0.004209 | 0.000849 | -1.000027 | 6398.8896 | -0.8649 | 4.2921 | 413 |
| 19 | 11.39511 | 0.02917 | -9.79254 | 0.004209 | 0.000849 | -1.000021 | 6398.8027 | -0.8624 | 4.2866 | 315 |
| 20 | 11.41895 | 0.02529 | -9.79391 | 0.004208 | 0.000849 | -1.000034 | 6398.8232 | -0.8676 | 4.2867 | 217 |
| 21 | 11.39735 | 0.01454 | -9.80444 | 0.004209 | 0.000849 | -1.000039 | 6398.8604 | -0.8654 | 4.2901 | 119 |
| 22 | 11.40087 | 0.02398 | -9.78951 | 0.004209 | 0.000850 | -1.000025 | 6398.8379 | -0.8684 | 4.2874 | 21 |
| 23 | 11.40399 | 0.01808 | -9.80502 | 0.004207 | 0.000850 | -1.000032 | 6398.8330 | -0.8744 | 4.2807 | 77 |
| 24 | 11.40935 | 0.01726 | -9.79181 | 0.004209 | 0.000850 | -1.000037 | 6398.8389 | -0.8791 | 4.2882 | 175 |
| 25 | 11.40488 | 0.02505 | -9.80653 | 0.004208 | 0.000850 | -1.000027 | 6398.8301 | -0.8835 | 4.2848 | 273 |
| 26 | 11.40924 | 0.01448 | -9.79986 | 0.004209 | 0.000851 | -1.000023 | 6398.1963 | -0.8641 | 4.2834 | 806 |
| 27 | 11.40154 | 0.02834 | -9.79280 | 0.004209 | 0.000851 | -1.000028 | 6398.9697 | -0.8669 | 4.2854 | 707 |
| 28 | 11.41099 | 0.01391 | -9.80882 | 0.004208 | 0.000850 | -1.000034 | 6398.9766 | -0.8706 | 4.2878 | 609 |
| 29 | 11.39878 | 0.02027 | -9.80204 | 0.004209 | 0.000851 | -1.000028 | 6398.8018 | -0.8681 | 4.2876 | 512 |
| 30 | 11.41077 | 0.02367 | -9.79667 | 0.004209 | 0.000851 | -1.000028 | 6398.8438 | -0.8709 | 4.2903 | 413 |

Figure F-I

BGSD file 100991b.dat Excel

| Data Point | X Gyro (Deg/hr) | Y Gyro (Deg/hr) | Z Gyro (Deg/hr) | X Accel. (Gs) | Y Accel. (Gs) | Z Accel. (Gs) | Heading (mils) | Roll (mils) | Pitch (mils) | Alignment or Navigation time (Sec) |
|---|---|---|---|---|---|---|---|---|---|---|
| 1 | 10.74550 | 3.90507 | -9.78412 | 0.004281 | 0.000851 | -1.000039 | 6044.2588 | -0.8900 | 4.3517 | 9940 |
| 2 | 10.71900 | 3.88573 | -9.79311 | 0.004281 | 0.000852 | -1.000029 | 6044.2520 | -0.8917 | 4.3434 | 10037 |
| 3 | 10.73006 | 3.90490 | -9.79461 | 0.004282 | 0.000852 | -1.000013 | 6044.2158 | -0.8679 | 4.3624 | 805 |
| 4 | 10.72986 | 3.89375 | -9.78857 | 0.004281 | 0.000851 | -1.000021 | 6043.9199 | -0.8647 | 4.3610 | 707 |
| 5 | 10.73842 | 3.91291 | -9.79157 | 0.004281 | 0.000851 | -1.000021 | 6044.0498 | -0.8710 | 4.3597 | 609 |
| 6 | 10.73842 | 3.91291 | -9.79157 | 0.004281 | 0.000851 | -1.000021 | 6044.1992 | -0.8689 | 4.3573 | 511 |
| 7 | 10.72644 | 3.88923 | -9.79165 | 0.004281 | 0.000852 | -1.000026 | 6044.2080 | -0.8719 | 4.3581 | 413 |
| 8 | 10.73204 | 3.90899 | -9.79306 | 0.004282 | 0.000852 | -1.000018 | 6044.2510 | -0.8721 | 4.3607 | 315 |
| 9 | 10.74068 | 3.91335 | -9.78606 | 0.004281 | 0.000852 | -1.000020 | 6044.2500 | -0.8677 | 4.3583 | 217 |
| 10 | 10.72074 | 3.88533 | -9.78949 | 0.004281 | 0.000851 | -1.000020 | 6044.2842 | -0.8709 | 4.3631 | 119 |
| 11 | 10.73236 | 3.90557 | -9.80209 | 0.004281 | 0.000852 | -1.000013 | 6044.2773 | -0.8688 | 4.3616 | 21 |
| 12 | 10.73883 | 3.90939 | -9.79039 | 0.004281 | 0.000852 | -1.000027 | 6044.2676 | -0.8663 | 4.3589 | 78 |
| 13 | -2.23041 | -2176.39063 | 706.46021 | -0.630854 | 0.000520 | -0.639096 | 6399.4746 | -0.8271 | -1066.8076 | 175 |
| 14 | -2.85036 | 0.00855 | -14.76690 | -0.866008 | 0.000419 | -0.499849 | 6399.4717 | -0.8293 | -1066.8018 | 273 |
| 15 | -2.84103 | 0.01507 | -14.78095 | -0.866008 | 0.000420 | -0.499844 | 6399.4707 | -0.8394 | -1066.8093 | 372 |
| 16 | -2.82303 | 0.03338 | -14.76448 | -0.866008 | 0.000421 | -0.499844 | 6399.4678 | -0.8364 | -1066.7983 | 469 |
| 17 | -2.84812 | 0.01104 | -14.77309 | -0.866011 | 0.000420 | -0.499847 | 6399.4639 | -0.8419 | -1066.7998 | 567 |
| 18 | -2.83739 | 0.01134 | -14.77515 | -0.866005 | 0.000421 | -0.499846 | 6399.4658 | -0.8439 | -1066.7979 | 666 |
| 19 | -2.84587 | 0.01555 | -14.76016 | -0.866015 | 0.000421 | -0.499853 | 6399.4785 | -0.8436 | -1066.7954 | 763 |
| 20 | -2.82062 | 0.02909 | -14.77332 | -0.866016 | 0.000421 | -0.499850 | 6399.4766 | -0.8507 | -1066.8010 | 861 |
| 21 | -2.83525 | 0.00770 | -14.78257 | -0.866015 | 0.000420 | -0.499852 | 6399.4736 | -0.8474 | -1066.7952 | 960 |
| 22 | -2.83136 | 0.02865 | -14.77679 | -0.866006 | 0.000420 | -0.499848 | 6399.4805 | -0.8447 | -1066.8030 | 1057 |
| 23 | -2.84638 | 0.01503 | -14.76882 | -0.866011 | 0.000421 | -0.499849 | 6399.4697 | -0.8415 | -1066.7969 | 1155 |
| 24 | -2.83067 | 0.01264 | -14.76763 | -0.865997 | 0.000421 | -0.499848 | 6399.4854 | -0.8478 | -1066.7986 | 1254 |
| 25 | -2.83226 | 0.02082 | -14.77657 | -0.866010 | 0.000421 | -0.499850 | 6399.4932 | -0.8505 | -1066.7974 | 1351 |
| 26 | -2.83641 | 0.00832 | -14.77275 | -0.866006 | 0.000421 | -0.499849 | 6399.4863 | -0.8330 | -1066.7949 | 1449 |
| 27 | -2.83219 | 0.02559 | -14.77044 | -0.866006 | 0.000421 | -0.499847 | 6399.4863 | -0.8440 | -1066.7883 | 1548 |
| 28 | -2.84111 | 0.01305 | -14.77480 | -0.866008 | 0.000420 | -0.499847 | 6399.5010 | -0.8530 | -1066.7952 | 1645 |
| 29 | -2.84929 | 0.00463 | -14.77313 | -0.866005 | 0.000422 | -0.499846 | 6399.4941 | -0.8514 | -1066.7932 | 1743 |
| 30 | -2.84044 | 0.01872 | -14.77283 | -0.866020 | 0.000420 | -0.499852 | 6399.5039 | -0.8616 | -1066.7930 | 1842 |

Figure F-II

F-4